UNLOADING USING AUGER TOOL AND FOAM AND

EXPERIMENTAL IDENTIFICATION OF LIQUID LOADING OF LOW

RATE NATURAL GAS WELLS

A Thesis

by

RANA BOSE

Submitted to the Office of Graduate Studies of
Texas A&M University
in partial fulfillment of the requirements for the degree of

MASTER OF SCIENCE

May 2007

Major Subject: Petroleum Engineering

UNLOADING USING AUGER TOOL AND FOAM AND

EXPERIMENTAL IDENTIFICATION OF LIQUID LOADING OF LOW

RATE NATURAL GAS WELLS

A Thesis

by

RANA BOSE

Submitted to the Office of Graduate Studies of
Texas A&M University
in partial fulfillment of the requirements for the degree of

MASTER OF SCIENCE

Approved by:

Chair of Committee,   Stuart L. Scott
Committee Members, Yassin Hassan
                               Walters B. Ayers
Head of Department, Stephen A.Holditch

May 2007

Major Subject: Petroleum Engineering

ABSTRACT

Unloading Using Auger Tool and Foam and Experimental Identification of

Liquid Loading of Low Rate Natural Gas Wells. (May 2007)

Rana Bose, B.E., Jadavpur University, India

Chair of Advisory Committee: Dr. Stuart L. Scott

Low-pressure, low-producing natural gas wells commonly encounter liquid loading during production. Because of the decline in the reservoir pressure and the flow capacity, wells can fall below terminal velocity. Identifying and predicting the onset of liquid loading allows the operators to plan and prepare for combating the liquid loading hence saving valuable reserves and downtime. The present industrial applications of artificial lift, wellhead pressure reduction by compressor installation at the wellheads and reduction in tubing size are costly and often intermittent. The thesis examines the above aspects to generate a workflow for identifying and predicting the liquid loading conclusively and also assessing the application of Auger Tool and foam combination towards achieving a cost effective and more efficient solution for liquid unloading.

In chapters I-IV, I describe the process of using production surveillance software of Halliburton Digital Consulting Services, named DSS (Dynamic Surveillance Software), to create a workflow of identifying the liquid loaded wells based on well data on daily basis for field personnel and engineers. This workflow also decides

the most cost effective solution to handle it. Moreover, it can perform decline analysis to predict the conditions of liquid loading.

In chapters V-VIII of the thesis, I describe the effort of handling the problem of liquid loading in a cost effective manner by introduction of an inexpensive Auger Tool in the bottomhole assembly and using WhiteMax surfactant soapstick from J&J Solutions. Four different combinations of well completion and fluid were tested for performance in respect to liquid hold up, pressure loss in the tubing, unloading efficiency and critical flow requirement. The test facilities and instruments, along with the operational methods, are discussed in chapter VI.

Except for the reduction of the operational envelope with the inclusion of Auger Tool, the performance improved with the insertion of Auger Tool. The best combination of Auger and foam system could be a result of flow modification by the Auger Tool caused by reduced pressure loss and increase in drag coefficient and also by reduced density and surface tension of foam.

DEDICATION

I would like to dedicate my thesis to my parents and my wife for their sincere support and love in every aspect of my life.

To my parents, who are really extremely special in bringing me up to this stage. You are the ones lending me support and strength and you made it happen. Thanks to both of you for guiding me the right way and standing by my decision.

To my wife, who is an example of strength and candid in all her opinions, thank you for helping me make such a courageous decision at a crucial juncture of my life and also for providing the right balance of life even in conditions which were not well suited, were sudden and which led to financial difficulties.

Without your support, understanding and encouragement, I could not have achieved anything.

ACKNOWLEDGEMENTS

I would like to thank my advisor, Dr. S.L. Scott, for his continued support and guidance, and for allowing me to work and decide on several directions and explore several possibilities during my research.

This research was made possible by the support of the ARCO. I would like to especially thank Crisman Research Institute for funding the work described in chapters V-VIII of the thesis and for making the project a reality.

I want to express my sincere gratitude to Ms. Lynn Babec of Halliburton Digital Consulting Services (HDCS) for believing in me and assigning me Section 1 of the project and for allowing me to publish the results.

The laboratory tests to check the performance of Auger tool and foam, described in chapters V-VII of the thesis were conducted as an extension of the previous work on similar Vortex tool by Ali et al.. I acknowledge the great influence he had on my work.

I also would like to thank Mr. J. Votaw of J&J Solutions for providing valuable guidelines for the use of soapsticks in the test.

I want to express my sincere thanks to my colleagues within the Multiphase Research

Group who have helped me set up the infrastructure for testing, especially since it needed to be changed several times. I am especially grateful to Ms. Luciana Cruz for helping me take the videos and photographs and Austin Gaskamp, Pat Thaiuboon, for constant support and helpful discussions throughout the project.

I would like to acknowledge my professors and committee members at Texas A&M University, from whom I have received guidance all through the difficult stages of the project.

Finally, I would like to thank my parents, family, and colleagues, who acted as a source of inspiration and helped me to finish the project successfully on time.

TABLE OF CONTENTS

LIST OF FIGURES

LIST OF TABLES

CHAPTER I

INTRODUCTION

The natural gas well loading phenomenon is considered as one of the most serious problems in the natural gas industry. It occurs as a result of liquid accumulation in the wellbore, when the natural gas phase is not able to provide sufficient energy to lift the produced fluids resulting in additional hydrostatic pressure in the reservoir and causes more reduction in the transport energy. The energy requirement increases and the natural gas flow reduce. The changing relative water saturation and natural gas saturation and corresponding relative permeability changes makes it increasingly difficult. If the reservoir pressure is low, then the accumulated liquids may completely kill the well. If the reservoir pressure is higher, then liquid slugging or churning may take place and gives more chance for liquid accumulation and the well may eventually die. The phenomenon is more important for marginally economic wells like low pressure, low flow gas wells. The technique to successfully operate these wells lies in the production rate to be above its critical natural gas flow rate.

It is thus very important to identify the liquid loading in a proper way and the liquid loading, if can be predicted, would lead to saving valuable reserves and well life. In

_____

This thesis follows the style of *SPE Production and Facilities.*

chapters II-IV, described is an effort to identify and predict the liquid phenomena through use of patented well monitoring software of Halliburton Digital Consulting Services (HDCS) named Dynamic Surveillance Software (DSS).The well site engineer can routinely identify wells that experience a liquid loading condition and take day-to-day remedial action based on the described workflow. This identification methodology will be used in excel sheet platform for site engineers and at surveillance software level by the well supervisors. The wellwise or fieldwise identification , will be followed by analysis through work flow. The workflow comprise of creation of graph, charts, bubble map to identify wells with different coloring through logic set in the software and then analyse and conclude for or against liquid loading. The necessary equipment procurement can be performed based on that workflow. The scheduling of workovers based on this kind of requirement can also be done.

The software can be used to perform a decline analysis and optimize the reserve and production operations by prior planning through obtaining a tentative idea of around what time the natural gas velocity would be below the terminal velocity level so that it onsets the liquid loading.

In creation of the workflow, the analytical equation of the four phase kinetic energy model proposed by B.Guo et al.[1] was solved programmatically to arrive at a different critical flow rate calculation, other than using traditional Turner[2] and Coleman's[3] correlation. The advantage in this approach that it can handle condensate, water and

solid production simultaneously and has also been proved superior to Turner correlation in lot of recent liquid loaded wells when matched with the actual well performance.

Chapter II will consist of the background and literature review regarding the basis of this work. Chapter III will discuss the methods of identifying and predicting liquid loading by a workflow. Chapter IV will consist of the results and discussions.

The solutions to the liquid loading problem had been dealt with in several ways as described below:

1. Different methods of artificial lift
2. To allow the well unload by itself
3. Wellhead compression of produced gas
4. Soap sticks or annular injection
5. Reduction in tubing size

The first method and the third methods are the most expensive because of operation costs and all installation involved, and the fourth method is an excellent solution since is easier to lift foam than water.

Low natural gas rate injection wells have an unstable performance due to non-utilisation of lift potential, occurrence of critical operating conditions and complicated production control and allocation.

Pressure drop in the tubing at low natural gas rate injection is controlled by hydrostatic pressure gradient and at high rates by frictional pressure gradient.

The solution to this liquid loading problem readily used and accepted in the industry are capital intensive and energy rich solutions. In terms of a field development planning for marginal wells, the number of wells requirement is higher with a lower wells spacing. The lead time and the involved in the procurement of all these capital items are much higher.

The solution like change in tubing size may be only an intermittent one, need several changes with subsequent declines and can also lead to a tubing limited situation if implemented in early well life.

All these combined provides the need for a less capital intensive, energy deficient solution. Both the Tools and methods applied in the form of self twisting Auger Tool and foam surfactant used in the wellbore can turn out to be a suitable solution to this liquid loading problem.

The Chapter V will deal with background pertaining to this work which involves certain standard flow pattern, discussion on pressure loss, usefulness of Auger Tool, working ideology of Auger Tool, usefulness of foam, certain standard definition concerning foam application, foam selection criteria ,certain industry practices and little bit of case

histories gathered from various sources. Chapter VI will be on literature review. Chapter VII will focus on the laboratory set up, all the metering and recording instruments used and the methodologies followed in arriving at the test results.

The Chapter VIII presents the results in the graphical form to compare the achievements and the benefits and also discusses the shortcomings of the tests conducted. The results in tabular form are presented in Appendix A to E.

The Chapter IX will be conclusion and recommendation where the scope for improvement and furthering the research effort to achieve the industrial applicability.

CHAPTER II

IDENTIFICATION OF LIQUID LOADING OF LOW RATE NATURAL

GAS WELLS: BACKGROUND AND LITERATURE REVIEW

The choosing of proper critical flow rate calculation model has an important role to play in predicting the minimum natural gas flow rate requirement. Results from different models suggested often show mismatch with the actual field results. The BP wells has been evaluated for its liquid loading onsetting with the existing Turner[2] model and in several wells, the prediction was not accurate, when matched with the field results. In quest of a better prediction, another model by B,Guo et al. has been used. Comparison with the field data described in the paper showed an improved accuracy in predicting the liquid loaded wells based on four phase model, when compared with the prediction with the Turner model.

Discussed below are the basics of Turner model and B.Guo's model considered for creation of the production engineering workflow.

2.1 Turner Model

Turner et al. (1969)[2] were the pioneer investigators who analyzed and predicted the minimum natural gas-flow rate to prevent liquid loading. They presented two mathematical models to describe the liquid-loading problem: the film-movement model and entrained drop-movement model. On the basis of analyses of field data, they concluded that the film movement model does not represent the controlling liquid-transport mechanism.

The liquid exists in the wellbore in two forms 1) the liquid film along the pipewall and 2) in the high velocity natural gas core in the middle as liquid droplets.

Turner predicted two models to predict the onset of liquid loading:

2.1.1 Continuous Film Movement Model: This model assumes that annular liquid film should have to be continuously moved upward along the wells to achieve liquid unloading. The model calculates the minimum flow rate requirement to move the film upward.
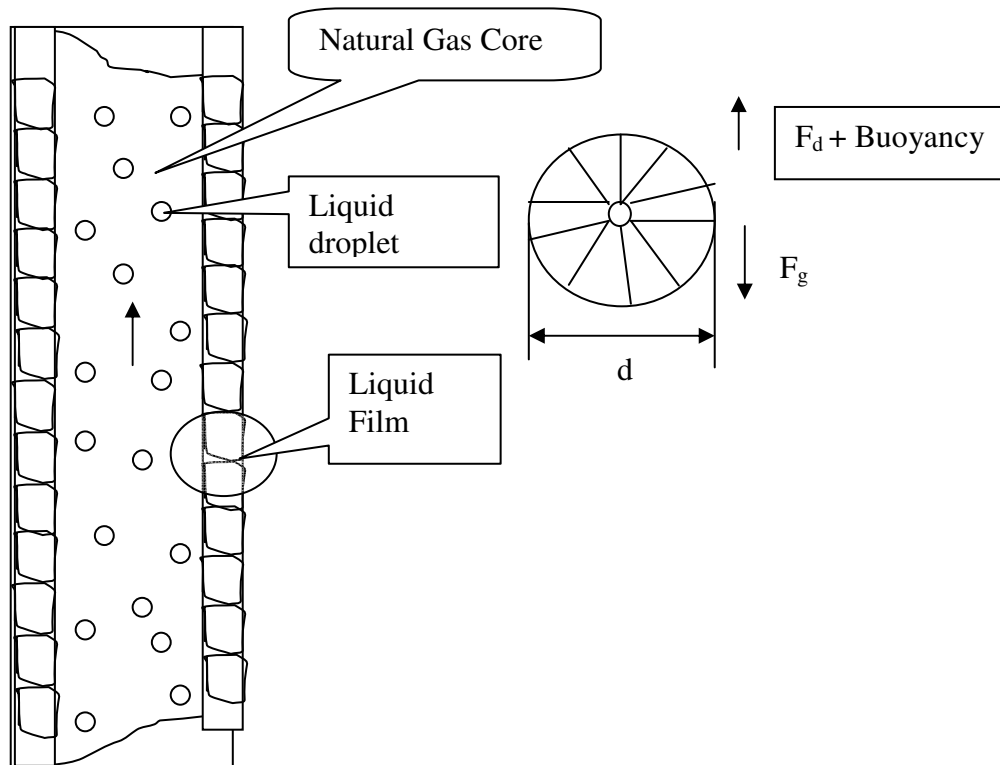
Figure 2.1 Turner model description

2.1.2 Liquid Droplet Model: The liquid droplet model assumes that the governing criteria are the lifting of the entrained droplets in the high velocity natural gas core. This model predicts the minimum flow rate requirement for raising the liquid droplets. Comparison with the field data has shown that the liquid droplet model represents the controlling mechanism.

2.1.3 Critical Rate Theory: Turner. et al. showed that a free falling particle in a fluid medium will reach a terminal velocity that is function of the particle size, shape, and density and of the fluid medium density and viscosity.

Applying this concept of liquid droplets in a flowing core of natural gas column, the terminal velocity, v_t of the drop is, which assumes a fixed droplet size, shape and drag coefficient and includes the 20% adjustment suggested by Turner, based on field results matching.

$$v_{sl} = \frac{1.3\sigma^{1/4}\left(\rho_l - \rho_g\right)^{1/4}}{c_d^{1/4}\rho_g^{1/2}} \dots\dots\dots\dots\dots\dots\dots\dots\dots\dots\dots\dots\dots\dots\dots\dots\dots(2.1)$$

The minimum natural gas-flow rate (in MMcf/D) for a particular set of conditions (pressure and conduit geometry) after considering this terminal velocity and correcting to standard conditions (MMscf/day).

$$Q_{gslMM} = \frac{3.06 p v_{sl} A}{Tz} \dots\dots\dots\dots\dots\dots\dots\dots\dots\dots\dots\dots\dots\dots\dots\dots\dots\dots(2.2)$$

The 20% adjustment is needed to conform to the test results but used mostly for wells with wellhead pressure 500 psia.

Coleman et al.[3] stated that for wells less than wellhead flowing pressure of 500 psia, this 20% upward adjustment is not required.

Li et al.[4] came up with a non spherical shape idea of the liquid particles and considered a drag coefficient of 1.0.

Turner et al. believed that the discrepancy was attributed to several facts, including the use of drag coefficients for solid spheres; the assumption of stagnation velocity; and the critical Weber number established for drops falling in air, not in compressed natural gas. The main problem that hinders the application of Turner et al.' s entrained drop model to natural gas wells comes from the difficulties of estimating the values of fluid density and pressure. The use of average value of natural gas-specific gravity (0.6) and natural gas temperature (120°F), did not represent natural gas pressure in a multiphase-flow wellbore.

Nosseir et al. (2000) cxpanded Turner et al.' s entrained drop model to more than one flow regime in a well.

2.2 Four Phase Model by B.Guo et al.

This paper of B, Guo et al.[1] claimed that Turner's method with 20% adjustment still underestimates the minimum natural gas velocity for liquid removal. The study is based on determining the minimum kinetic energy of natural gas required to lift liquids.

The model proposed can handle a four-phase mist-flow in natural gas wells with water, oil and solid production. The minimum kinetic energy criterion requires that natural gas kinetic energy exceed a minimum value to transport liquid droplets up in the natural gas well. The four-phase mist-flow model considered accurate predictions of pressure, and thus fluid density that are used in the kinetic energy calculation, against the average specific gravity value and temperature considered in Turner model.

2.2.1 Minimum Kinetic Energy: Kinetic energy per unit volume of natural gas can be expressed as

$$E_k = \frac{\rho_g v_g^{\,2}}{2g_c} \quad\text{...(2.3)}$$

Substituting Eq. 2.1 into Eq. 2.3 gives an expression for the minimum kinetic energy required to keep liquid droplets from falling:

$$E_{ksl} = 0.026 \sqrt{\frac{\sigma(\rho_l - \rho_g)}{C_d}} \quad\text{...(2.4)}$$

When C_d = 0.44 and the natural gas density is neglected,

$$E_{ksl} = 0.04 \sqrt{\sigma \rho_l} \quad\text{..(2.5)}$$

In natural gas wells producing water, σ = 60 dynes/cm and ρ_l = 65 lbm/ft^3 , E_{ksl}= 2.5 lbf-ft/ft^3.

The minimum natural gas velocity for transporting the liquid droplets upward=floating velocity plus transporting velocity.

$$V_{gm} = V_{sl} + V_{tr} \text{...(2.6)}$$

The transport velocity V_{tr} may be calculated on the basis of liquid production rate, geometry of the conduit, and liquid volume fraction, which is difficulty to quantify. Considering nonstagnation velocity, drag coefficients for solid spheres, and the critical Weber number established for drops falling in air, v_{tr} has been taken as 20% of v_{sl} in this study. Use of this value results in

$$V_{gm} \approx 1.2 V_{sl} \quad\text{..(2.7)}$$

Substituting Eqs. 2.1 and 2.7 into Eq. 2.3 results in the expression for the minimum kinetic energy required for transporting the liquid droplets as

$$E_{km} = 0.0576 \sqrt{\sigma \rho_l}$$ ....(2.8)

For typical natural gas wells producing water, this equation yields the minimum kinetic energy value of 3.6 lbf-ft/ft^3. which is approximately twice of that in condensate-producing natural gas wells.

The E_k in equation 2.3 requires the values of natural gas density ρ_g and natural gas velocity V_g need to be determined.

Ideal gas law:

$$\rho_g = \frac{2.7 S_g p}{T}$$ ....(2.9)

$$V_g = 4.71 * 10^{-2} \frac{TQ_g}{A_i p}$$ ....(2.10)

Equation 2.9, 2.10 and 2.3 yields

$$E_k = 9.3 * 10^{-5} \frac{S_g TQ_g^{2}}{A_i^{2} p}$$ ....(2.11)

Eq. 2.11 indicates that the natural gas kinetic energy is inversely proportional to the pressure, which relates to the bottomhole conditions, in which natural gas has higher pressure and lower kinetic energy.

However, this analysis is in contradiction with Turner et al.'s results that indicated that the wellhead conditions are, in most instances, controlling.

2.2.2 Four-Phase Flow Model: To accurately predict the bottomhole pressure p in Eq. 2.11, a natural gas/oil/water/solid four-phase mist-flow model has been developed. According to the four-phase flow model, the flowing pressure p at depth L can be solved numerically from the following equation:

$$144(p-p_{hf})+\frac{1-2bm}{2}\ln\left|\frac{(144p+m)^2+n}{(144p_{hf}+m)^2+n}\right|-\frac{m+\frac{b}{c}n-bm^2}{\sqrt{n}}\left[\tan^{-1}\left(\frac{144p+m}{\sqrt{n}}\right)-\tan^{-1}\left(\frac{144p_{hf}+m}{\sqrt{n}}\right)\right]$$

$$=a(1+d^2e)L \quad\text{………………………………………………..(2.12)}$$

Where

$$a=\frac{15.33S_sQ_S+86.07S_WQ_w+86.07S_0Q_0+18.79S_gQ_g}{10^3T_{av}Q_G}\cos(\theta)\text{………………. (2.13)}$$

$$b=\frac{0.2456Q_s+1.379Q_w+1.379Q_0}{10^3T_{av}Q_G}\text{……………………………………… (2.14)}$$

$$c=\frac{6.785X10^{-6}T_{av}Q_G}{A_i}\text{……………………………………………………… (2.15)}$$

$$d = \frac{Q_s + 5.615(Q_w + Q_0)}{600 A_i} \qquad \text{(2.16)}$$

$$e = \frac{6f}{gD_h \cos(\theta)} \qquad \text{(2.17)}$$

$$f = \left[\frac{1}{1.74 - 2\log\left(\frac{2\varepsilon'}{D_h}\right)} \right]^2 \qquad \text{(2.18)}$$

$$m = \frac{cde}{1 + d^2 e} \qquad \text{(2.19)}$$

$$n = \frac{c^2 e}{\left(1 + d^2 e\right)^2} \qquad \text{(2.20)}$$

2.2.3 Minimum Required Natural Gas Production Rate: Predicting the minimum natural gas flow rate Q_{gm} involves calculation of natural gas density ρ_g, natural gas velocity V_g and natural gas kinetic energy E_k at bottomhole condition using an assumed natural gas flow rate Q_G (non-zero), and compare E_k with E_{km}.

The value of Q_G should be reduced iteratively until E_k is very close to E_{km} which corresponds to Q_{gm}. Under the minimum unloaded condition equation 2.11 becomes

$$E_{km} = 9.3 X 10^{-5} \frac{S_g T_{bh} Q_{gm}^{2}}{A_i^2 p} \qquad \text{(2.21)}$$

Which gives

$$p = 9.3 \times 10^{-5} \frac{S_g T_{bh} Q_{gm}^2}{A_i^2 E_{km}} \dots \dots \dots \dots \dots \dots \dots \dots \dots \dots \dots \dots \dots \dots \dots \dots (2.22)$$

Substituting equation 2.22 into equation 2.12 results in

$$144 b\alpha_1 + \frac{1 - 2bm}{2} \ln \alpha_2 - \frac{m + \frac{b}{c} n - bm^2}{\sqrt{n}} \left[\tan^{-1} \beta_1 - \tan^{-1} \beta_2\right] = \gamma \dots \dots \dots (2.23)$$

Where

$$\alpha_1 = 9.3 \times 10^{-5} \frac{S_g T_{bh} Q_{gm}^2}{A_i^2 E_{km}} - p_{hf} \dots \dots \dots \dots \dots \dots \dots \dots \dots \dots \dots \dots \dots (2.24)$$

$$\alpha_2 = \frac{\left(1.34 \times 10^{-2} \frac{S_g T_{bh} Q_{gm}^2}{A_i^2 E_{km}} + m\right)^2 + n}{\left(144 p_{hf} + m\right)^2 + n} \dots \dots \dots \dots \dots \dots \dots \dots \dots \dots (2.25)$$

$$\beta_1 = \frac{1.34 \times 10^{-2} \frac{S_g T_{bh} Q_{gm}^2}{A_i^2 E_{km}} + m}{\sqrt{n}} \dots \dots \dots \dots \dots \dots \dots \dots \dots \dots \dots \dots (2.26)$$

$$\gamma = a\left(1 + d^2 e\right) L \dots \dots \dots \dots \dots \dots \dots \dots \dots \dots \dots \dots \dots \dots \dots (2.27)$$

Equation 2.23 is a one to one function of Q_{gm} for all values greater than zero. Newton Raphson can be used for Q_{gm}.

Sensitivity analysis has been carried out with 3 major governing parameters tubing id, tubing head pressure, presence of condensate.

Dousi, N., Veeken, C.A.M., and Currie, P.K[5] in their work on modeling the liquid loading process described and modeled the water build up and drainage process. Their work shows clearly that the wells can operate at two different rates, a stable rate during their full production cycle and a lower metastable rate at which liquid loading effects play a role. The metastable rate operation has been modeled and sensitivity analysis carried out. They derived an analytical solution for the metastable rate and stabilized water column height confirming the numerical analysis results.

Kumar, N[6] in his paper provided an improved multiphase flow correlation for natural gas wells experiencing liquid loading over the existing Gray correlation for flowing bottomhole pressure.

Lea, J.F., and Nickens, H.V[7] describes the problem of liquid accumulation in a natural gas well. Recognition of natural gas-well liquid-loading problems and solution methods are discussed including the stability and nodal analysis.

Jelinek, W., Wintershall, and Schramm, L.L[8] talk about the several aspects of surfactant use including the technical and economical aspects in a liquid loaded wells to prevent reserve loss through production enhancement.

CHAPTER III

IDENTIFICATION OF LIQUID LOADING OF LOW RATE NATURAL GAS WELLS: METHODS

The work of Guo, B et al.[1] suggested a kinetic energy model where the minimum kinetic energy criteria is used to predict the minimum natural gas flow rate. According to the authors, the Turner et.al[2] calculation underestimated the flow rate requirement even after 20% upward adjustment.

The new flow correlation and the flow equation for the minimum flow requirement is based on the minimum energy requirement to transport the entrained droplets. Comparison with the field data used in the paper showed an improved accuracy in predicting the liquid loaded wells based on four phase model, when compared with the prediction with the Turner model.

Equation 2.23 is a one to one function of Q_{gm} for all values greater than zero. Newton Raphson can be used for Q_{gm}. The solver functionality which comes with Microsoft Excel can also be used for iteration. However, the solver is a single row based function in Microsoft Excel and cannot be repeated for multiple rows at a time, which is what is needed for the well monitoring .This was solved by using a VBA program (Ref. Appendix I) and later referenced to well surveillance software through interfaces for well monitoring and decision making workflow on liquid loading.

The analytical model was solved by a Visual basic application and the resulting minimum natural gas flow calculated was then interfaced to DSS for further analysis purpose.

- The job involved writing a code to solve the nonlinear minimum kinetic energy equation in B.Guo's work[1] which is being accomplished by a macro in VBA Excel platform

- The excel interface is for site engineers monitoring to identify the liquid loaded wells marked by different color

- The DSS interface with bubblemap created through preset criteria and decision workflow is used for analysis by supervisors

- Presently it was being tested for 4 different wells

- Running the program with one set of data had established that the turner predicted flow rate was underestimating the minimum flow rate in at east one of the wells. These needs further validation with further well data.

- A form was created where from the user will be choosing a particular data set of their choice and also choose the range of data (days of operation) they are interested in and perform minimum flow rate calculation. Presently the program needs to be changed with changing of the worksheet name to perform that. The master datasheet would consist of the list of the wells and the program would consider the first well in that master database as well 1 and so on. In order to change the program sequence, the master table has to be altered.

- The wells can be colored suitably with different colors for liquid loaded and liquid unloaded wells using the program itself.

- The program automatically generates the casing pressure versus tubing pressure comparison by a graph and feeds to DSS.

- The DSS analyses the data based on calculated minimum flow rate and conclude on liquid loading while considering the other relevant well data vide workflow. All these alongwith the decision space management which has an optimizer for well economics module leads to a workflow defined later in this section (Figure 3.1).

- The decline analysis feature of DSS was utilized to perform the decline analysis for predicting the onset of liquid loading, based on the present day production data. This analysis can be suitably run and updated with the changing production profile with time. It would find its effectiveness in well monitoring and workover planning to save valuable production downtime.

The proprietary well surveillance software DSS of Halliburton Digital Consulting Services used to create suitable table, workbook, and chart, bubble map and were configured according to the needs. The B, Guo model was incorporated to calculate the minimum flow requirement while retaining the flexibility of using Turner model.

Different steps that must be followed in DSS to generate this workflow are being explained through screenshots in Appendix-J.

Liquid Unloading Workflow

```
Well Production Data from          Configure Data with Key Indexes
SCADA                               For Evaluation By DSS

            Calculated
            Qgm By
4 Phase     Excel/VBA      Dynamic Surveillance
Model                      Software(DSS)

                    Creation of Workbook, Table with
                    Primary Index, Criteria, Bubble
                    Maps, Configuration of Properties

   No                                         Yes
                     Qg>Qgm

No Liquid                                  Probable
Loading                                    Liquid Loading

                                  Check On Well     Check On Well Production      Well Monitoring
      Need                        Completion i.e    History,Decline Curves,Differential   i.e any
No    Prediction    Yes           Packer Or No      Casing Head Pressure and Tubing   particular
      of Liquid                   Packer ,Plunger Lift   Head Pressure,Production   workover/well
      Loaduig                                       Fluctuations,Field Production Trend   intervention

Liquid                 Decline
Unloaded well          Analysis in
                       DSS

                                            Decision On Liquid Loading
         Tabulate the results for
         onset of Liquid Loading
         and send it to decision                              No      Liquid      Yes
         Logic                                                        Loading

                                              Well Services Team For
                                              necessary Remedial Job
                                              based on EUR, Cost Of
                                              Recompletion, Re-
                                              stimulation , Artificial Lift
                                              Vis.A.Vis New Well Cost
                                              With Well Optimiser
```

Figure 3.1 Liquid loading workflow

CHAPTER IV

IDENTIFICATION OF LIQUID LOADING OF LOW RATE NATURAL

GAS WELLS: RESULTS AND DISCUSSION

The analysis method of identifying and predicting the liquid loading has improved the workflow used by the field engineers to quite a great extent. The basic logic and process outlined above has been suitably incorporated in Dynamic Surveillance Tool Project Model .It enables the field engineer to monitor, detect and correct the wells performance on a daily basis on scenario analysis. This also paves way for the project engineers to plan and procure the required capital items and helps reducing the downtime. It also enhances the decision making and improves the workover rigtime. Most importantly, it optimizes the well operation and increases well life.

The work of B, Guo et al.[1] worked well with 30 wells scenario with the wells considered by him in his paper. However, it encountered a mixed results when an analysis is done by using the four phase model and compared with the turner model. More wells and fields are to be dealt with before conclusively accepting or rejecting either of the models.

The prediction of liquid loading by Turner flow rate corresponding to terminal velocity was found wanting in most of the real BP well scenario. The actual well names which can be referred to master table, are not disclosed due to technical reasons. The wells tended to show signs of liquid loading even if the predicted Turner[2] critical flowrate was not suggesting that. This had necessitated considering B.Guo's model as an alternative

model of predicting flowrate.If found successful, it was to be considered for inclusion in DSS upcoming releases and also include it in the engineering workflows.

Results displaying the values and the percentage difference between the minimum flowrate predicted by the 4 phase model and Turner model are in Appendix J.

In field1, well 4,5,7,13,20 and Field2 well1, 2 justified claim of B.Guo. Most of the wells deviated by 5-6% which proves that the arbitrary 20% adjustment is close enough. It has got more scientific explanation.

The claim of B.Guo[1] of Turner flow rate underprediction was found true around 40% wells and 20% more wells was very close by 5-6%. Needs more data to conclude on the applicability range of the model.

CHAPTER V

LIQUID UNLOADING OF NATURAL GAS WELLS BY USING AUGER TOOL

AND FOAM: BACKGROUND

The natural gas well loading phenomenon is considered as one of the most serious problems in the natural gas industry. It occurs as a result of liquid accumulation in the wellbore, when the natural gas phase is not able to provide sufficient energy to lift the produced fluids resulting in additional hydrostatic pressure in the reservoir and causes more reduction in the transport energy. The energy requirement increases and the natural gas flow reduces. The changing relative water saturation and natural gas saturation and corresponding relative permeability changes makes it increasingly difficult. If the reservoir pressure is low, then the accumulated liquids may completely kill the well. If the reservoir pressure is higher, then liquid slugging or churning may take place and gives more chance for liquid accumulation and the well may eventually die. The phenomenon is more important for marginally economic wells. The technique to successfully operate these wells lies in the production rate to be above its critical natural gas flow rate.

The solutions to prevent this are:

1. To unload the liquid mechanically by natural gas lift injection, submersible pump, plunger lift, other methods of artificial lifts and so on

2. To allow the well unload by itself

3. Reduction in wellhead pressure by inclusion of a compressor at the wellhead

4. Use of some chemical liquids for instance surfactants (soap sticks or annular injection)

5. Reduction in tubing size

The first method and the third methods are the most expensive because of operation costs and all installation involved, and the fourth method is an excellent solution since is easier to lift foam than water.

High natural gas rate injection wells have a stable performance, however low natural gas rate injection wells have an unstable performance and some of the disadvantages unstable system are:

1 The total lift potential is not well used

2 Due to the rush in production, critical operational conditions might occur

3 Production control and allocation turned out to be complicated.

Pressure drop in the tubing at low natural gas rate injection is controlled by hydrostatic pressure gradient and at high rates by frictional pressure gradient.

The solutions to this liquid loading problem readily used and accepted in the industry are capital intensive and energy rich solutions. In terms of a field development planning for marginal wells, the number of wells requirement is higher with a lower wells spacing. The lead time and the involved in the procurement of all these capital items are much

higher. The fifth solution may be only an intermittent one and can also lead to a tubing limited situation quickly.

All these combined provides the need for a less capital intensive, energy deficient solution. Both the Tools and methods applied in the form of self twisting Auger Tool and foam surfactant used in the wellbore can turn out to be a suitable solution to this liquid loading problem.

The created test set up was utilized to achieve a technique for continuous liquid unloading initially with the inexpensive Auger Tool in place, with and without surfactant to see the effectiveness of the Auger Tool and surfactant in liquid unloading. The Turner equation of the terminal velocity and the critical flow rate was validated by the result. The test was conducted with the Auger at the middle of the tubing since it was felt that most of the pressure drop which leads to slippage of natural gas and liquid falling, occurs at that part of the tubing.

Operation envelope was determined with the set up not having Auger Tool, set up with the Auger Tool without surfactant, and also with the Auger Tool and the surfactant and finally with the surfactant alone.

Flow pattern changes with transition was observed and recorded during the terminal velocity determination for all the above scenarios.

Suitable software was considered to be used after the initial set up for data acquisition and see the effect of liquid slugging and the effect of injection of natural gas at a certain rate and varying the simulated rate.

During the surfactant test, GLCC –the gas liquid cyclone separator was used for defoaming with higher retention time and effective separation through a helical movement and handling of surfactant effectively. This has been proposed in the work at Tulsa University, the working principle described later in the Section 6.4.5.

Metering equipment and transmission equipment available in the Lab were used to effectively communicate the data to the Data acquisition system (DAQ).

The job included setting up vertical casing in tower for experiment, followed by visualizing and investigating the flow pattern changes with the Auger Tool compared to the set up without Auger Tool and also the Auger Tool and surfactant in combination in terms of operating envelope and also to determine the operating envelope and terminal velocity in each of these conditions. The pumping facility was selected with proper judgement to carry out the test with widely varying flowrates and pressures and also with varying fluid qualities.

Industry application wise the use of surfactant at the bottom of the riser in subsea applications is thought to be of significant cost effective importance in terms of creating

pressure drop and will stimulate achieving higher recovery.

Tight natural gas sand wells and low pressure, low producing natural gas wells are really significant areas of applications of the above two methodologies.

The Chapter V will provide background which deals with the outline of the liquid loading phenomena and the objective of the research. The Chapter VI will deal with literature review pertaining to this work which involves certain standard flow pattern, discussion on pressure loss, usefulness of Auger Tool, working ideology of Auger Tool, dimension of Auger Tool, usefulness of foam, certain standard definition concerning foam application, foam selection criteria, certain industry practices and the details of the foam being used and use of GLCC to handle foam carryover. Chapter VII will focus on the laboratory set up, all the metering and recording instruments used and the methodologies followed in arriving at the test results.

The Chapter VIII presents the results in graphical form to compare the achievements and the benefits and also discusses the shortcomings of the tests conducted.

The Chapter IX will discuss the scope for improvement and furthering the research effort to achieve the industrial applicability in the conclusion and recommendation.

CHAPTER VI

LIQUID UNLOADING OF NATURAL GAS WELLS BY USING AUGER TOOL

AND FOAM: LITERATURE REVIEW

During the declining stages of a well sourced without any reservoir pressure support mechanism, the produced liquid transporting energy reduces leading to liquid hold up and pressure loss through the tubing requiring more natural gas flow.

The demand of natural gas increased over the years due to primarily 3 reasons 1) comparatively lower cost 2) cleaner fuel 3) non discovery of major oil fields which can be produced in a cost effective way. The newer level of energy demand continue to outgrow the supply. The depleting of natural gas wells shifts the focus for increasing the recovery.

The natural gas production from the reservoir is associated with the production of water and condensate in the wellbore. Due to its discontinuous nature of production, different multiphase flow regimes are encountered during the production life of the well.

With sufficiently high natural gas flows, the annular mist flow condition can be maintained .With the decline in the flow rate in a depleting field, the flow regime changes and finally give in to the liquid accumulation in the wellbore. This effects a backpressure on the formation that can affect the producibility of the well by also changing the saturation around the wellbore. This necessitates to maintain the flow rate

of natural gas above the critical rate.

Liquid removal varies during all the regimes but the continuous liquid removal happens only in the mist flow regime. The rest of the regimes produce natural gas intermittently. It is very important to visually observe the terminal velocity onset and correlate that with the annular mist flow transition.

6.1 Multiphase Flow in a Natural Gas Well

Almost all the natural gas wells go through the following flow regimes in a wells history.

Bubble Flow—Free natural gas bubbling through the liquid filled tubing, where the liquid contacts the wall surface, and the bubbles reduce the density.

| Bubble | Slug | Slug-annular transition | Annular-mist |
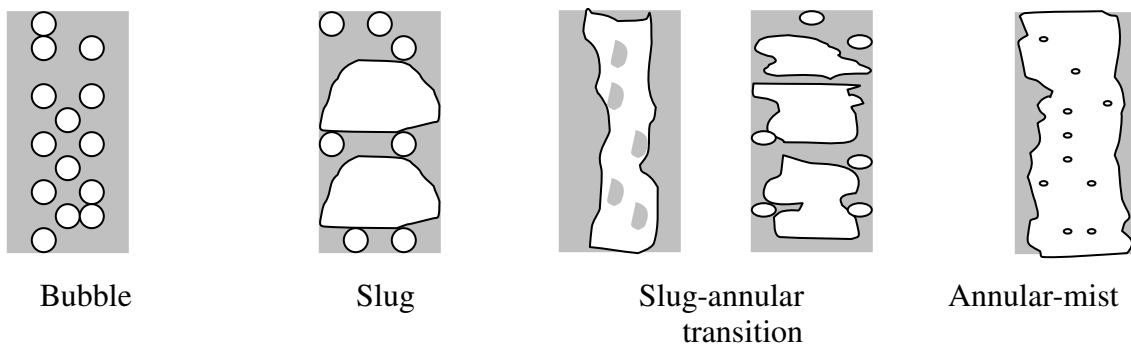
Figure 6.1 Flow regimes in vertical multiphase flow

Slug Flow—Larger natural gas bubbles due to expansion cause slugs with liquid as continuous phase. Slipping of the liquid film occurs. Intermittent flow pattern observed.

Churn Flow-increased natural gas velocity breaks slugs, change of continuous phases occurs with the liquid near the wall churning.

Slug-Annular Transition—Continuous natural gas phase observed with some liquid entrainment.

Annular-Mist Flow—Natural gas phase is continuous with all liquid entrained. The pipe wall coated has thin film of liquid.

It needs corrective action to prevent the well decline to produce and continue to be the annular-mist flow region.

The mist flow pattern where the liquids are dispersed in the natural gas which causes less low liquid "holdup", resulting in a low gravitational pressure drop fluids.

Improper tubing design can greatly affect the life of the well caused by low natural gas velocity. The balance between frictional pressure drop and gravitational pressure drop are detailed in the Appendix G and H.

The water production sourcing can be natural production, condensation or water coning. The well producing rate can be predicted by the reservoir inflow performance relationship (IPR) curve. Lea and Tighe[9] provide an introduction to loading and some discussion of field problems and solutions. Coleman et al.[3] suggested newer means of predicting the liquid loading.

Possible methods and criteria to deliquefy natural gas wells within different operating pressure ranges are detailed in[10]. The method that is most economic for the longest period of operation is the optimum method.

As the reservoir pressure declines, the condensation increases and it is more effective with increase in temperature.

This phenomenon occurs when liquids (interstitial water and hydrocarbon condensates) entrained in the produced natural gas; accumulate in the wellbore to the extent that they can severely reduce production by backpressure and by reduced natural gas relative permeability in the surrounding formation. The accumulating fluid may eventually balance out the available natural gas reservoir energy and cause the well to die.

A terminal velocity exists when natural gas can no longer transport liquid upwards through the well tubing. The critical natural gas rate is defined as the minimum natural gas flow rate that will ensure the continuous removal of liquids from the wellbore. The

most widely used equation to estimate critical rate is Turner's equation derived from the spherical liquid droplet model, assuming a constant turbulent flow regime. A slight variation of this equation was proposed by Coleman. And more recently, an enhancement of the model was proposed by Nosseir[11] who considered the prevailing flow regimes, and by Li[4] who, to obtain a match to the behavior of the wells he studied, considered the shape of entrained droplets to more like convex bean than spherical.

All the methods are essentially Turner's equation with different constant terms corresponding to different flow conditions.

The relevant equations are:

Turner's Equation:

$$v_{gc} = 1.912[\sigma^{1/4}(\rho_l - \rho_g)^{1/4}] / [(\rho_g)^{1/2}]; \text{ assumed } C_d = 0.44 \text{ ------------------------(6.1)}$$

Coleman's Equation:

$$v_{gc} = 1.593[\sigma^{1/4}(\rho_l - \rho_g)^{1/4}] / [(\rho_g)^{1/2}]; \text{ assumed } C_d = 0.44 \ldots\ldots\ldots\ldots\ldots\ldots.(6.2)$$

Nosseir's Equation-I (Transition flow regime):

$$v_{gc} = 0.5092[\sigma^{0.35}(\rho_l - \rho_g)^{0.21}] / [(\mu_g)^{0.134}(\rho_g)^{0.426}]; \ldots\ldots\ldots\ldots\ldots\ldots\ldots\ldots\ldots(6.3)$$

Nosseir's Equation-II (Highly turbulent flow regime):

$$v_{gc} = 1.938[\sigma^{1/4}(\rho_l - \rho_g)^{1/4}] / [(\rho_g)^{1/2}]; \text{ assumed } C_d = 0.2 \ldots\ldots\ldots\ldots\ldots\ldots\ldots.(6.4)$$

Li's Equation:

$$v_{gc} = 0.724[\sigma^{1/4}(\rho_l - \rho_g)^{1/4}] /[(\rho_g)^{1/2}]; \text{ assumed } C_d=1.0 \ldots\ldots\ldots\ldots\ldots\ldots\ldots\ldots(6.5)$$

Natural gas density can be related to natural gas gravity (Dake[12])

$$\rho_g = 2.699*\gamma_g*p/[Tz] \ldots\ldots\ldots\ldots\ldots\ldots\ldots\ldots\ldots\ldots\ldots\ldots\ldots\ldots\ldots\ldots\ldots\ldots\ldots\ldots(6.6)$$

Finally, the critical flow rate can be determined from terminal velocity by

the expression:

$$q_c = 3.06pv_{gc}A/Tz \ldots\ldots\ldots\ldots\ldots\ldots\ldots\ldots\ldots\ldots\ldots\ldots\ldots\ldots\ldots\ldots\ldots\ldots.(6.7)$$

Guo, B et al. proposed Four Phase Model where he suggested that the minimum gas flow rate corresponds to minimum kinetic energy required for entraining the liquid droplets. The derivation of the analytical equation leading to   minimum flow rate has been described in chapter II.

6.2 Physical Observation of Liquid Loading

Early detection of the liquid loading can lead to prevention of the liquid loading occurrence and instrumental in sustenance of the well continuous production. Presence of the phenomenon of liquid loading recorded through the natural gas measuring device pressure fluctuations, slugging production and a trended decline rate more than predicted smooth exponential rate, correlation of tubing pressure decrease with simultaneous increase in casing pressure, steep change in pressure gradient than usual and significant

decrease in liquid unloading rate. Pressure gradient survey could be an indication which then can be matched by a liquid level measurement. Higher natural gas gradient above liquid and a lower liquid gradient below liquid is observed through acoustic measurement.

Large tubing results in lower frictional pressure loss and the presence of the liquid in the increases the tubing pressure gradient.

At low natural gas rates, the proportional increase of pressure loss in the tubing caused by liquids is higher than at high natural gas rates.

The minimum lift curves (and erosion natural gas rate) placed directly on the wellhead backpressure curve[10] help identify when liquid loading (or erosion rates) threatens to reduce production.

"The Auger separator is a device which partially separates liquid and gas. It has no moving parts, and requires no power or level controls[13]".

This device has been shown to be particularly useful in gas wells where the Multiphase Meters are not as accurate. The cost is ≈ 2% of installing a conventional separator vessel.[14] Even though each case is singular and different costs apply for each case, this is an estimated number where the magnitude should be analyzed.

6.3 Vortex Applications: Working Principle

6.3.1 Surface: Two-phase flow (gas and liquid), the device ideally creates two distinct flows within the overall laminar flow: (Figure 6.2)."Spiral" flow is established along the outer wall of the pipe-carries liquid phase which carries most or all of the liquid phase of the pipe flow. Center of the spiral is occupied by a strong laminar flow of gas phase (Figure 6.2).The fluids remain entrained in the laminar flow, reducing drop out. This boundary layer cushioning effect reduces pressure drop compared to turbulent flow.

Pipe wall

Liquids

Heavier fluids

Gas   Lighter fluids

Heavier fluids
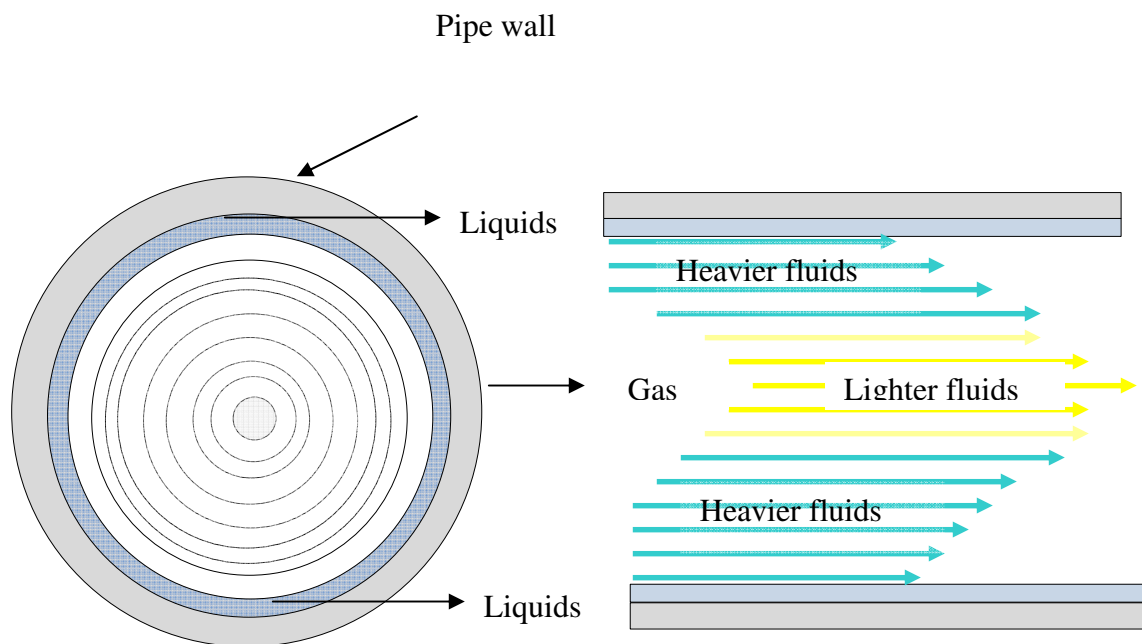
Liquids

Figure 6.2 Organized flow pattern[15]

Random flow pattern (Figure 6.3) is observed without Vortex.

Pipe wall
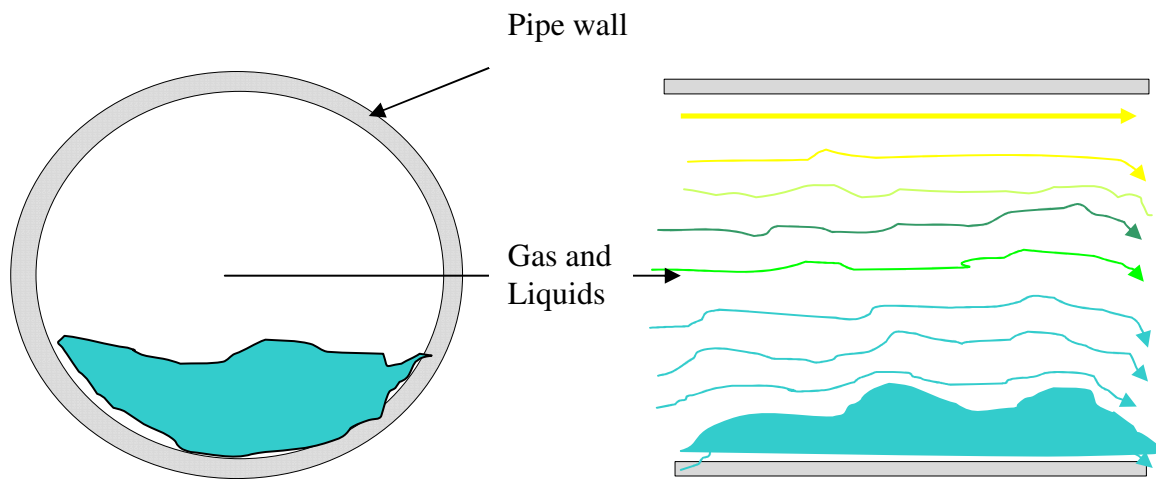
Gas and
Liquids

Figure 6.3 Random flow pattern[15]

6.3.2 Downhole: The combined flow stream of gas and liquids on entering the Vortex

tool is subjected to rapid spinning by the helical forces caused by the bluff body placed

at an attacking angle of 450 with respect to the mandrel. The heavier fluid is moved to

the pipe wall with the high angular acceleration. The gas starts moving centrally with the

no-flow boundary at the edge of the gas stream and along the pipe wall. This results in a

lower differential velocity between the gas and liquid of the flow, which lowers the shear

force and frictional pressure. Reduction of this slip force between liquid droplets in the

flow and the natural gas stream reduces amount of work performed by the natural gas

mist- reducing the total pressure drop. (Ref. website: http://www.jeffreymachine.com/

earthAuger3d.html) .

Flanged connection

Angle of attack 45^0

High Velocity Gas Core

Liquid spirally moving in the wall

Liquid particle

Gas particle

E-27
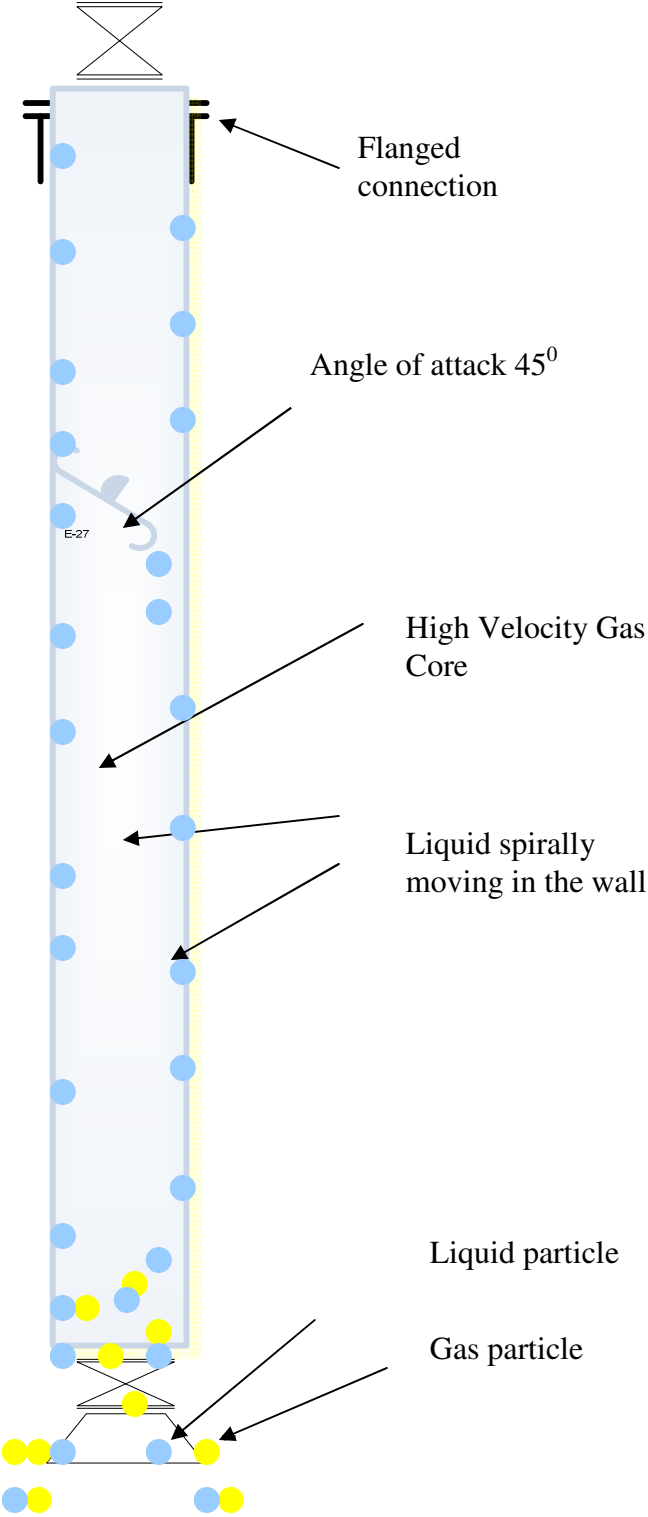
Figure 6.4 Downhole display of fluid motion with Vortex tool[16]

Illobi and Ikoku17 characterized the flow regime to be an upward moving continuous smooth to wavy film of liquid on the tube wall. Natural gas containing entrained liquid droplets of varying concentration moves through centrally .They described the annular mist flow regime in two categories small ripple regime and disturbance wave regime. In the small ripple regime, small waves develop in the interface and move at about interfacial velocities and disappear quickly. At higher flow rates, the waves are higher and travel at 2-3 times the interfacial velocity. These are called disturbance waves.

6.4 Foam Application

Foams used as a circulation medium for drilling wells, well cleanouts, and as fracturing fluids can be used in natural gas well liquid removal applications. The principal benefit of foam as a natural gas well de-watering method is that liquid is held in the bubble film and exposed to more surface area, resulting in less natural gas slippage and a low-density mixture[18]. The foam is effective in transporting the liquid to the surface in wells with very low natural gas rates.

Natural gas bubbles are separated by a liquid film in foam. Surface active agents reduce the surface tension of the liquid to cause more natural gas-liquid dispersion. The liquid film between bubbles has two surfactant layers with liquid between them. This method of binding the liquid and natural gas is instrumental in removing liquid from natural gas wells.

The tests carried out reflected the pressure gradient reduction realized with foam.
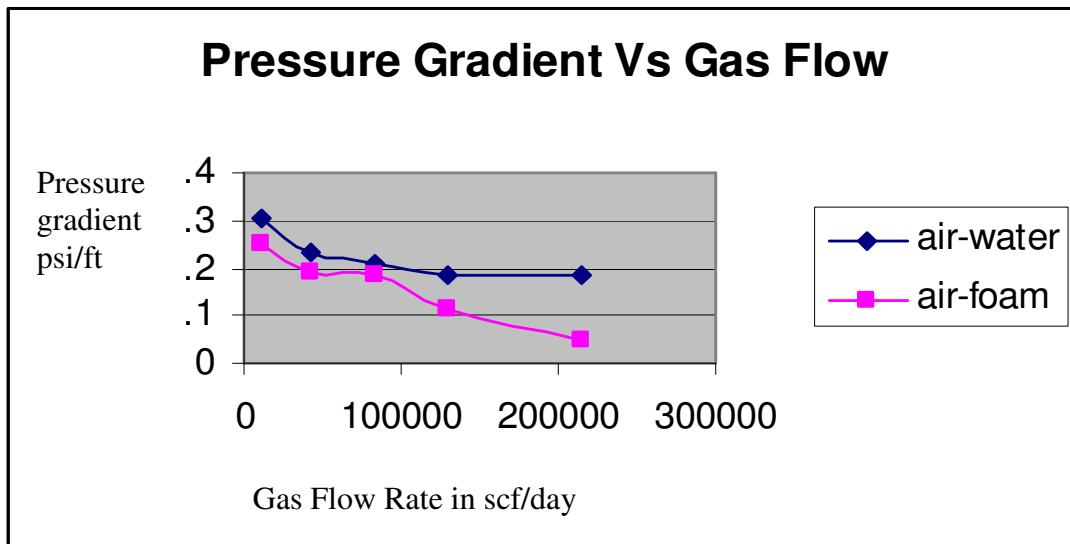
Figure 6.5 Pressure gradient versus gas flow comparison

Campbell et al.[18] described the foam effect on production of liquids using the terminal velocity. He discussed that foam will reduce the surface tension and therefore reduce the required terminal velocity. They indicated surface tension should be measured under dynamic conditions.

They also discussed that foam will reduce the density of the liquid droplets to a complex structure containing formed water and/or condensate and natural gas. Thus, the

beneficial effects of foam are described by the fact that the foamed liquid droplet density and surface tension both combine to reduce the required terminal velocity.

The percentage of natural gas in the foam mixture at operating pressure and temperature is termed foam quality (i.e., foam that is 80% natural gas by mass is called 80 quality foam).

At higher foam qualities, the liquid film becomes thinner and distorted because of surface tension.

The minimum stress required to overcome the interlocking of the bubble structures is called a yield point. The apparent viscosity, which is dependent on the shear rate.

6.4.1 Foam Selection[19,20] : Economics plays a major role in choosing surfactants in reducing bottomhole pressure .While the low-rate natural gas wells with GLRs 1000 - 8000 scf/bbl are better candidates for foaming; where high GLR wells is suitable for plunger lift to produce with less bottomhole pressure than foam.

Foam quality appears to vary with the amount of liquids and the natural gas volume fraction. The viscosity of foam varies with quality and with the amount and type of surfactant used. The viscosity which is dependent on the kind of foam determines shear

stress and thus shear rate and thinning, is an important consideration, which however was not determined during the test. The test was carried out by anionic surfactant.

6.4.2 Anionic Surfactants: Supplier data suggested Anionic surfactants are excellent water foamers. This kind of surfactant is more polar and anionic in character and has an increased solubility in water.

During this test, the product of J & J Solutions was used. Soapsticks were 1" in diameter. The composition is either a hard, wax-like stick with a water soluble paper jacket.

The product is tradenamed WhiteMax sticks is specially formulated of nonionic and anionic surfactants and foaming agents .It comes in clean water soluble stick form. It was advised by the manufacturer to restrict the application to preferably in fresh water and limited condensate. The WhiteMax stick dissolves to release highly effective foaming agents.

It was also being advised on personal discussion that in absence of online ppm measurement or surface concentration measurement, the way to control the foam use is to maintain a density to 0.7 g/cc.It was decided to drop one soapstick each at the wellhead and the return tank to achieve that, once the recorded density goes above 0.7 g/cc.

Water has a surface tension of approximately 65-72 dyne/cm in air-water system, which is generally reduced to the 20 to 35 dyne/cm range with surfactants used for foaming based on surfactants used. In absence of surface tension measurement, the literature values were considered for terminal velocity calculation and comparison.

6.4.3 Foam Stability: Foams tend to deteriorate with time.Drainage of liquids from the bubble film causes thinning of the bubble wall. Also, the bubble grows by expansion of natural gas and and eventually the liquid film breaks.

Campbell et al.[18] describes the thinning of the foam film in terms of the critical micelle concentration (CMC). The CMC is the point at which the addition of surfactant molecules to a solution results in the formation of colloidal aggregates.

The determining role is the film structure. Based on this model, the following effects are predicted. The more micelles present in solution, the easier the film ordering. The foamer with the lower CMC would at the same concentration have more micelles present and be more stable.

If the foam is used at many times the CMC, the produced foam would be more stable. A solution that is too dilute will not allow the range of surface effects (i.e., surface tension reduction, film elasticity, repair of ruptured bubbles, etc.) required for foaming.

A solution that is too concentrated may cause excessive foam stiffness, high apparent foam viscosity, and/or excessive liquid-oil emulsions, as well as increasing the cost of treating the well.

Laboratory tests indicate that many surfactants have an optimum effectiveness at approximately .1% to .2% concentration in the water phase. Campbell et al.[18] indicates that experience dictates a surfactant dosage of 1000-4000 ppm.

Vosika, J.L[21] in his paper illustrated that the use of foaming agents as an inexpensive yet effective solution to liquid loading problems in area natural gas wells. They described the necessity of selecting different foaming agents based on liquid ppm, past well performance and wellbore configuration.

Scott, S.L., Wu, Y., and Bridges, T.J[22] presented foam staged operations by air-foam unit as an alternative to the costlier N_2 and coil tubing applications. The authors discussed and handled the concerns regarding utilizing air foam: 1) lower available pressures and rates; 2) flammability; and, 3) corrosion.

6.4.4 Foam Density Calculation

Table 6.1 Foam Density Calculation Example

Foam Density Calculation example:						
Base Data:						
Liquid Injection Rate (Q_l):					400	gpm
Mud Weight (W_m):					8.4	ppg
Surface Temperature:					530	°R
Natural gas Specific Gravity (Sg):					1	air=1
Backpressure (P_s):					50	psia
Natural gas Injection Rate (Q_o):					50	scfm
$Q_{natural\ gas}$ **ft^3**	Q_{liquid} **ft^3**	Foam Quality	Foam Density lb/ft^3			
15.0	**53.5**	**22%**	**52.63**			

Foam Density= ((Mud Weight/8.33)-((Mud weight/8.33)-(Backpressure in psia*144/53.3/Surface Temperature in ^{O}R))*Foam Quality)*62.4

The different observation of the use of soapsticks in the lab at Texas A&M University is being discussed separately.

The foam quality could not be measured on a continuous basis and the foam density calculation being a dependent function of that was not calculated. However, the foam density was monitored in data acquisition unit.
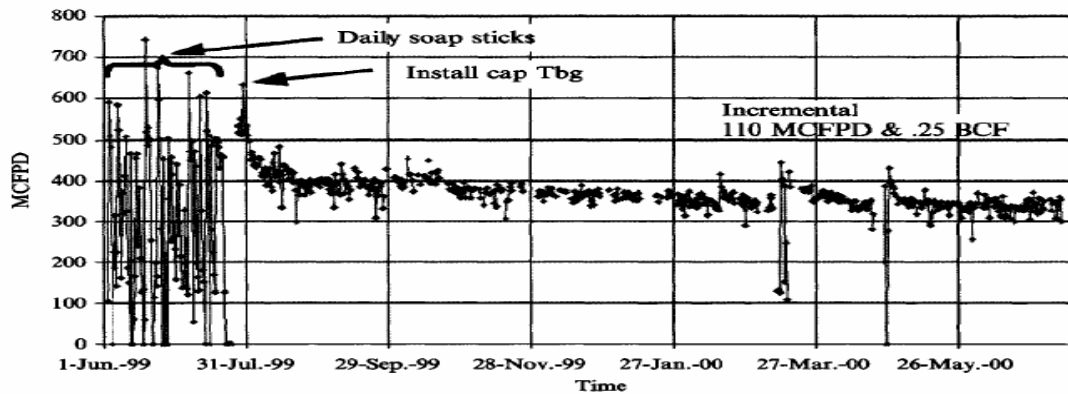
Figure 6.6 Case history 2 -3/8 inch tubing with packer injecting surfactant
with capillary tubing system to bottom of tubing[18]

6.4.5 Foam Carryover: Foam carryover into lines and separators sometimes causes

upsets and interferes with level controls. De-foamer chemicals can be effective in

suppressing the foam. When the foam is broken, the liquid phases are separated in the

production separator. If foam carryover or persistent emulsions continue with existing

separation equipment, it may be desirable to chemically treat the produced stream to

destroy the foam surfactant activity. In the scope of the thesis, it is controlled by cyclone

separator. Heating the produced foam above the cloud point (approximately 150^0F) helps

break the foam. The temperature achievement was not permissible .Earlier work at Tulsa

University suggested use of gas liquid cyclone separator(GLCC).

The gas liquid cyclone separator was able to handle the situation .It works in the

following mechanism.

The return foamed fluid through the 4" return line enters a sloped tangential inlet nozzle, to deliver the flow stream into the separator. The fluid momentum combined with the tangential inlet design generates a liquid vortex with sufficient G-forces for gas and liquid separation to rapidly occur. Finally, the gaseous component of the foam exits through the top of the GLCC and the liquid exits though the bottom of the GLCC, reducing the chance of turbulence in the tank due to reduction of gas volume fraction which debottlenecked the return tank.

The diameter of the nozzle was comparable to the diameter of the GLCC. the inclination angle was 30^0,nozzle area was 40% of the GLCC area.

At low gas flow rate, the foam tend to carryover into the gas stream at the top.

With higher gas velocities, foam breaks and a swirling liquid film tend to move up half way through the vertical length and then fall back to the liquid leg and the gas moves over to the gas leg and the gaseous foam gets to the drain. The resulting lesser gas volume then recombines with the liquid stream and returns to the return tank, from where it is pumped back to the tower system.
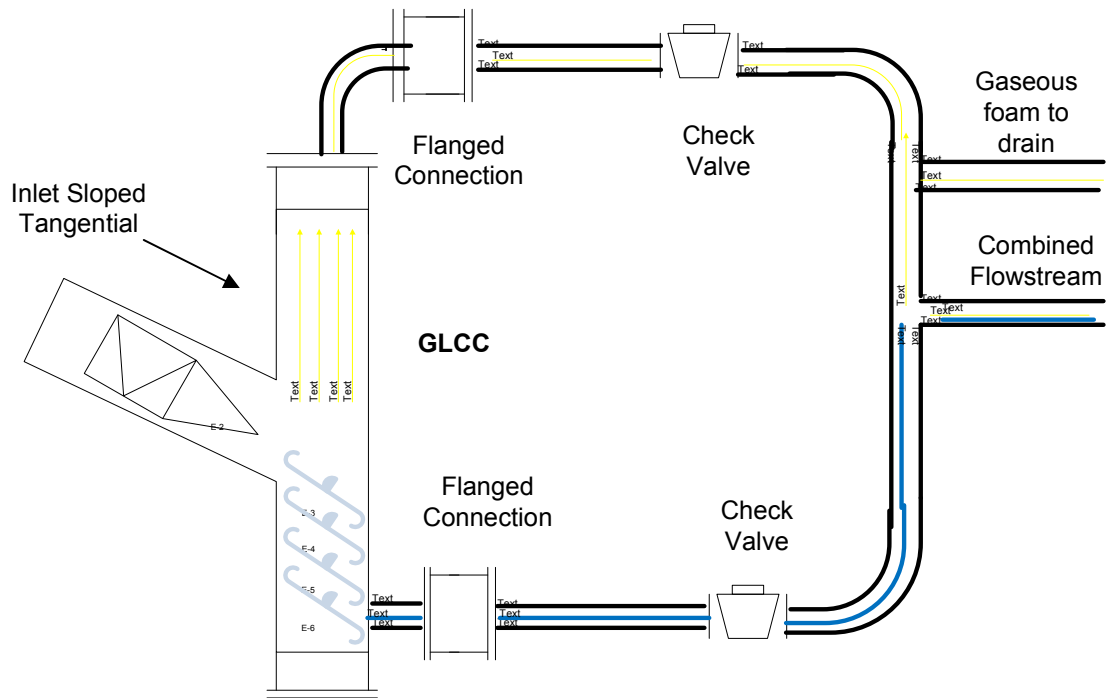
Gaseous
foam to
drain

Combined
Flowstream

Check
Valve

Check
Valve

Flanged
Connection

Flanged
Connection

GLCC

Inlet Sloped
Tangential

Figure 6.7 Gas liquid cyclone separator (GLCC)

CHAPTER VII

LIQUID UNLOADING OF NATURAL GAS WELLS BY USING AUGER TOOL

AND FOAM: TEST FACILITY AND TESTING METHODS

7.1 Use of Auger Tool in the Laboratory Facility at Texas A&M University

A laboratory test facility was created for this test bring in the required modification in the vertical loop, existing in the University Petroleum Engineering building and running all through the 10th floor to check the effectiveness of the Auger Tool in obtaining the pressure drops which culminates eventually in the desired flow regime changes at lesser natural gas flow rate.

Increase in the natural gas rate causes turbulence in the liquid film, decrease in the film thickness, development of wave at the interface and droplets are torn off the film and entrained in the natural gas. The mist regime occurs when the wavy film is completely destroyed and liquid entrainment moves with natural gas in droplets.

7.1.1 Laboratory Setup for the Test with and without Auger: The empty place inside the Richardson building of the Petroleum Engineering running all along the height of the building was being used for the test loop. The tubing string consists of PVC pipes of 10 ft joints of 2 inch diameter (upto 6th floor) and changed over to 1-1/2 inch diameter from 6th floor onwards to the 9th floor where the wellhead valve is placed. The total height of tower that was utilized was 76 ft. The PVC pipes are coupled with suitable unions and

the end bottom plug. To prevent the pressure drop and any liquid accumulation, the unions used was of the same diameter as of the pipe diameter. The tubing string is anchored through clamps and fixed supports.

The 24 inch vessel with a height of 54 ft at the 3rd floor was used as the surge vessel .The opening at the top of the surge vessel comes and joins the natural gas distribution line from the compressor. The water is being pumped through a progressive cavity pump onto the vessel and the compressor at the ground floor supplies the natural gas .The PC pump due to its rating based on RPM, can be operated at various range of liquid flow with the use of a variable frequency drive which was set at different level to vary the speed, hence the torque and alongwith that the flow rate. The compressed air comes into the 2nf floor and runs through the choke before being metered and supplied to the wellbore.

The joining point immediately after the surge vessel simulates a wellbore. All the PVC pipes used were expensive PVC transparent schedule 80 pipes so as to observe flow pattern changes and also help in proper terminal velocity determination.

To eliminate the exit effects of liquid fall back into the $2"/1\frac{1}{2}"$ loop, a bend was installed on the top of the tubing string at the 9th floor. The produced air-water mixture overflows into a 4 inch return line. One valve at the wellhead is used to close and open to control the pressure at the wellhead.

The air-water mixture comes back onto the water supplying vessel where the air is being separated and vented to the atmosphere. The water is pumped back onto the reservoir. This system provides the means for continuous testing and no loss of water happens. (Ref. Figure 7.1 and 7.2)
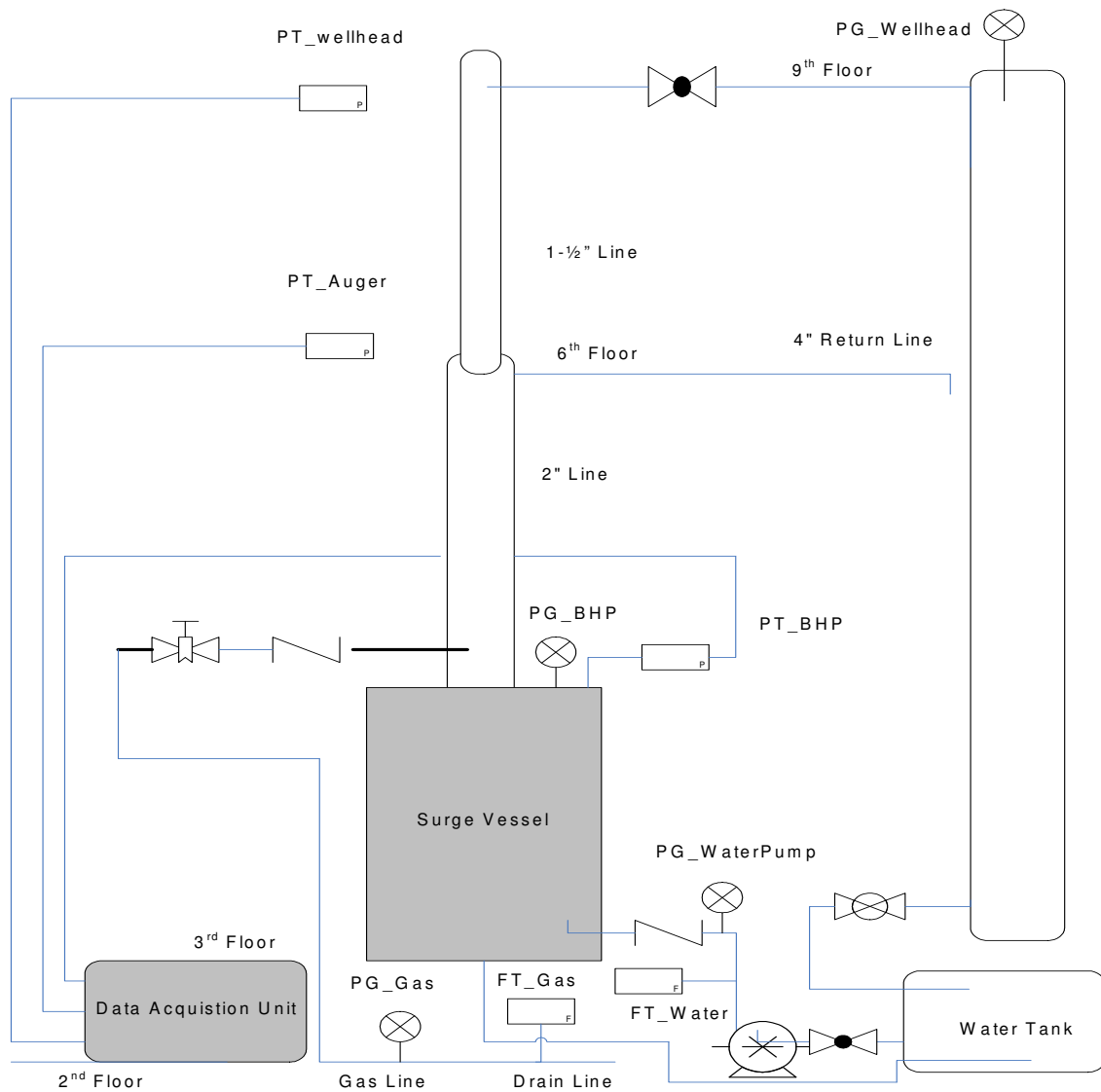

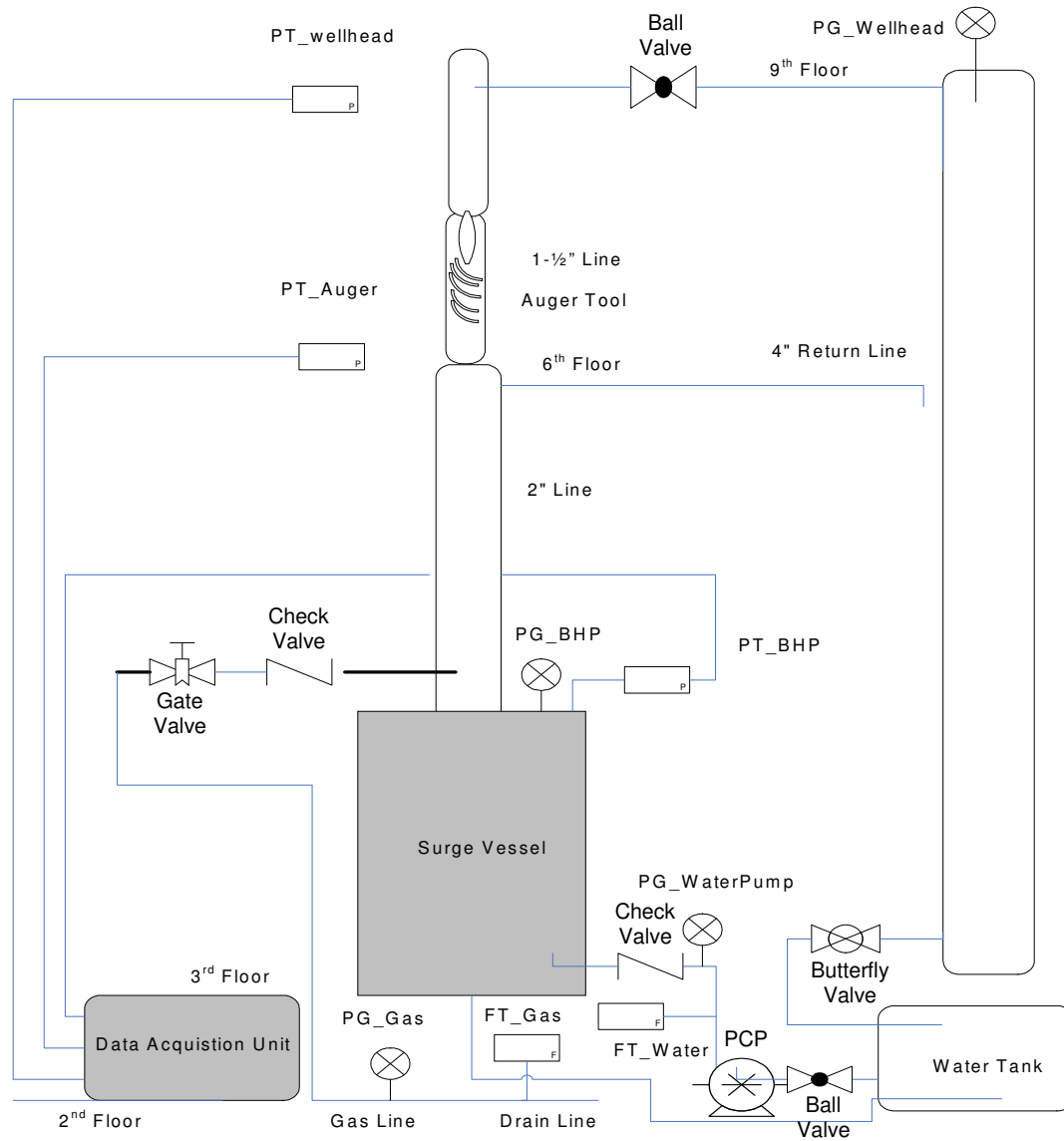**Figure 7.1** Laboratory setup without Auger

Figure 7.2 Laboratory setup with Auger

The details of the Auger Tool dimension and configuration is described below. The description would cover the angle of attack, pitch and the flange connection and casing.
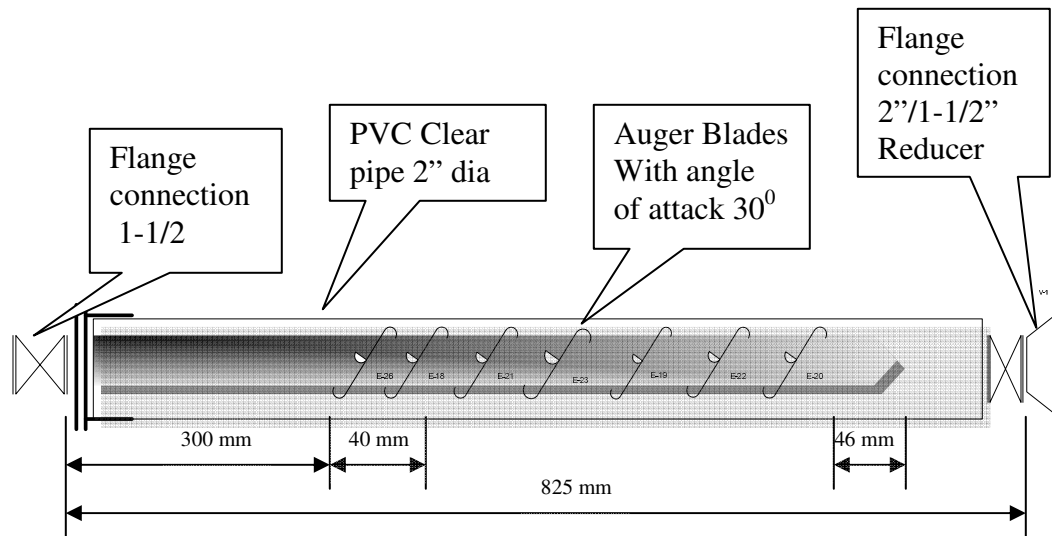
Figure 7.3 Description of the Auger Tool and its dimension.

The water metering is being carried out by the use of 2 inch Model D (Sensor model S150) Coriolis meter .The air flow rate is metered by ½ inch Elite type (sensor model CMF050) Micromotion Coriolis meter.

Analog pressure transducers were used to measure the wellhead, middle tubing and also the bottomhole pressure. The details of the Pressure sensor: Rosemount, Analog output Range: 4-20 ma, Pressure Range: 0-100 psia.

Voltage: 45 volts .The pressures are corroborated by the use of pressure gauges at every

place where the pressure transducers were used. These transducers were calibrated to measure pressures between 0 and 100 psig.

Temperature was measured from the 2nd variable from the air flowmeter: ½" Elite Type (sensor model CMF050).The error factor could be upto $\pm$ 0.5 %- $\pm$ 1% in pressure and flowmeters.

Progressive cavity pump was used for better solid handling capacity, foam handling capacity, desired pressure range and its provision of operating at a variable operating range with the use of a Variable frequency drive.

Data acquisition unit consists of a Pentium 333 MHz system equipped with a strawberry 16-channel acquisition card. Data are recorded in 8-bit blocks at 15 Hz. It receives signals from all the pressure transducers, temperature transmitters and the flowmeters on realtime and records into a predetermined excel file. The scanning rate and the loop logic was set before the tests were conducted. The physical channel from all the metering equipments come s and joins into a junction box which feeds the DAQ with all the analog signals and all the ports are designed and calibrated in DAQ to measure a particular designated variable with a preset range based on the meter range. The real time graph option was utilized for all the metering .The screen shots of the front end of DAQ and the backend logic loop is displayed. Continuous periodic screenshots were recorded during the pressure envelope test and the terminal velocity determination with all kinds of set up i.e.

tests without the Auger Tool and only with tubing, tests with the Auger Tool and also during the tests with the Auger Tool in combination with the surfactant.

Unloading can also be achieved by reducing the pressure drop in the tubing string. This would increase the value of the drag coefficient in the velocity equation, which would translate into more efficient use of the existing reservoir energy. As a result unloading would occur at lower natural gas rates.

Mingaleeva[23] studied the lowering of pressure drop in self- twisting helical flow. He observed the mechanism from an energy standpoint, and concluded that the liquids and natural gases will flow through a path of least resistance. Also the power spent to overcome the hydraulic drag for raising an air column in a helical trajectory, was compared to the motion and rising of an equivalent air mass at the same velocities by a straight column, was significantly lower. Therefore he concluded that the helical path was more favorable from an energy-use viewpoint. As a result the air column suffered a lower pressure drop when is moved in a helical path.

In the ARCO Tool there is no rotation from any parts of the Auger Tool but the fluid changes its flow pattern through the blades placed at an angle which adds to the separation efficiency and thus makes it cheap compared to any rotary equipment involved.

Displayed below are the pictures of various important equipment, pipeline, measuring instruments used during the test and described individually above.

Figure 7.4 Pressure transducer in the wellbore with the surge vessel (3rd floor)

Figure 7.5 Pressure transmitter connection at the wellbore and pressure gauge to measure the wellbore pressure

Figure 7.6 The air and water connection meeting at the wellbore (3rd floor)

Figure 7.7 Close picture of the Auger Tool with its blades (6th floor)

Figure 7.8 Pressure gauge and pressure transmitter connection at the 6th floor to measure the pressure at the middle of the tower around Auger Tool

Figure 7.9 The wellhead connections at the 9th floor with the wellhead loop and pressure transmitter

Figure 7.10 The soapstick dropping connection and 4" loop with the pressure gauge connection at the wellhead (9th floor)

Figure 7.11 Junction box connection from different test component

Figure 7.12 Junction box with instructions

Figure 7.13 Progressive cavity pump

Figure 7.14 Micromotion meter for water flow measurement

Figure 7.15 Variable frequency drive (VFD) controller to provide operability range with the pump

Figure 7.16 Covered tank used for water and foam storage during the test with water and foam

Figure 7.17 Air flow and temperature recorder Elite Type (sensor model CMF050) reading from Coriolis meter

Figure 7.18 Water flow recorder displaying the reading recorded from a Micromotion meter

Figure 7.19 Air flow measurement by Coriolis meter

7.1.2 Laboratory Setup with Foam: The same set up used for the Auger test is being used with 2 changes being brought about in the form of an arrangement with a valve to drop surfactant soapstick and a cyclone separator to effectively provide separation and retention time to effectively defoam the liquid returning from the tower. (Diagram attached).

Figure 7.20 The Auger Tool in the downhole string (6th floor)

Figure 7.21 Soapstick used for the test

Figure 7.22 Picture from inside the return tank during a foam treatment test

Figure 7.23 Setup of the cyclone separator and the buffer vessel

Figure 7.24 Elbow and the cyclone separator during foam test

Figure 7.25 Straight portion after GLCC slot

Figure 7.26 Buffer vessel and the natural gaseous foam bleeding lines

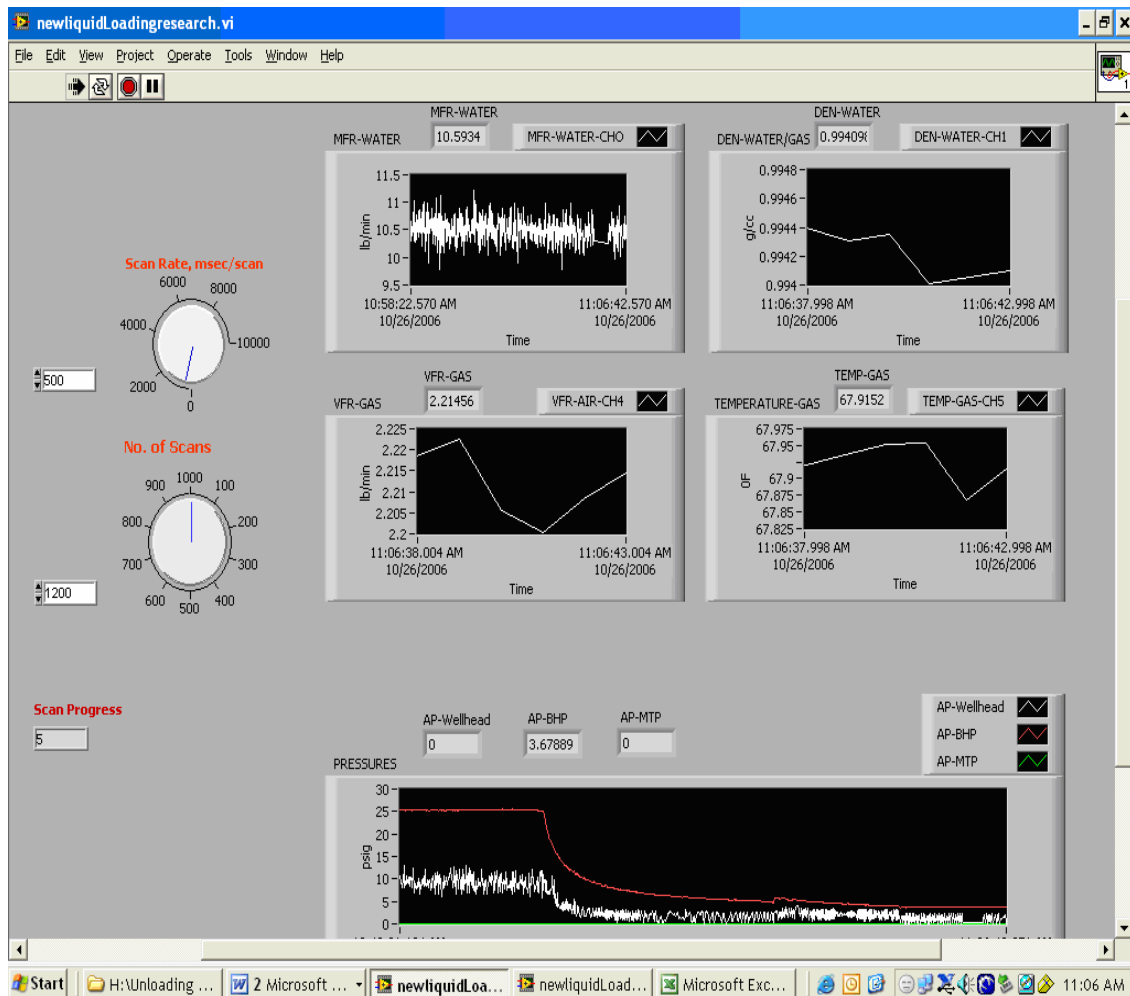**7.1.3 Data Acquisition Unit (DAQ):**

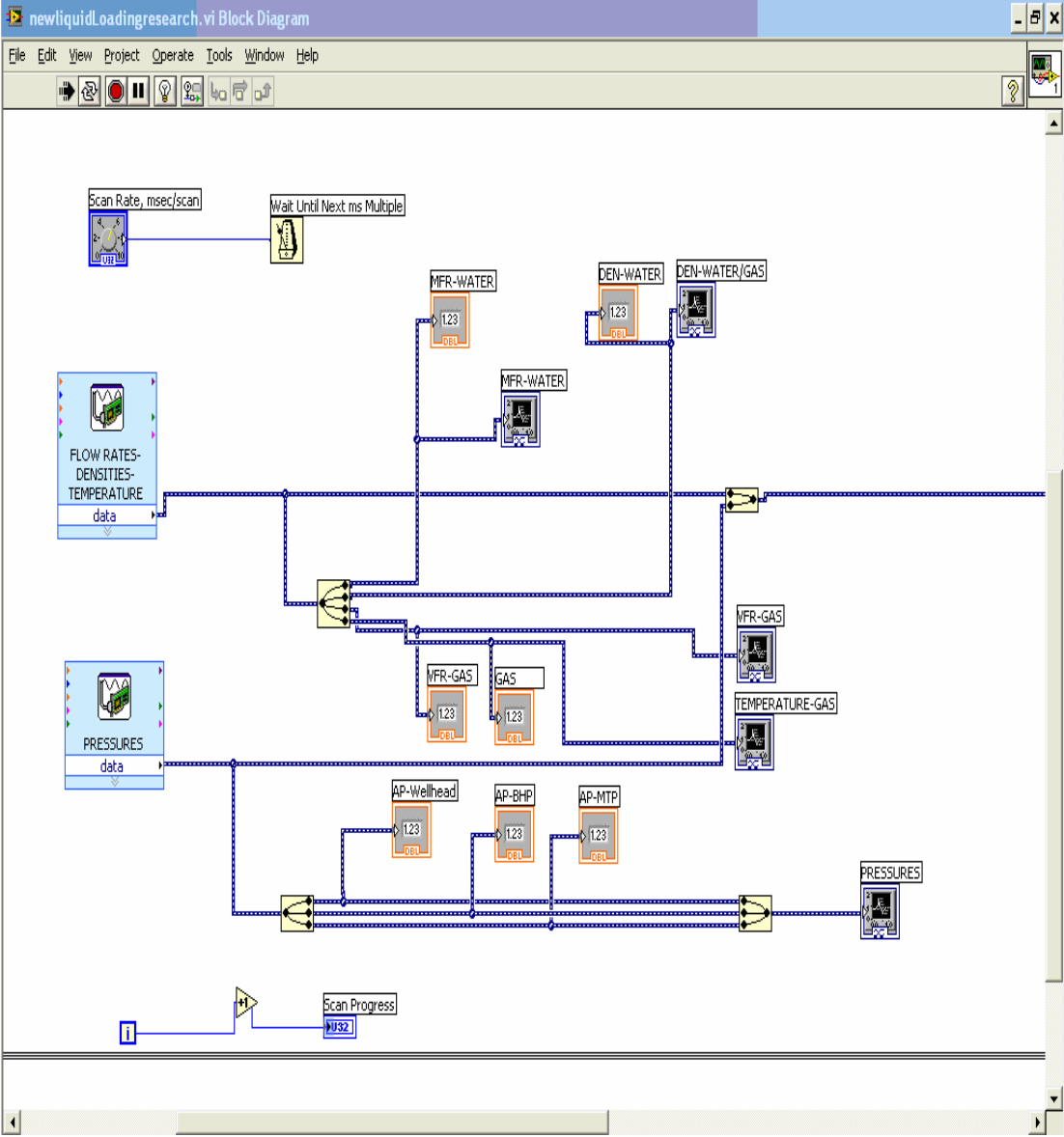**Figure 7.27** Data acquisition system (DAQ) – operations

Figure 7.28   Data acquisition system (DAQ) – block diagram

7.1.4 Determination of Operational Envelope: The well bore was made free of liquid and the wellhead valve completely open, air was passed through the flow loop until the wellhead and bottom hole pressures had stabilized, Water was then slowly introduced into the well bore, Liquid level after reaching the bottom of the surge vessel, it started flowing up the tubing string where it meets the air line. This was accompanied by an increase in the bottomhole pressure. The liquid rate was then increased until the desired bottomhole pressure was achieved. This was carried out in 15 psi, 22 psi and finally at 30 psi during this test. The flow was allowed to stabilize for 30 minutes to ensure the average bottomhole pressure was within the required range.

If the pressure exceeded the desirable pressures in each of the scenarios, then the liquid rate was decreased. Conversely, if the pressure fell below the corresponding pressure designated for the test, the liquid rate was increased. The flow was allowed to re-stabilize. The procedure was repeated until the average bottomhole pressure fell within the desired range.

Once the desired pressure had been achieved, the values for the different flow variables being fed into the NI DAQ system were recorded for 5 minutes, Simultaneous video recordings were taken for the flow visualizations at the different points along the tubing string with a high intensity digital camera. The procedure was repeated at increasing air flow rates. The air rates were fixed at an increasing increment of 4 ft^3/minute i.e. 1.5,

5.5, 9.5 .13.5 and 19 ft^3/minute.The rates were fixed to observe the pressure envelope on a comparison basis for all the tests at 15 psi, 22 psi and 30 psi bottomhole pressure.

Similar tests were conducted with placement of Auger in the middle of the tower at the 6th floor. Once the data s were recorded and the analysis made on the performance on the Auger in terms of liquid hold up, pressure loss efficiency and the critical flow rate reduction aspect, the tests were repeated with the similar objective but with the fluid changed through the induction of surfactant on the wellhead.

7.1.5 Critical Rate Determination: The determination of the critical gas rate involved determining the annular mist-flow transition. This transition is marked by an increased turbulence in the liquid film, a decrease in the film thickness and the development of waves at the natural gas/liquid interface. Droplets are torn off the film and entrained into the natural gas. Several empirical and graphical methods have been proposed to determine the flow regime changes, most of them being plotted with superficial gas versus superficial liquid velocity. However, during this lab test, "Determination of this transition point depended largely on visual observations and personal judgment." (Ref. SPE 84136).[24]

Water has been introduced into the wellbore at a low rate, after the gas pressure in the wellbore and wellhead had reached equilibrium and stable. Once the liquid level reached the bottom of the surge vessel, it was accompanied by an increase in the wellbore

pressure if the air flow rate was not sufficient to carry the liquid. If this happened, then the air rate was increased.

Once the well was continuously unloading liquids and the bottomhole and wellhead pressure had stabilized, the liquid flow pump was stopped. The flow of the liquid onto the wellhead earlier was contributed by the hydrodynamic energy of the pump and the viscous drag of the air. Once the pump was stopped, the only contributing factor for liquid removal was gas viscous drag force. At a certain air flow rate controlled by the opening and closing of the air valve , the drag force balances off the gravitational force of the liquid resulting in a near mist flow condition within the wellbore. It was tried to obtain that condition at the bottomhole since that is the place where the liquid loading is most likely to occur and if that is taken care of , the whole column will be in mist flow condition and liquid will be removed continuously in that flow regime.

Once the liquid had been removed of the bottomhole and the only liquid in the tubing was the wavy film, the wellhead valve was closed slightly to cause liquid fallback. Once this happened, the wellhead choke was reopened slowly until the liquid started to rise. The wellhead pressure and the air rates were recorded during all times of the terminal velocity determination. These conditions were maintained until the flow loop was completely dry, usually approximately one hour, to ensure that the correct critical gas rate had been determined. The procedure was repeated at different air rates.

CHAPTER VIII

LIQUID UNLOADING OF NATURAL GAS WELLS BY USING AUGER TOOL

AND FOAM: RESULTS AND DISCUSSION

This chapter details the results obtained from all the different tests conducted with changed fluid medium and well completion sequence. The tabular results of the test data and the related calculations of all the governing criteria i.e. pressure loss in the tubing, liquid hold up, liquid unloading ability and efficiency , are displayed in Appendix A though F.

Each of the deciding parameters and the corresponding observation obtained during the tests with various combinations are combined in single graph and sequenced for the three pressure regimes 30 psi, 22 psi and 15 psi; under consideration.

The normal flow pattern that was observed without the use of the Tool or the foam system was the bubble flow at the intersection of the natural gas and water meeting point right near the wellbore at the 3rd floor, a slug flow at some distance away from the wellbore up the vertical tower and the 4 inch return line showing an annular flow. The primary objective of the test was to check the effectiveness of the Auger Tool and the surfactant to change the flow pattern gradually to the ideal mist flow condition.

Operational envelope is determined by measuring the liquid flow versus natural gas flow at the no backpressure being maintained at the wellhead.

8.1 Operational Envelopes

While testing with the four different scenarios involving the test with only tubing, with tubing and Auger, Auger and foam combined and only foam with water, the following observations were made. The greatest operational envelope was observed with only the tubing as the downhole completion and water being the only fluid. The next largest operational envelope which could be extended to all 5 sequential air flow rate to the battery limit was with foam and only tubing. The Auger when placed in the tubing string could provide slightly lower envelope than the foam and tubing combination. The lowest operational envelope, which however was more efficient in other respect, was with Auger and foam combination. This trend was observed with all the pressure regimes 30 psi, 22 psi and 15 psi. Ref. Figure 8.1a to 8.1c.

The trend that was observed during determination of operational envelope was that the increase in gas flow caused the decrease in liquid handling capacity, in all the pressure regimes. This observation was different from that of intermittent liquid production scenario, where the liquid unloading is a direct function of gas rate increase.

This contrasting behavior finds explanation in the fixed chamber volume of the wellbore .When the pressure in the wellbore is achieved to be constant, the gas pressure and the hydrostatic components balance each other to account for the constant pressure at the wellbore. Lower gas rates would result in higher hydrostatic head and thus more fluid handling and vice versa.
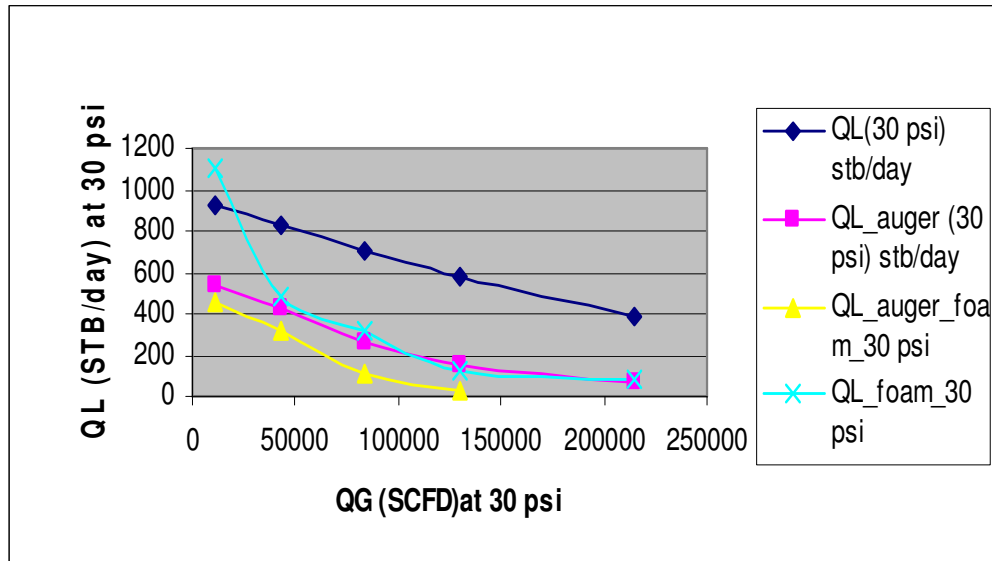
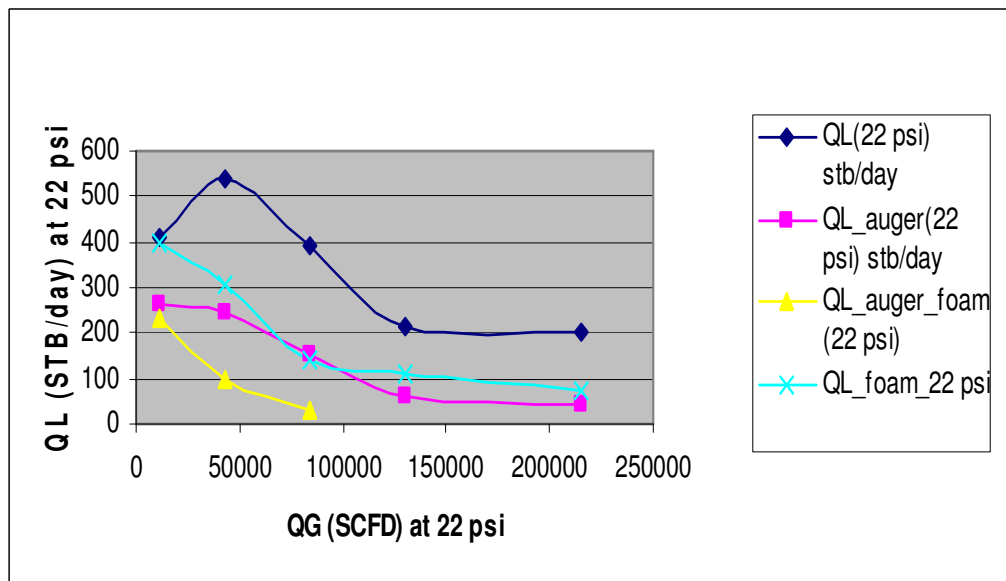**Figure 8.1a** Air flow rate versus liquid flow rate at 30 psi

Figure 8.1b Air flow rate versus liquid flow rate at 22 psi
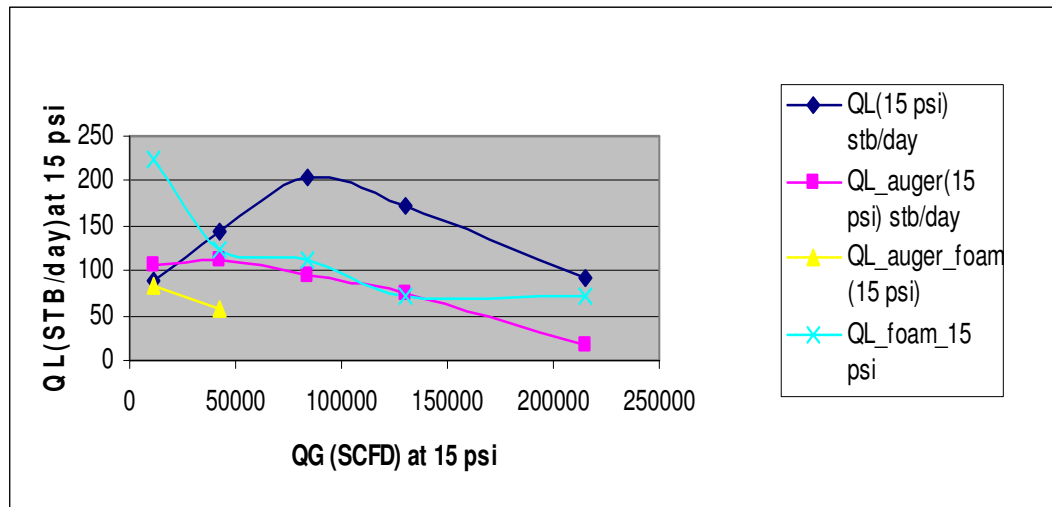
Figure 8.1c Air flow rate versus liquid flow rate with air-foam at 15 psi

8.2 Liquid Holdup

The liquid hold up trend was also observed with all the combinations: test with only

tubing, with tubing and Auger, Auger and foam combined and only foam with water.

For the pressure regimes of 30 psi and 22 psi wellbore pressure, the largest liquid

hold up was with only tubing followed by the tubing with foam combination which

was greatly reduced with the incorporation of the Auger Tool which suggested that

the Auger Tool reduced the liquid hold up but the best result was with the

combination of the Auger and the foam. The results have been slightly erratic with

lower pressures regime due to instability of the foam, where the foam looses its

stability with higher gas volume fraction. (Figure 8.2a through c)

The liquid hold up is displayed with varying gas flow rates. Liquid hold up at all the tested pressure regimes, after a declining trend evens out to take a linear trend. This trend was associated with increase in gas rates and suggested a possible flow pattern change from slug flow to transition and eventually to annular mist flow regimes.

In low gas flow,the flow regime was observed predominantly in the slug flow regime .Increase in the gas flow rate changes the flow pattern to churn and subsequently to annular flow. The slug pattern resulted in lot of gas slippage , which reduces with increase in gas rate and corresponding gas velocity. The resulting insitu gas and liquid velocities becoming the same during annular-mist flow pattern causes the hold up to be linear with increasing gas velocities .
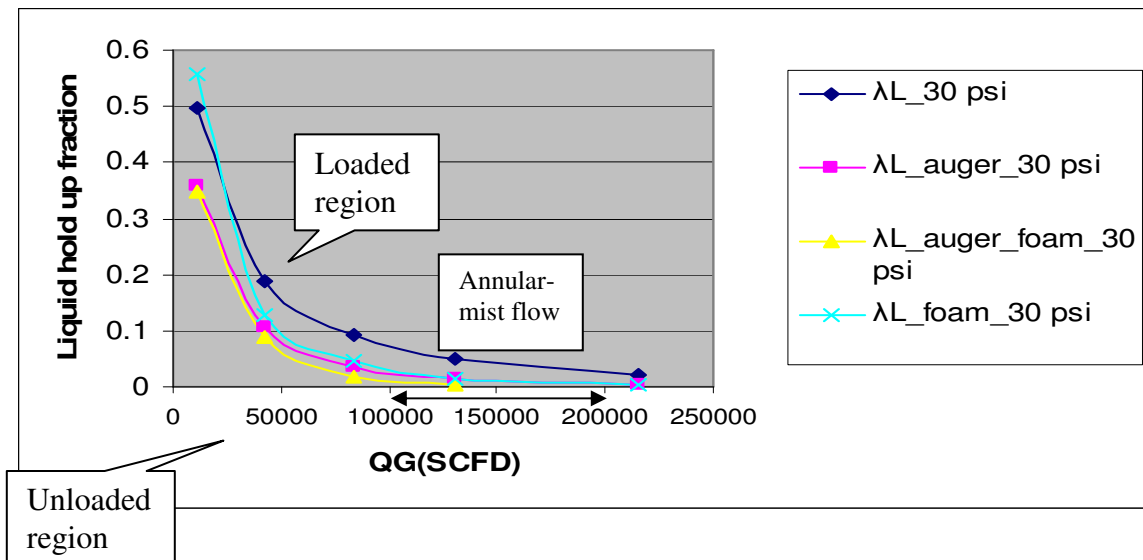

Figure 8.2a Liquid holdup through the tubing at 30 psi with and without Auger (air-water) and with and without Auger (air-foam)
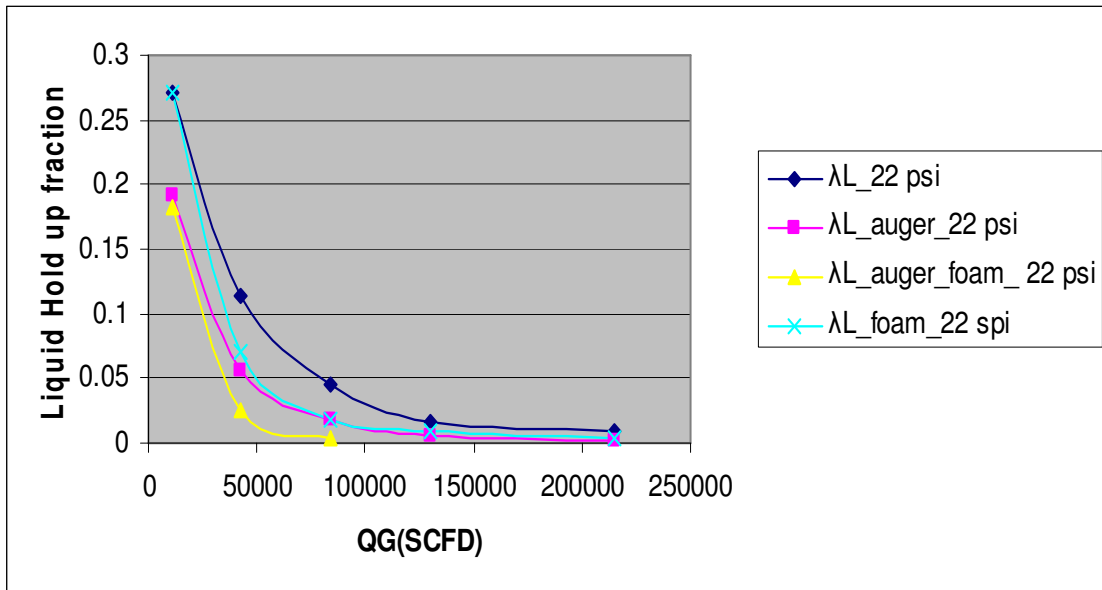
Figure 8.2b Liquid holdup through the tubing at 22 psi with and without Auger
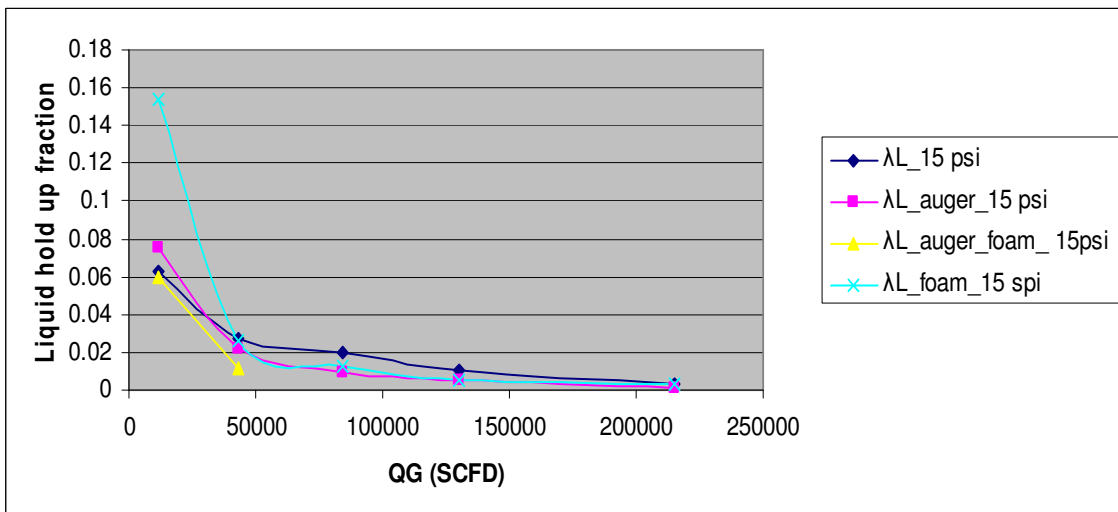(air-water) and with and without Auger (air-foam)

Figure 8.2c Liquid holdup through the tubing at 15 psi with and without Auger
(air-water) and with and without Auger (air-foam)

8.3 Pressure Drop through the Tubing String

The pressure drop which was quite higher with only tubing in the string and water being lifted, has been gradually reduced with insertion of Auger Tool. For the pressure regimes 30 psi and 22 psi, the tubing suffered the greatest pressure loss followed by foam being used as a fluid with tubing as completion, but with the Auger Tool in place it reduced by quite an extent and further reduced by using of foam in combination with the tubing. In the testing of 15 psi, the foam and only water both suffered similar pressure loss whereas the situation improved with Auger Tool and greatly improved with Auger and foam combination. (Figure 8.3a to c)

The pressure loss through the tubing is a prime concern to achieve the liquid unloading. The faster reserve depletion caused by higher pressure loss greatly reduces the marginal economics of the low pressure, low flowing wells. It is significant in more than one way. The reduction in pressure loss causes the increase in the drag coefficient which in turn causes the lower minimum terminal velocity and thus reduces the critical flow rate requirement.[25]
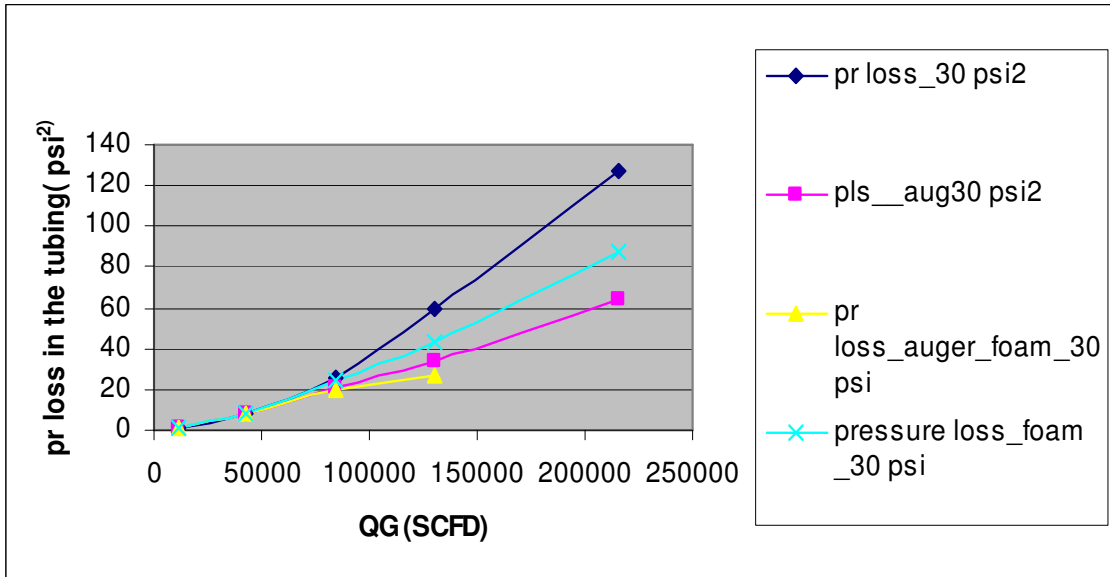
Figure 8.3a Pressure loss through the tubing at 30 psi with and without Auger
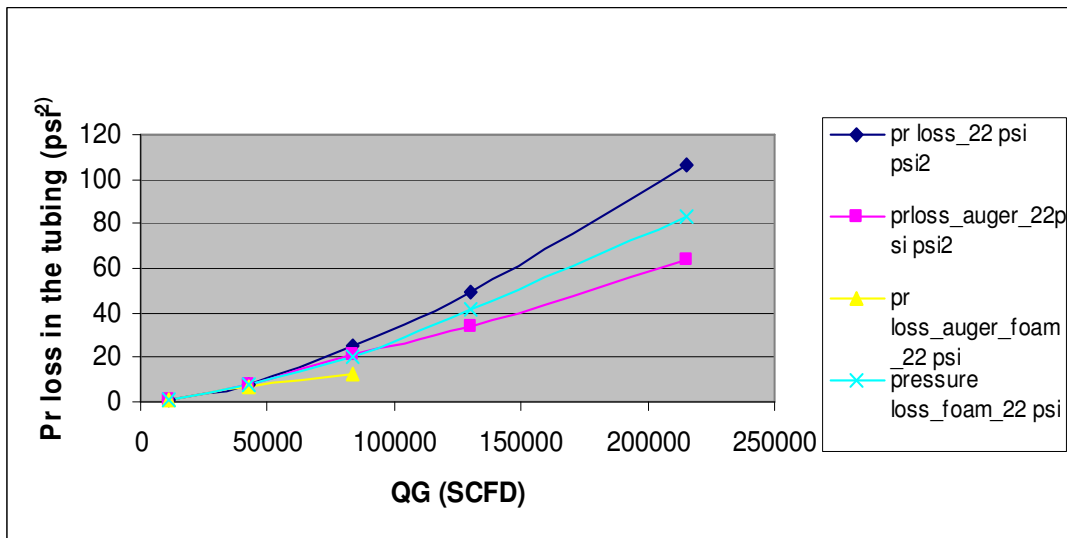(air-water) and with and without Auger (air-foam)

Figure 8.3b Pressure loss through the tubing at 22 psi with and without Auger
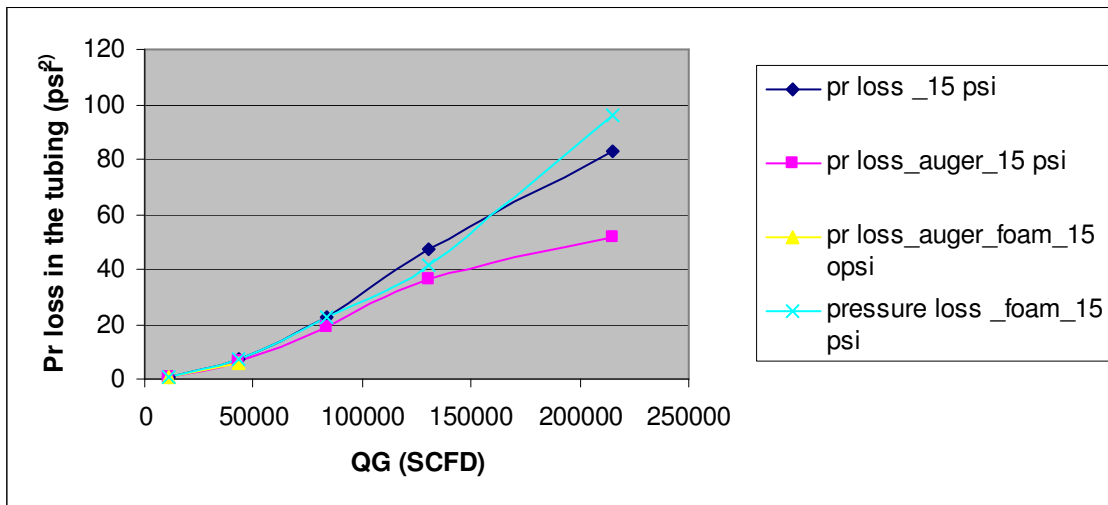(air-water) and with and without Auger (air-foam)

Figure 8.3c Pressure loss through the tubing at 15 psi with and without Auger (air-water) and with and without Auger (air-foam)

8.4 Wellhead Backpressure Analysis

The back pressure analysis was carried out to see the liquid unloading performance vis.a. vis the pressure loss through the tubing. This was to quantify the improvement observed by the addition of flow modifying device and also using of foam as a carrier fluid. The trend shows that the increase in liquid unloading was earlier associated with a higher pressure loss when only tubing was used. The most efficient system that emerged was the Auger and the foam combination which has the similar or higher unloading in all the pressure regimes but underwent a much less pressure loss thus reducing the terminal velocity requirement due to the change in the drag coefficient. (Figure 8.4a to c)
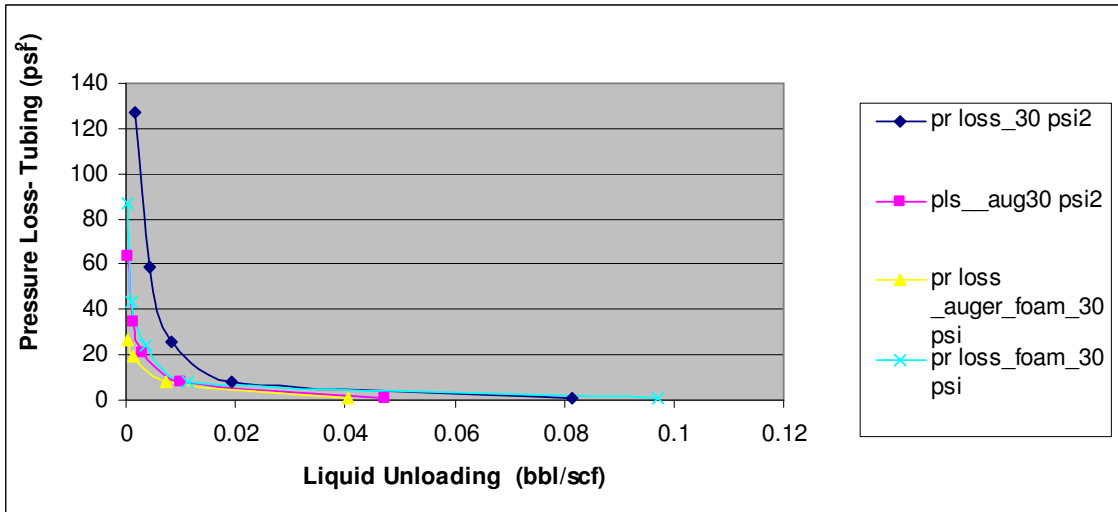
Figure 8.4a Liquid unloading ability versus pressure loss through the tubing at 30 psi with and without Auger (air-water) and with and without Auger (air-foam)

Figure 8.4b Liquid unloading ability versus pressure loss through the tubing at 22 psi with and without Auger (air-water) and with and without Auger (air-foam)

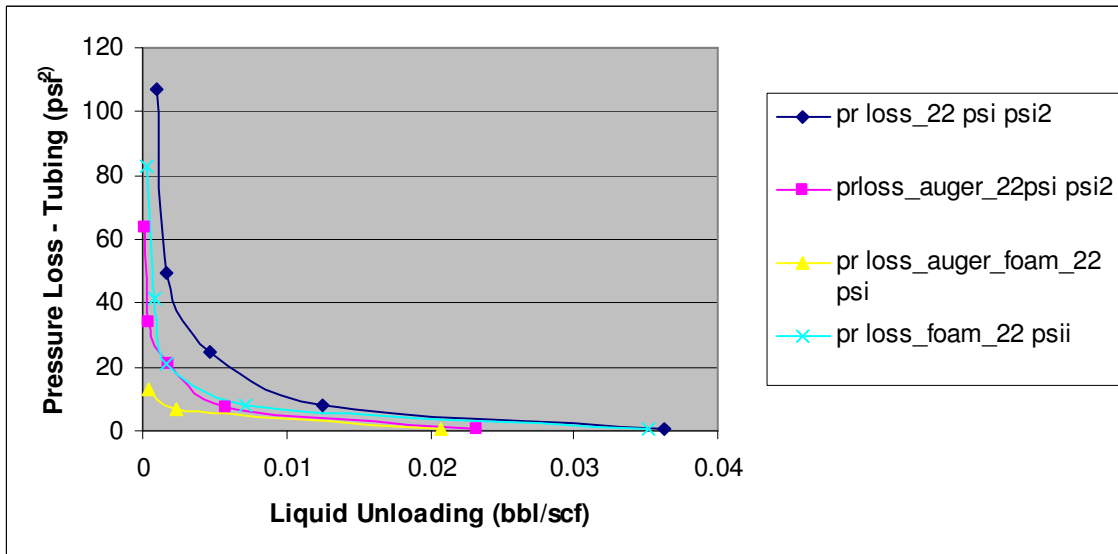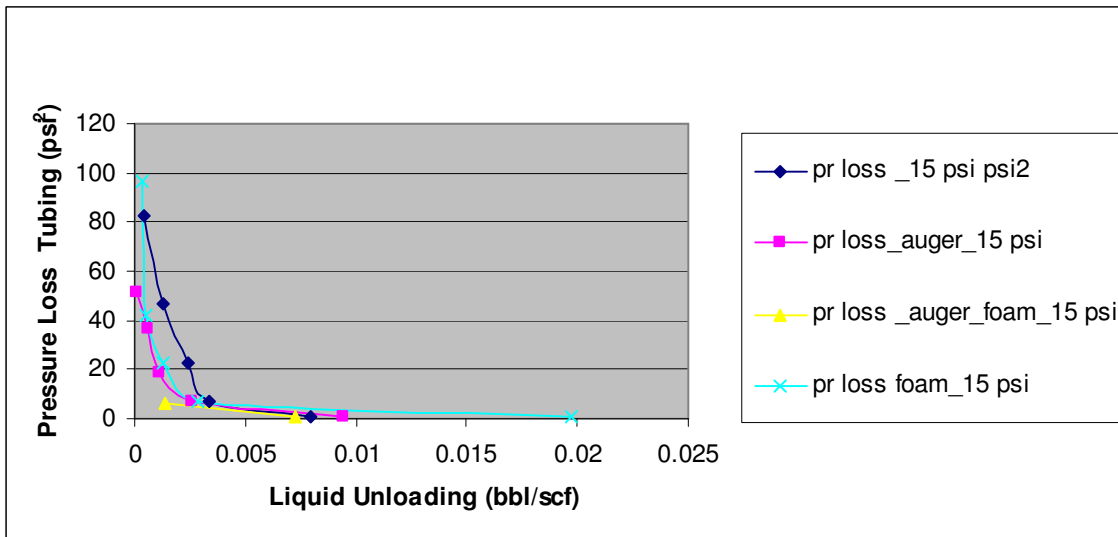**Figure 8.4c** Liquid unloading ability versus pressure loss through the tubing at
15 psi with and without Auger (air-water) and with and without Auger (air-foam)

8.5 Terminal Velocity

The critical rates of the gas with and without flow modifying Tools were observed
.Although it was a mere visual observation in absence of high performance camera,
effort has been put to have a close look at the transition of flow from slug flow and
annular flow in the tubing and also at the wellbore to the mist flow which is the desirable
flow conditions. Observing the changing in gas flow which marked the onset of mist
flow thus making the wellbore free of liquid , was considered a flowrate corresponding
to the critical flowrate.The highest terminal velocity was with only tubing trying to
unload water followed by the terminal velocity with only foam and tubing combination.
The terminal velocity required for continuous unloading of water was reduced with

inclusion of Auger Tool in the middle of the downhole string with air-water system which however was the lowest when the surfactant foam in the form of soapsticks was introduced. The terminal velocity observation when tabulated showed the consistency with the other determining parameters discussed earlier in this chapter.

Table 8.1 Terminal Velocity

Tubing

	M_G	Q_G	P_{WH}	P_{WH}
	lb/min	MSCFD	psig	psia.
1	6.25	117.94	0.64	15.336
2	8	150.9632	24	38.696
3	10.2	192.4781	37	51.696

Foam

	M_G	Q_G	P_{WH}	P_{WH}
	lb/min	MSCFD	psig	psia
1	4.872134	91.9391	1.6	16.296
2	7.9806	150.5971	27	41.696
3	8.862434	167.2376	40	54.696

Auger and Foam

	M_G	Q_G	P_{WH}	P_{WH}
	lb/min	MSCFD	psig	psia
1	4.384921	82.74519	1.7	16.4
2	6.78351	128.0075	30	44.7
3	7.151984	134.9608	42	56.7

Auger

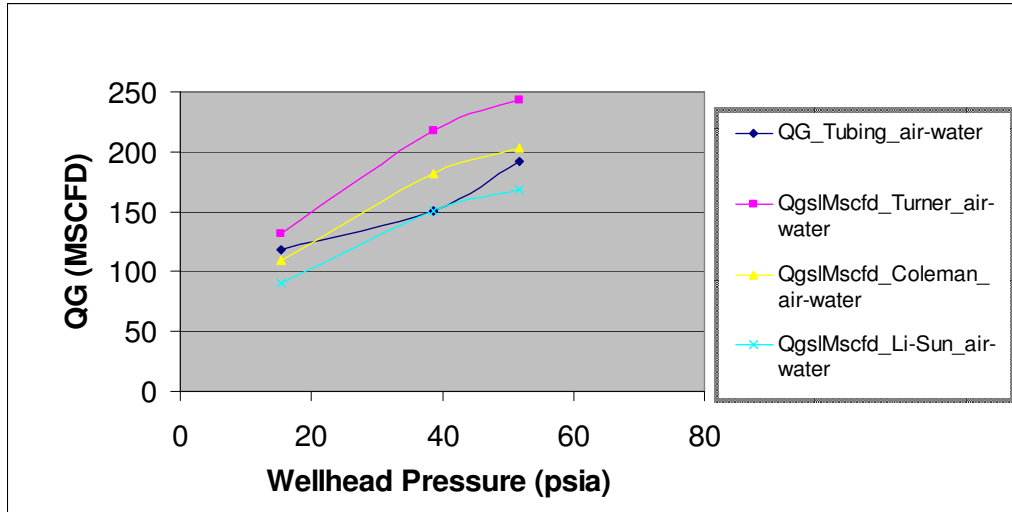|	M_G	Q_G	P_{WH}	P_{WH}
	lb/min	MSCFD	psig	psia
1	4.604167	86.88245	1.9	16.6
2	7.258355	136.968	36	50.7
3	7.795663	147.1073	46	60.7

Tubing_air-water

Figure 8.5a Comparison of terminal velocities tubing_air-water
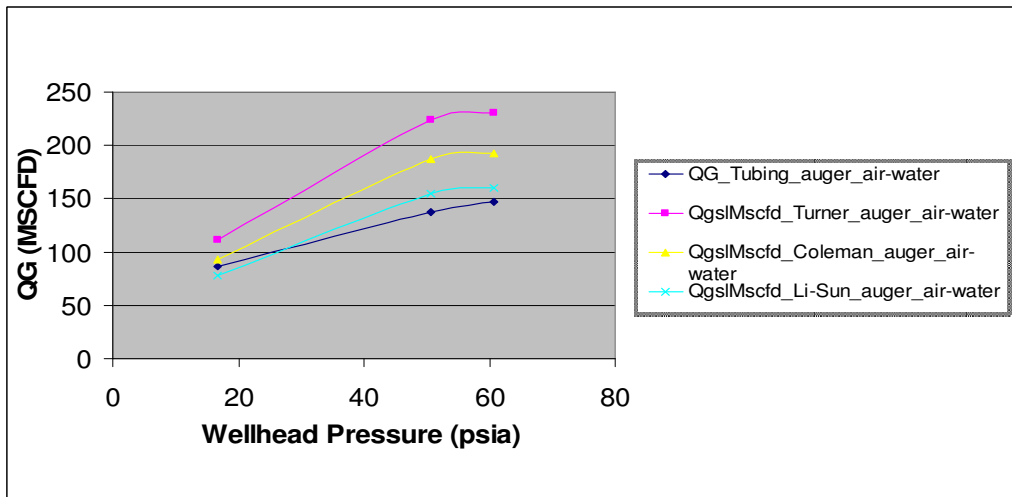
Tubing_Auger_air-water

Figure 8.5.b Comparison of terminal velocities tubing_Auger_air-water
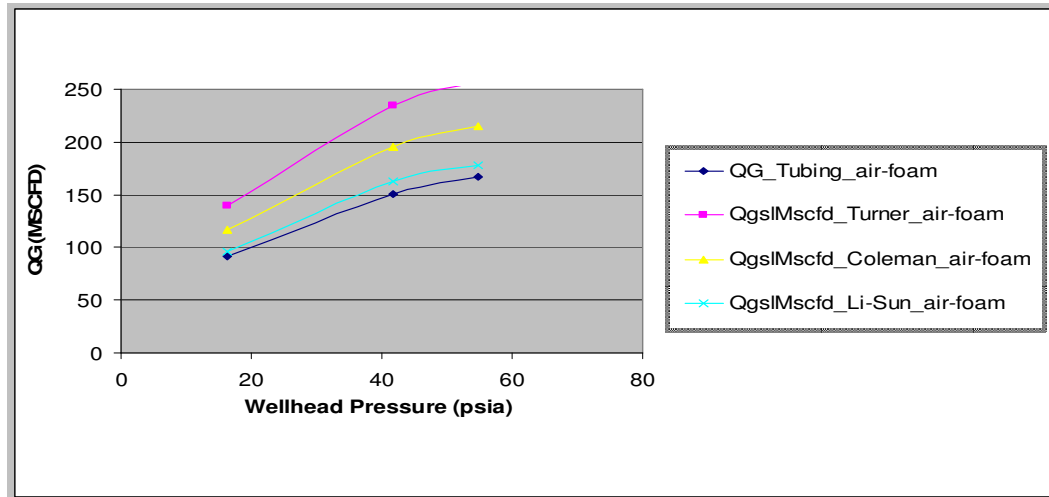
Tubing_air-foam

Figure 8.5c Comparison of terminal velocities tubing_air-foam

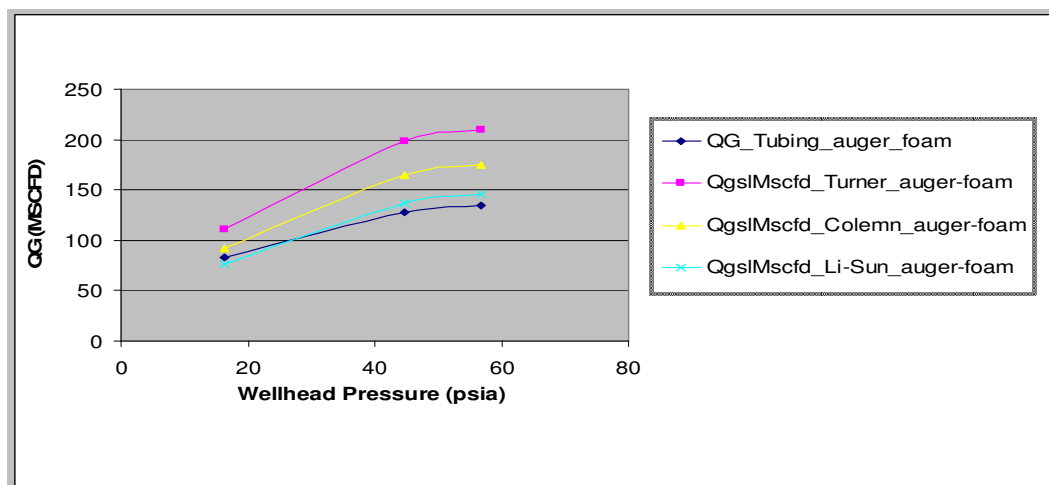**Tubing_Auger_air-foam**

Figure 8.5d Comparison of terminal velocities tubing_Auger_air-foam

CHAPTER IX

CONCLUSIONS AND RECOMMENDATIONS

The prediction of liquid loading by Turner flow rate corresponding to terminal velocity was found wanting in real BP well example. The actual well names which can be referred to master table, are not disclosed due to confidentiality. The wells tended to show signs of liquid loading even if the predicted Turner[2] critical flowrate exceeding was achieved. This had necessitated considering B.Guo's model as an alternative model of predicting flowrate. If found successful, it was to be considered for inclusion in DSS upcoming releases and also include it in the engineering workflows.(Ref. Chapter I-IV)

Results displaying the values and the percentage difference between the minimum flowrate predicted by the 4 phase model and Turner model are in Table J.4.1.

In Field1, well 4,5,7,13,20 and Field 2 well1and 2 justified claim of B.Guo. Most of the other wells deviated by 5-6% which proves that the arbitrary 20% adjustment is close enough.

The claim of B.Guo[1] of Turner flow rate underprediction was found true around 40% wells and 20% more wells was very close by 5-6%. Needs more data to conclude on the applicability range of the model.

The results of the tests carried out in the laboratory (Ref. Chapter V-VIII) have shown

the effectiveness of the flow modifying Auger Tool. It was quantified in terms of resulting lower pressure drop, lower liquid hold up, terminal velocity reduction, and also the liquid unloading ability.

Introducing the Auger Tool into the wellbore could bring in the above features but the best performance in the context of all the above parameters came with the Auger Tool used in combination with the surfactant foam. Lower pressure drop would account for higher recovery from the wells. The only point of concern with the use of Auger Tool was reduction of the operating envelope i.e. less quantity of water handling ability observed in both the forms of fluid system air-water and air-foam.

However, when compared the pressure loss associated with the higher quantity of liquid unloading without Auger, the Auger Tool provides the merit.

The position of the Auger Tool plays a major role in determining the performance of the Tool. The previous works by a similar Tool placed at the wellbore was able to increase the operating envelope. There has been literature reviews suggesting the same. In this particular test ideology, it was felt that the pressure drop which was found to be more prominent from the middle of the tubing string, would be lessened by the introduction of the Auger Tool at the middle. The basic flow modifying design would take care of the pressure drop.

The two basic phenomenons that were observed in all he cases studied that, the performance and the stability of the tests were increasingly better in the higher pressure envelope. The tests could not be extended further into the higher regime due to operational constraints.

All the performance at almost all the pressure regimes showed consistency in the results of the defining parameters and that was reflected in the critical flow rate observation also.

Lots of fluctuations were encountered in the low pressure regime without the Auger Tool which was much more stabilized with the inclusion of Auger Tool in the wellbore.

Liquid unloading ability increases at lower gas flow rates which fulfill the objective of the low flow, low pressure natural gas wells under consideration. However, for wider acceptance of the Tool, the flow envelope should be enhanced to meet the high flow requirements. Literature review suggests that the requisite change could be brought about by the changes in designs in blade angle, angular spacing and frequency of occurrence of the blades.

A significant improvement was contributed by the foam also. The combination worked well in contrasting ways. Where the pressure drop caused by the Auger was owing to flow modification by the helical twisting, the foam resulted in reduced pressure gradient.

The foam also contributed in reducing surface tension. The reduction in pressure drop in the tubing increased the drag coefficient which all in combination contributed to reducing the required minimum terminal velocity and thus the minimum flow rate.

The slower response time of the pressure transducers were detrimental to the critical needs of pressure measurement.

The surface tension values were obtained only from literature. The viscocity of the foam which affects the shear rate, if measured, would give a better indication of the results. The results when compared with the terminal velocity calculation by Turner et al. showed slight departure in some cases higher or lower. This might be owing to the surface tension values considered and in calculation of the exact foam density measurement. The variation of the drag coefficient with pressure drop, if obtained by a laboratory test, can be used to more accurately determine the terminal velocity. The temperature measurement is considered average in the absence of the any wellhead temperature measuring device.

Insertion of the Tool was very time consuming and work intensive. Methodology like insert tubing Tool or sidepocket mandrel is suggested for easier operability. Foam is now being inserted manually after every certain duration. An automated injection based on the ppm measurement suggested by the literature and operational websites will be a more suited adoption to achieve the otherwise encouraging results.

NOMENCLATURE

A	=	Cross-sectional Area of the Pipe, ft^2
B_G	=	Formation Volume Factor for the Gas , ft^3/SCF
B_L	=	Formation Volume Factor for the Liquid,ft^3/SCF
ρ_G	=	Gas Density , lbm/ft^3
ρ_L	=	Liquid Density , lbm/ft^3
C_1	=	Constant,25
C_2	=	Constan,0.0375
D	=	Diameter of the Pipe, in.
TVD	=	True Vertical Depth,ft
MD	=	Measured Depth,ft
f	=	Friction Factor, in.
GLR	=	Gas Liquid Ratio, SCF/STB
γ_m	=	Specific Gravity of Air-Water Mixture
γ_G	=	Natural Gas Gravity,(air=1)
γ_L	=	Liquid Gravity(water=1)
λ_L	=	No Slip Liquid Holdup
λ_G	=	No-Slip Gas Holdup
M_{AIR}	=	Molecular Weight of Air
M_G	=	Natural Gas Mass Rate, lb/minute
M_L	=	Liquid Mass Rate,lb/minute
η	=	Efficiency , fraction
P_{AVG}	=	Average Pressure, psia.
P_{PC}	=	Pseudocritical Pressure,psia
P_{PR}	=	Pseudoreduced Pressure, fraction
P_{SC}	=	Pressure, 14.69 psia.
P_{WF}	=	Flowing Bottomhole Pressure,psig
P_{WH}	=	Wellhead Pressure,psig
P_{PR}	=	Pseudoreduced Pressure, fraction
ΔP	=	Pressure difference,psi
$(p_{wf}^2-p_{wh}^2 e^s)_{Auger}$	=	Pressure Loss with Auger,$psia^2$
$(p_{wf}^2-p_{wh}^2 e^s)_{only\ tubing}$	=	Pressure Loss without Auger , $psia^2$
T_{AVG}	=	Temperature Average within the Wellbore System,^0R
T	=	Temperature ^0R
Tsc	=	520^0R
T_{PR}	=	Pseudoreduced Temperature, fraction
T_{PC}	=	Pseudocritical Temperature,^0R
Q_G	=	Volumetric Gas Flow Rate, SCFD
Q_L	=	Volumetric Liquid Flow Rate,SCFD
q_G	=	Gas Flow Rate,ft^3/day
q_L	=	Liquid Flow Rate, ft^3/day
q_{sc}	=	Flow Rate , MMSCFD

R	=	Gas/Liquid Ratio, Scf/Stb
S	=	Static Gas Column Constant
σ	=	Surface Tension of Liquid to Gas, dyne/cm
v_t	=	Terminal Gas Velocity For Settling,ft/s
v_{SL}	=	Superficial Liquid Velocity , ft/s
v_{SG}	=	Superficial Gas Velocity , ft/sec
Z	=	Compressibility Factor at T_{AVG} and P_{AVG}
v_{gc}	=	Critical Gas Velocity, ft/sec.
q_c	=	Critical Gas Flow Rate, MMscf/day
ρ_l	=	Density of Liquid, lbm/ft^3
ρ_g	=	Density of Gas, lbm/ft^3
γ_g	=	Gas Gravity (air = 1)
μ_g	=	Viscosity of Gas, lbm/ft/sec
C_d	=	Drag coefficient (dimensionless)
p	=	Pressure, psia
z	=	Gas Compressibility Factor, dimensionless

REFERENCES

1. Guo, B., Ghalambor, A., and Xu, C.: "A Systematic Approach to Predicting Liquid Loading in Gas Wells," paper SPE 94081 presented at the SPE Production Operations Symposium, Oklahoma City, Oklahoma, (16-19 April 2005).

2. Turner, R.G., Hubbard, M.G and Dukler, A.E.: "Analysis and Prediction of Minimum Flowrate for Continuous Removal of Liquids from Natural Gas Wells," *Journal of Petroleum Technology* (November 1969), 1475-82.

3. Coleman, S.B., Clay, H.B., McCurdy, D.G., and Norris III, L.H.: "A New Look at Predicting Natural Gas Well Liquid Loadup," *Journal of Petroleum Technology,* (March 1991), 329-332.

4. Li, M., Li, S.L., and Sun, L.T.: "New View on Continuous Removal of Liquids from Natural Gas Wells," *SPE Production and Facilities*, (February 2002), 42-46.

5. Dousi, N., Veeken, C.A.M., and Currie, P.K.: "Modeling the Natural Gas Well Liquid Loading Process," paper SPE 95282 presented at the Offshore Europe, Aberdeen, United Kingdom, (6-9 September 2005).

6. Kumar, N.: "Improvements for Flow Correlations for Natural Gas Wells Experiencing Liquid Loading," paper SPE 92049 presented at the SPE Western Regional Meeting, Irvine, California (March 30 - April 01 2005).

7. James, F.L., Nickens, H.V.: "Solving Gas-Well Liquid-Loading Problems," paper SPE 72092, *Journal of Petroleum Technology*, Vol. 56, No. 4, (April 2004), 30-36.

8. Jelinek, W., Wintershall., and Schramm, L.L.: "Improved Production from Mature Natural Gas Wells by Introducing Surfactants into Wells," paper SPE 11028 presented at the International Petroleum Technology Conference, Doha, Qatar (21-23 November 2005).

9. Lea, J.F., and Tighe, R.E.: "Natural Gas Well Operation with Liquid Production," paper SPE 11583 presented at the 1983 Production Operation Symposium, Oklahoma City, Oklahoma, (February 27- March 1, 1983).

10. Gilbert, W.E.: "Flowing and Natural Gas-Lift Well Performance," presented at the spring meeting of the Pacific Coast District, Division of Production, Los Angeles, (May 1954) Drilling and Production Practice, 126-157.

11. Nosseir, M.A., Darwish, T.A., Sayyouh, M.H., and El Sallaly, M.:"A New Approach for Accurate Prediction of Loading in Natural Gas Wells under Different Flowing Conditions," *SPE Production and Facilities*, (November 2000), 241-246.

12. Dake, L.P.: *Fundamentals of Reservoir Engineering*, Elsevier Scientific Publ. Co., Amsterdam, Netherlands, (1978), Chapter. 1.

13. Weingarten, J.S., Kolpak, M.M., Mattison, S.A., and Williamson, M.J.: "Development and Testing of a Compact Liquid-Natural Gas Auger Partial Separator for Downhole or Surface Applications," paper SPE 30637, *SPE Production and Facilities,* Vol. 12, No. 1,(February 1997), 34-40.

14. Weingarten, J.S.: "Field Results of Separation-Vessel and Multiphase- Flowline Debottlenecking Using an In-line Natural Gas/Liquid Auger Separator," paper

SPE 65072, *SPE Production and Facilities,* Vol.15, No. 3, (August 2000), 196-200.

15. Vortex Tools, http://www.vortexTools.com/HTML/howitworks.php, Accessed April 5, 2007.

16. Vortex Flow LLC, Internet Homepage: http:/www.vortexflowllc.com, Accessed April 5, 2007.

17. IIobi, M.I. and Ikoku, C.U.: "Minimum Natural Gas Flow Rate for Continuous Liquid Removal in Natural Gas Wells," paper SPE 10170 presented at the SPE Annual Technical Conference and Exhibition, San Antonio, Texas, (4-7 October 1981).

18. Campbell, S., Ramachandran, S., and Bartrip, K., "Corrosion Inhibition/Foamer Combination Treatment to Enhance Natural Gas Production," paper SPE 67325 presented at the SPE Production and Operations Symposium, Oklahoma City, Oklahoma,(March 24-27, 2001).

19. Letz, R.S., "Capillary Strings to Inject Surfactants," SWPSC School on De-Watering Natural Gas Wells, Lubbock, Texas, (April 24, 2001).

20. Libson, T.N., and Henry, J.R., "Case Histories: Identification of and Remedial Action for Liquid Loading in Gas Wells. Intermediate Shelf Gas Play," paper SPE 7467 presented at 53rd Annual Fall Meeting of SPE of AIME, Houston, Texas, (October 1-3, 1978).

21. Vosika, J.L.: "Use of Foaming Agents to Alleviate Liquid Loading in Greater Green River TFG Wells," paper SPE 11644 presented at the SPE/DOE Low

Permeability Natural Gas Reservoirs Symposium, Denver, Colorado (14-16 March 1983).

22. Scott, S.L., Wu, Y., and Bridges, T.J.: "Air Foam Improves Efficiency of Completion and Workover Operations in Low Pressure Natural Gas Wells," paper SPE 27922, *SPE Drilling & Completion* ,Vol. 10, No. 4, (December 1995), 219-225.

23. Mingaleeva, G.R.: "On the Mechanism of a Helical Motion of Fluids in Regions of Sharp Path Bending," *Technical Physics Letters*, (March 2002), 657-659.

24. Ali, A.J., Scott, S.L., and Fehn, B.: "Investigation of New Tool to Unload Liquids from Stripper-Natural gas Wells," paper SPE 84136 presented at the SPE Annual Technical Conference and Exhibition, Denver, Colorado, (October 5-8, 2003).

25. Brill, J.P., and Beggs, H.D.: "Two Phase Flow in Pipes," Sixth Edition, University of Tulsa , Tulsa, Oklahoma (January 1991).

26. Standing, M.B., and Katz, D.L.: "Density of Natural Gases," *Petroleum Transactions, AIME*, Vol. 146, (1942), 140-149.

27. Cullender, M.H., and Smith, R.V.: "Practical Solution of Natural Gas Flow Equations for Wells and Pipelines with Large Temperature Gradients," *Petroleum Transactions, AIME*, Vol. 207, (1956) , 281-287.

28. Gray, H. E., *Vertical Flow Correlation in Natural Gas Wells.* User Manual for API 14B Subsurface Control Safety Valve Sizing Computer Program, App. B., (June 1974).

29. Rawlins, E.L., and Schellhardt, A.A.: *Back Pressure Data on Natural Gas Wells and Their Applications to Production Practices*, Bureau of Mines Monograph 7, Bartlesville, Oklahoma, 1935.

30. Neely, A.B.: "The Effect of Compressor Installation on Natural Gas Well Performance," HAP Report 65-1, (January 1965).

31. Fetkovich, M.J.: "The Isochronal Testing of Oil Wells," paper SPE 4529, 48th Annual Fall Meeting of SPE, Las Vegas, Nevada, 1973.

32. Russell, D.G., Goodrich, J.H., Perry, G.E., and Bruskotter, J.F.: "Methods for Predicting Natural Gas Well Performance," paper SPE 1242, *Journal of Petroleum Technology*, (January 1966), 99-108.

33. Thrasher, T.S., "Well Performance Monitoring: Case Histories," paper SPE 26181 presented at the SPE Natural gas Technology Symposium, Calgary, Alberta, Canada,(June 28-30, 1993).

APPENDIX A

TABLES OF RESULTS AIR-WATER SYSTEM, ONLY TUBING

FLUID SYSTEM	WELLBORE CONFIGURATION
AIR-WATER SYSTEM	COMBINATION OF 2 IN AND 1-1/2" TUBING ONLY

Table A.1 Summary of Data without Auger Tool (air-water)

Test without Auger

Pressure envelope test results				
30 psig				
No	Water rate(lb/min)	Gas rate (ft3/minute)	Pwf	Pwh
1	224	1.5	30	5.5
2	200	5.5	30	11.5
3	170	9.5	30	13.2
4	140	13.5	30	15
5	94	19	30	15
22 psig			Pwf	Pwh
1	100	1.5	21	4.6
2	131	5.5	21	4.8
3	96	9.5	22	8.5
4	52	13.5	22	10
5	48.5	19	22.5	10.3
15 psig			Pwf	Pwh
1	22	1.5	14	1.3
2	35	5.5	13.7	2
3	49.4	9.5	14.1	3
4	42	13.5	14.3	4
5	22.5	19	15	5.4

Table A.2 Calculation without Auger Tool (air-water)

(a) 15 Psi without Auger

M_L	ρ_L	Q_L	M_G	Q_G	p_{WF}	p_{WH}	Δp	GLR	T	q_G	Pavg
lb/min	lb/ft³	stb/day	lb/min	scf/day	psig	psig	psig	scf/stb	deg F	ft³/day	psia
22	62.415	90.398	0.6	11322.24	14	1.3	12.7	125.24877	76	7640.51301	22.34
35	62.415	143.815	2.27	42835.8	13.7	2	11.7	297.8535	74	28906.6075	22.54
49.4	62.415	202.9846	4.45	83973.27	14.1	3	11.1	413.6928	72	56667.1381	23.24
42	62.415	172.578	6.9	130205.7	14.3	4	10.3	754.47473	72	87865.8996	23.84
22.5	62.415	92.4525	11.4	215122.5	15	5.4	9.6	2326.8438	70	145169.747	24.89

C_1	C_2	C_3	B_L	q_L ft³/day	γ_g	λ_L	λ_m
1.0008356	8.53624E-07	-9.39928E-12	1.000855	508.0186	1	1	3.778292
1.0004536	8.59247E-07	-1.02561E-11	1.000473	807.9032	1	1	3.440786
1.0000784	8.64907E-07	-1.11243E-11	1.000098	1139.871	1	1	3.256795
1.0000784	8.64907E-07	-1.11243E-11	1.000099	969.1214	1	1	2.847162
0.99971	8.70603E-07	-1.2004E-11	0.999732	518.9815	1	1	2.005263

T_{PC} (°R)	P_{PC} (psia)	P_{PR}	T_{PR}	a	b	c	d	Z	B_G
238.69	546.9	0.040848	2.237211	0.688905	0.0043253	0.0200937	1.3412121	0.998933	0.6748236

v_{sL} ft/sec	area ft²	v_{sG} ft/sec	λ_L	f	Pressure Loss (psia²)	s
0.354913225	0.016566993	5.337834	0.062345	0.018	0.708371	3.40497E-06
0.564419337		20.19481	0.027189	0.014	7.181854	4.43839E-05
0.796339404		39.58894	0.019719	0.012	22.3932	0.000161446
0.677050047		61.3851	0.010909	0.012	47.07114	0.000339333
0.362572155		101.4189	0.003562	0.011	82.96689	0.000652374

(b) 22 Psi without Auger

M_L	ρ_L	Q_L	M_G	Q_G	p_{WF}	p_{WH}	Δp	GLR	T	q_G	Pavg
lb/min	lb/ft³	stb/day	lb/min	scf/day	psig	psig	psig	scf/stb	deg F	ft³/day	psia
100	62.415	410.9	0.6	11322.24	21	4.6	16.4	27.554729	76	6206.39743	27.496
131	62.415	538.279	2.27	42835.8	21	4.8	16.2	79.57918	74	23480.8703	27.596
96	62.415	394.464	4.45	83973.27	22	8.5	13.5	212.87942	72	46030.781	29.946
52	62.415	213.668	6.9	130205.7	22	10	12	609.38343	72	71373.5705	30.696
48.5	62.415	199.2865	11.4	215122.5	22.5	10.3	12.2	1079.4636	70	117921.551	31.096

C_1	C_2	C_3	B_L	q_L ft^3/day	γ_g	λ_L	λ_m
1.0008356	8.53624E-07	-9.39928E-12	1.000859	2309.186	1	1	4.014198
1.0004536	8.59247E-07	-1.02561E-11	1.000477	3023.879	1	1	3.883802
1.0000784	8.64907E-07	-1.11243E-11	1.000104	2215.146	1	1	3.596043
1.0000784	8.64907E-07	-1.11243E-11	1.000105	1199.872	1	1	3.001866
0.99971	8.70603E-07	-1.2004E-11	0.999737	1118.699	1	1	2.5746

T_{PC} (^{0}R)	P_{PC} (psia)	P_{PR}	T_{PR}	a	b	c	d	Z	B_G
238.69	546.9	0.050276	2.237211	0.688905	0.0053288	0.0200937	1.34121	0.998711	0.5481

v_{sL} ft/sec	area ft^2	v_{sG} ft/sec	λ_L	f	Pressure Loss (psia^2)	s
1.613249021	0.016566993	4.335929	0.271172	0.018	0.752445	3.61838E-05
2.112550114		16.40426	0.114088	0.014	8.106595	0.000501096
1.547551131		32.15814	0.045914	0.012	24.74037	0.001783024
0.838257406		49.86318	0.016533	0.012	49.69823	0.003578507
0.781548644		82.38265	0.009398	0.011	106.9118	0.008377836

(c) 30 Psi without Auger

M_L	ρ_L	Q_L	M_G	Q_G	p_{WF}	p_{WH}	Δp	GLR	T	q_G	P_{avg}
lb/min	lb/ft^3	stb/day	lb/min	scf/day	psig	psig	psig	scf/stb	deg F	ft^3/day	psia
224	62.415	920.416	0.6	11322.24	30	5.5	24.5	12.301218	76	5258.93367	32.443
200	62.415	821.8	2.27	42835.8	30	11.5	18.5	52.124363	74	19896.2991	35.443
170	62.415	698.53	4.45	83973.27	30	13.2	16.8	120.21426	72	39003.7581	36.293
140	62.415	575.26	6.9	130205.7	30	15	15	226.34242	72	60477.7372	37.193
94	62.415	386.246	11.4	215122.5	30	15	15	556.95729	70	99919.7398	37.193

C_1	C_2	C_3	B_L	q_L ft^3/day	γ_g	λ_L	λ_m
1.0008356	8.53624E-07	-9.39928E-12	1.000863	5172.597	1	1	4.054696
1.0004536	8.59247E-07	-1.02561E-11	1.000484	4616.641	1	1	3.951177
1.0000784	8.64907E-07	-1.11243E-11	1.00011	3922.677	1	1	3.789543
1.0000784	8.64907E-07	-1.11243E-11	1.000111	3230.442	1	1	3.570141
0.99971	8.70603E-07	-1.2004E-11	0.999742	2168.213	1	1	3.064338

T_{PC} (^{0}R)	P_{PC} (psia)	P_{PR}	T_{PR}	a	b	c	d	Z	B_G
238.69	546.9	0.059321631	2.237211	0.688905	0.0062934	0.02009375	1.34121217	0.998503	0.4644783

v_{sL} ft/sec	area ft^2	v_{sG} ft/sec	λ_L	f	Pressure Loss (psia^2)	s
3.613693043	0.016566993	3.67401	0.495862	0.018	0.759878	3.65564E-05
3.22528907		13.9	0.188335	0.014	8.245546	0.000509895
2.740470157		27.2489	0.091381	0.012	26.06746	0.001879358
2.256859531		42.25111	0.050707	0.012	59.11421	0.00425683
1.514762108		69.80618	0.021239	0.011	127.3236	0.009973535

APPENDIX B

TABLES OF RESULTS AIR-WATER SYSTEM, TUBING WITH AUGER

FLUID SYSTEM	WELLBORE CONFIGURATION
AIR-WATER	COMBINATION TUBING 2 IN AND 1-1/2 IN WITH AUGER TOOL

Table B.1 Summary of Data with Auger (air-water)

Test with Auger

Pressure envelope test results					
30 psig					
No	Water rate(lb/min)	Gas rate(ft^3/minute)	P_{wf}	P_{middle}	P_{wh}
1	130	1.5	30	18.06	4
2	104	5.5	30	21.2	5.678
3	63	9.5	30	23.8	6.45
4	37	13.5	30	23.94	4.8
5	16	19	30	26	3.93
22 psig			P_{wf}	P_{middle}	P_{wh}
1	64	1.5	23	10.5	2.4
2	60	5.5	22	13.6	3
3	37	9.5	22	15.9	3.5
4	15	13.5	22	17.2	3
5	10	19	22.5	21.37	3.7
15 psig			P_{wf}	P_{middle}	P_{wh}
1	26	1.5	14	6.58	2.88
2	27	5.5	14.1	6.3	2.73
3	23	9.5	14.1	8.43	2.69
4	18.33	13.5	14.3	8.68	2.31
5	4	19	15	9	2

Table B.2 Calculation with Auger (air-water)

(a)15 Psi with Auger

M_L	ρ_L	Q_L	M_G	Q_G	p_{WF}	p_{WH}	Δp	GLR	T	q_G	Pavg
lb/min	lb/ft³	stb/day	lb/min	scf/day	psig	psig	psig	scf/stb	deg F	ft³/day	psia
26	62.415	106.834	0.6	11322.24	14	2.88	11.12	105.97973	76	7379.29864	23.13
27	62.415	110.943	2.27	42835.8	14.1	2.73	11.37	386.10639	74	27918.3465	23.105
23	62.415	94.507	4.45	83973.27	14.1	2.69	11.41	888.54018	72	54729.7983	23.085
18.33	62.415	75.31797	6.9	130205.7	14.3	2.31	11.99	1728.7473	72	84861.9344	22.995
4	62.415	16.436	11.4	215122.5	15	2	13	13088.496	70	1402006.674	23.19

C_1	C_2	C_3	B_L	q_L ft³/day	γ_g	λ_L	λ_m
1.0008356	8.59247E-07	-1.02561E-11	1.000855	600.3861	1	1	3.821853
1.0004536	8.64907E-07	-1.11243E-11	1.000474	623.24	1	1	3.298049
1.0000784	8.64907E-07	-1.11243E-11	1.000098	530.709	1	1	2.724052
1.0000784	8.70603E-07	-1.2004E-11	1.000098	422.952	1	1	2.216097
0.99971	0.000001093	-5E-11	0.999735	92.26371	1	1	1.244028

T_{PC} (°R)	P_{PC} (psia)	P_{PR}	T_{PR}	a	b	c	d	Z	B_G
238.69	546.9	0.042293	2.237211	0.688905	0.004479	0.0200937	1.3412127	0.998899	0.6517526

v_{sL} ft/sec	area ft²	v_{sG} ft/sec	λ_L	f	Pressure Loss (psia²)	s
0.419443239	0.016566993	5.155344	0.075239	0.018	0.716513	3.44435E-06
		19.50439	0.021836	0.014	6.883678	4.25441E-05
		38.23547	0.009604	0.012	18.72925	0.000135041
		59.28646	0.004959	0.012	36.63531	0.00026413
		97.95154	0.000658	0.011	51.46297	0.000404735

(b) 22 Psi with Auger

M_L	ρ_L	Q_L	M_G	Q_G	p_{WF}	p_{WH}	Δp	GLR	T	q_G	P_{avg}
lb/min	lb/ft³	stb/day	lb/min	scf/day	psig	psig	psig	scf/stb	deg F	ft³/day	psia
64	62.415	262.976	0.6	11322.24	23	2.4	20.6	43.054264	76	6230.44447	27.39
60	62.415	246.54	2.27	42835.8	22	3	19	173.74788	74	23571.8483	27.19
37	62.415	152.033	4.45	83973.27	22	3.5	18.5	552.33579	72	46209.1298	27.44
15	62.415	61.635	6.9	130205.7	22	3	19	2112.5292	72	71650.1114	27.19
10	62.415	41.09	11.4	215122.5	22.5	3.7	18.8	5235.3986	70	118378.445	27.79

C_2	C_3	B_L	q_L ft³ /day	γ_g	λ_L	λ_m
8.59247E-07	-1.02561E-11	1.000859	1477.879	1	1	3.974133
8.64907E-07	-1.11243E-11	1.000477	1384.983	1	1	3.674383
8.64907E-07	-1.11243E-11	1.000102	853.7525	1	1	3.070033
8.70603E-07	-1.2004E-11	1.000102	346.1158	1	1	2.071849
0.000001093	-5E-11	0.99974	230.6604	1	1	1.54542

T_{PC} (°R)	P_{PC} (psia)	P_{PR}	T_{PR}	a	b	c	d	Z	B_G
238.69	546.9	0.050082	2.237211	0.688905	0.0053081	0.0200937	1.34121217	0.998715	0.5502838

v_{sL} ft/sec	area ft²	v_{sG} ft/sec	λ_L	f	Pressure Loss (psia²)	s
1.032479438	0.016566993	4.352729	0.191725	0.018	0.744926	3.58224E-06
			0.055495	0.014	7.667773	4.74074E-05
			0.018141	0.012	21.10436	0.000152221
			0.004807	0.012	34.24412	0.000246983
			0.001945	0.011	63.92239	0.000502883

(c) 30 Psi with Auger

M_L	ρ_L	Q_L	M_G	Q_G	p_{WF}	p_{WH}	Δp	GLR	T	q_G	P_{avg}
lb/min	lb/ft³	stb/day	lb/min	scf/day	psig	psig	psig	scf/stb	deg F	ft³/day	psia
130	62.415	534.17	0.6	11322.24	30	4	26	21.195946	76	5383.0419	31.696
104	62.415	427.336	2.27	42835.8	30	5.678	24.322	100.23916	74	20365.8419	32.535
63	62.415	258.867	4.45	83973.27	30	6.45	23.55	324.38769	72	39924.2275	32.921
37	62.415	152.033	6.9	130205.7	30	4.8	25.2	856.43077	72	61904.9819	32.096
16	62.415	65.744	11.4	215122.5	30	3.93	26.07	3272.1241	70	102277.796	31.661

C_1	C_2	C_3	B_L	q_L ft^3/day	γ_g	λ_L	λ_m
1.0008356	8.59247E-07	-1.02561E-11	1.000863	3001.952	1	1	4.030949
1.0004536	8.64907E-07	-1.11243E-11	1.000482	2400.648	1	1	3.835096
1.0000784	8.64907E-07	-1.11243E-11	1.000107	1453.694	1	1	3.396041
1.0000784	8.70603E-07	-1.2004E-11	1.000106	853.7561	1	1	2.752019
0.99971	0.000001093	-5E-11	0.999745	369.0583	1	1	1.789056

T_{PC} (^{0}R)	P_{PC} (psia)	P_{PR}	T_{PR}	a	b	c	d	Z	B_G
238.69	546.9	0.057956	2.237211	0.688905	0.0061476	0.0200937	1.34121217	0.998534	0.4754397

v_{sL} ft/sec	area ft^2	v_{sG} ft/sec	λ_L	f	Pressure Loss (psia^2)	s
2.097231606	0.016566993	3.760714	0.358015	0.018	0.755438	3.63412E-06
1.677146438		14.22804	0.105447	0.014	8.001707	4.949E-05
1.01558304		27.89196	0.035132	0.012	23.34139	0.000168416
0.596453215		43.24821	0.013604	0.012	45.47975	0.000328125
0.257832413		71.45357	0.003595	0.011	73.98928	0.000582268

APPENDIX C

TABLES OF RESULTS AIR-FOAM SYSTEM, TUBING WITH AUGER

FLUID SYSTEM	WELLBORE CONFIGURATION
AIR-FOAM	COMBINATION TUBING 2 IN AND 1-1/2 IN WITH AUGER TOOL

Table C.1 Summary of Data with Auger (air-foam)

No	Water rate(lb/min)	Gas rate(ft³/minute)	P_{wf}	P_{middle}	$P_{wh\_after\ foam}$
	30 psig				
1	78	1.5	30	18.385	11.068
2	53	5.5	30	21.803	12.1742
3	19	9.5	30	26	16
4	5	13.5	30	28	21
5		19			
	22 psig		Pwf	Pmiddle	Pwh
1	40	1.5	23	14.552	7.5128
2	17	5.5	22	16	7.87
3	5.02	9.5	22	19	11
4		13.5			
5		19			
	15 psig		Pwf	Pmiddle	Pwh
1	14	1.5	14	9	3.27
2	10	5.5	14.1	9.45	3.48
3		9.5			
4		13.5			
5		19			

Table C.2 Calculation Auger and Foam-Air

(a) 30 Psi with Auger and foam

M_L	ρ_L	Q_L	M_G	Q_G	p_{WF}	p_{WH}	Δp	GLR	T	q_G	P_{avg}
lb/min	lb/ft³	stb/day	lb/min	scf/day	psig	psig	psig	scf/stb	degF	ft³/day	psia
78	43.6905	457.86	0.6	11322.24	30	11.068	18.932	24.728603	76	4842.76112	35.227
53	43.6905	311.11	2.27	42835.8	30	12.1742	17.8258	137.687	74	18321.7796	35.7801
19	43.6905	111.53	4.45	83973.27	30	16	14	752.92089	72	35917.145	37.693
5	43.6905	29.35	6.9	130205.7	30	21	9	4436.3114	72	55691.7529	40.193

Continued

C₁	C₂	C₃	B_L	q_L ft³/day	γ_g	λ_L	λ_m
1.0008356	8.53624E-07	-9.39928E-12	1.000866	2573.109	1	1	4.02162
1.0004536	8.59247E-07	-1.02561E-11	1.000484	1747.729	1	1	3.750881
1.0000784	8.64907E-07	-1.11243E-11	1.000111	626.3105	1	1	2.848692
1.0000784	8.64907E-07	-1.11243E-11	1.000113	164.8189	1	1	1.623818

T_{PC} (⁰R)	P_{PC} (psia)	P_{PR}	T_{PR}	a	b	c	d	Z	B_G
238.69	546.9	0.0644 12141	2.237211	0.688905	0.006837	0.02009375	1.3412 1217	0.9983 88	0.427721 2

v_{sL} ft/sec	area ft²	v_{sG} ft/sec	$λ_L$	f	Pressure Loss (psia²)	s
1.797632182	0.016566 993	3.383262	0.346973	0.018	0.753592	3.62624E-05
1.221002644		12.80001	0.087084	0.014	7.826555	0.000484103
0.437554588		25.09253	0.017139	0.012	19.58872	0.001412922
0.115146193		38.90751	0.002951	0.012	26.85282	0.00193637

(b) 22 Psi with Auger and foam

M_L lb/min	$ρ_L$ lb/ft³	Q_L stb/day	M_G lb/min	Q_G scf/day	p_{WF} psig	p_{WH} psig	Δp psig	GLR scf/stb	T deg F	q_G ft³/day	Pavg psia
40	43.69 05	234.8	0.6	11322. 24	21	7.51 28	13.48 72	48.2207 76	76	5893.831 27	28.95 24
17	43.69 05	99.79	2.27	42835. 8	21	7.87	13.13	429.259 46	74	22298.32 83	29.13 1
5.02	43.69 05	29.46 74	4.45	83973. 27	22	11	11	2849.70 06	72	43712.58 2	31.19 6

C₁	C₂	C₃	B_L	q_L ft³/day	γ_g	λ_L	λ_m
1.0008356	8.53624E-07	-9.39928E-12	1.00086	1319.536	1	1	3.961013
1.0004536	8.59247E-07	-1.02561E-11	1.000479	560.589	1	1	3.234163
1.0000784	8.64907E-07	-1.11243E-11	1.000105	165.4769	1	1	1.872958

T_{PC} (^0R)	P_{PC} (psia)	P_{PR}	T_{PR}	a	b	c	d	Z	B_G
238.69	546.9	0.052939	2.237211	0.688905	0.0056126	0.0200937	1.34121217	0.9986459	0.5205535

v_{sL} ft/sec	area ft^2	v_{sG} ft/sec	λ_L	f	Pressure Loss (psia^2)
0.921857728	0.016566993	4.117563	0.182929	0.018	0.742429
0.391640123		15.57811	0.024524	0.014	6.749914
0.115605879		30.53859	0.003771	0.012	12.87944

(c)15 Psi with Auger and foam

M_L lb/min	ρ_L lb/ft^3	Q_L stb/day	M_G lb/min	Q_G scf/day	p_{WF} psig	p_{WH} psig	Δp psig	GLR scf/stb	T deg F	q_G ft^3/day	P_{avg} psia
14	43.6905	82.166	0.6	11322.24	14	3.27	10.73	137.792	76	7317.54467	23.325
10	43.6905	58.69	2.27	42835.8	13.7	3.48	10.22	729.865	74	27684.7107	23.28

C_1	C_2	C_3	B_L	q_L ft^3/day	γ_g	λ_L	λ_m
1.0008356	8.53624E-07	-9.39928E-12	1.000856	461.7568	1	1	3.750641
1.0004536	8.59247E-07	-1.02561E-11	1.000474	329.7004	1	1	2.871696

T_{PC} (^0R)	P_{PC} (psia)	P_{PR}	T_{PR}	a	b	c	d	Z	B_G
238.69	546.9	0.042649	2.237211	0.688905	0.0045169	0.0200937	1.34121217	0.99889	0.6462984

v_{sL} ft/sec	Area ft^2	v_{sG} ft/sec	λ_L	f	Pressure Loss (psia^2)
0.322593691	0.016566993	5.112202	0.059357	0.018	0.703157
0.23033614		19.34116	0.011769	0.014	5.993727

APPENDIX D

TABLES OF RESULTS AIR-FOAM SYSTEM, ONLY TUBING

FLUID SYSTEM	WELLBORE CONFIGURATION
AIR-FOAM SYSTEM	COMBINATION TUBING 2 IN AND 1-1/2 IN ONLY

Table D.1 Summary of Data without Auger (with only foam)

Test with foam only

Pressure envelope test results					
30 psig					
No	Water rate (lb/min)	Gas rate (ft^3/minute)	P_{wf}	P_{middle}	$P_{wh\ after\ foam}$
1	187	1.5	30	14	10
2	83	5.5	30	20.42	14.84
3	54	9.5	30	26	15.32
4	22	13.5	30	28	21
5	14	19	30	26	26
22 psig			Pwf	Pmiddle	Pwh
1	68	1.5	23	13	6
2	52	5.5	22	14	11
3	24	9.5	22	14	13
4	19	13.5	22	13	12
5	12	19	22.5	15	13
15 psig			Pwf	Pmiddle	Pwh
1	38	1.5	14	9	6
2	21	5.5	15	8	5
3	21	9.5	14.1	7	7
4	12	13.5	14.3	13	10
5	12	19	15	12	12

Table D.2 Calculation with Foam

(a) 30 Psi with foam

M_L lb/min	ρ_L lb/ft³	Q_L stb/day	M_G lb/min	Q_G scf/day	p_{WF} psig	p_{WH} psig	Δp psig	GLR scf/stb	T deg F	q_G ft³/day	P_{avg} psia
187	43.6905	1097.69	0.6	11322.24	30	10	20	10.314605	76	4917.40969	34.693
83	43.6905	487.21	2.27	42835.8	30	14.84	15.16	87.920612	74	18604.2	37.113
54	43.6905	316.98	4.45	83973.27	30	15.32	14.68	264.91661	72	36470.7885	37.353
22	43.6905	129.14	6.9	130205.7	30	21	9	1008.2526	72	56550.2115	40.193
14	43.6905	82.18	11.4	215122.5	30	26	4	2617.6993	74	93430.7841	42.693

C_1	C_2	C_3	B_L	q_L ft³/day	γ_g	λ_L	λ_m
1.0008356	8.53624E-07	-9.39928E-12	1.000865	6168.862	1	1	4.060051
1.0004536	8.59247E-07	-1.02561E-11	1.000485	2737.012	1	1	3.863937
1.0000784	8.64907E-07	-1.11243E-11	1.000111	1780.04	1	1	3.498709
1.0000784	8.64907E-07	-1.11243E-11	1.000113	725.2031	1	1	2.627212
1.0004536	8.59247E-07	-1.02561E-11	1.00049	461.6669	1	1	1.927099

T_{PC} (°R)	P_{PC} (psia)	P_{PR}	T_{PR}	a	b	c	d	Z	B_G
238.69	546.9	0.063435729	2.237211	0.688905	0.0067327	0.02009375	1.34121217	0.99841	0.4343143

v_{sL} ft/sec	area ft²	v_{sG} ft/sec	λ_L	f	Pressure Loss (psia²)	s
4.309705963	0.016566993	3.435413	0.556442	0.018	0.76081	3.66081E-05
1.912138403		12.99731	0.12825	0.014	8.062692	0.000498683
1.243575832		25.47931	0.046536	0.012	24.0629	0.001735286
0.506643249		39.50725	0.012662	0.012	43.47274	0.003132828
0.322530913		65.27285	0.004917	0.012	87.18061	0.006272736

(b) 22 Psi with foam

M_L	ρ_L	Q_L	M_G	Q_G	p_{WF}	p_{WH}	Δp	GLR	T	q_G	P_{avg}
lb/min	lb/ft³	stb/day	lb/min	scf/day	psig	psig	psig	scf/stb	deg F	ft³/day	psia
68	43.6905	399.16	0.6	11322.24	21	6	15	28.365162	76	6052.13601	28.196
52	43.6905	305.24	2.27	42835.8	21	11	10	140.33482	74	22897.2479	30.696
24	43.6905	140.88	4.45	83973.27	22	13	9	596.06237	72	44886.6754	32.196
19	43.6905	111.53	6.9	130205.7	22	12	10	1167.4504	72	69599.5642	31.696
12	43.6905	70.44	11.4	215122.5	22	13	9	3053.9825	72	114990.584	32.196

C_1	C_2	C_3	B_L	q_L ft³/day	γ_g	λ_L	λ_m
1.0008356	8.53624E-07	-9.39928E-12	1.00086	2243.21	1	1	4.012077
1.0004536	8.59247E-07	-1.02561E-11	1.00048	1714.745	1	1	3.745115
1.0000784	8.64907E-07	-1.11243E-11	1.000106	791.1252	1	1	3.017379
1.0000784	8.64907E-07	-1.11243E-11	1.000106	626.3072	1	1	2.514113
1.0000784	8.64907E-07	-1.11243E-11	1.000106	395.5626	1	1	1.830264

T_{PC} (°R)	P_{PC} (psia)	P_{PR}	T_{PR}	a	b	c	d	Z	B_G
238.69	546.9	0.05155 6	2.237 211	0.688905	0.005 4652	0.0200 937	1.34121217	0.998681	0.5345 353

v_{sL} ft/sec	area ft²	v_{sG} ft/sec	λ_L	f	Pressure Loss (psia²)
1.567157127	0.016566993	4.228159	0.270418	0.018	0.752025
1.197959632		15.99653	0.069671	0.014	7.816815
0.552697907		31.35884	0.01732	0.012	20.75563
0.437552321		48.62382	0.008918	0.012	41.60975
0.276348954		80.33501	0.003428	0.012	82.80922

(c) 15 Psi with foam

M_L	ρ_L	Q_L	M_G	Q_G	p_{WF}	p_{WH}	Δp	GLR	T	q_G	P_{avg}
lb/min	lb/ft³	stb/day	lb/min	scf/day	psig	psig	psig	scf/stb	deg F	ft³/day	psia
38	43.6905	223.022	0.6	11322.24	14	6	8	50.76736	76	6912.58136	24.69
21	43.6905	123.249	2.27	42835.8	15	5	10	347.55496	74	26152.5995	24.69
19	43.6905	111.511	4.45	83973.27	14.1	7	7.1	753.04918	72	51268.3118	25.24
12	43.6905	70.428	6.9	130205.7	14.3	10	4.3	1848.778	72	79494.6857	26.84
12	43.6905	70.428	11.4	215122.5	15	12	3	3054.5028	72	131339.046	28.19

C_1	C_2	C_3	B_L	q_L ft^3/day	γ_g	λ_L	λ_m
1.0008356	8.53624E-07	-9.39928E-12	1.000857	1253.341	1	1	3.954589
1.0004536	8.59247E-07	-1.02561E-11	1.000475	692.3717	1	1	3.358293
1.0000784	8.64907E-07	-1.11243E-11	1.0001	626.197	1	1	2.848566
1.0000784	8.64907E-07	-1.11243E-11	1.000102	395.4934	1	1	2.166978
1.0000784	8.64907E-07	-1.11243E-11	1.000103	395.4939	1	1	1.830161

T_{PC} (^{0}R)	P_{PC} (psia)	P_{PR}	T_{PR}	a	b	c	d	Z	B_G
238.69	546.9	0.045145	2.237211	0.688905	0.00478 25	0.0200 937	1.34 121 217	0.998831	0.6105 313

v_{sL} ft/sec	area ft^2	v_{sG} ft/sec	λ_L	f	Pressure Loss (psia^2)	s
0.875612467	0.016566993	4.829285	0.153484	0.018	0.741348	3.56422E-06
0.483706479	0.016566993	18.27079	0.025791	0.014	7.008949	4.33242E-05
0.43747534	0.016566993	35.8172	0.012067	0.014	22.8481	0.000141223
0.276300597	0.016566993	55.53678	0.00495	0.014	41.79092	0.000258293
0.276300919	0.016566993	91.75642	0.003002	0.014	96.36103	0.000595469

APPENDIX E

TABLES OF COMBINED RESULTS

Table E.1 Unloading versus Pressure Loss Data

With and without Auger (air-water)

Unloading 30 psi	Pr loss_30 psi (psi^2)	Unloading 30 psi_Auger	Pls__Auger_30 psi (psi^2)
0.08129276	0.759878	0.047179	0.744926
0.019184887	8.245546	0.009976	7.667773
0.008318481	26.06746	0.003083	21.10436
0.004418085	59.11421	0.001168	34.24412
0.00179547	127.3236	0.000306	63.92239
Unloading 22 psi	Pr loss_22 psi (psi^2)	Unloading 22 psi_Auger	pls_Auger_22psi (psi^2)
0.036291	0.752445	0.023227	0.744926
0.012566	8.106595	0.005755	7.667773
0.004697	24.74037	0.00181	21.10436
0.001641	49.69823	0.000473	34.24412
0.000926	106.9118	0.000191	63.92239
Unloading 15 psi	pr loss _15 psi (psi^2)	Unloading 15 psi_Auger	pr loss_Auger_15psi (psi^2)
0.00798411	0.708371	0.009436	0.716513
0.003357355	7.181854	0.00259	6.883678
0.002417253	22.3932	0.001125	18.72925
0.001325425	47.07114	0.000578	36.63531
0.000429767	82.96689	7.64E-05	51.46297

Table E.2 Liquid Hold Up versus Air Flow Rate

With And without Auger (air-water)

Q_G	λ_L_30 psi	λ_L_Auger _30 psi	λ_L_22 psi	λ_L_Auger _22 psi	λ_L_15 psi	λ_L_Auger_15 psi
11322.24	0.495862	0.358015	0.271172	0.191725	0.062345	0.075239
42835.8	0.188335	0.105447	0.114088	0.055495	0.027189	0.021836
83973.27	0.091381	0.035132	0.045914	0.018141	0.019719	0.009604
130205.7	0.050707	0.013604	0.016533	0.004807	0.010909	0.004959
215122.5	0.021239	0.003595	0.009398	0.001945	0.003562	0.000658

Table E.3 Air Flow Rate versus Liquid Flow Rate Operational Envelope

With and without Auger (air-water)

Q_G (30 psi) scf/day	Q_L(30 psi) stb/day	Q_{L_Auger} (30 psi) stb/day
11322.23824	920.416	534.17
42835.80134	821.8	427.336
83973.26694	698.53	258.867
130205.7397	575.26	152.033
215122.5265	386.246	65.744
Q_G (22 psi) scf/day	Q_L(22 psi) stb/day	Q_{L_Auger}(22 psi) stb/day
11322.24	410.9	262.976
42835.8	538.279	246.54
83973.27	394.464	152.033
130205.7	213.668	61.635
215122.5	199.2865	41.09
Q_G scf/day	Q_L(15 psi) stb/day	Q_{L_Auger}(15 psi) stb/day
11322.24	90.398	106.834
42835.8	143.815	110.943
83973.27	202.9846	94.507
130205.7	172.578	75.31797
215122.5	92.4525	16.436

Table E.4 Pressure Loss Efficiency versus Air Flow Rate

Q_G scf/day	η_30 psi	η_22psi	η_15 psi
11322.24	0.005842	0.009993	0.001
42835.8	0.029572	0.054132	0.041518
83973.27	0.104578	0.146967	0.163619
130205.7	0.230646	0.310959	0.341703
215122.5	0.418888	0.402101	0.479717

Table E.5 Air Flow Rate versus Wellhead Pressure

Q_G (scf/day)	$p_{WH\_30 psi}$ (psig)	$p_{WH\_Auger\_30psi}$ (psig)	$p_{WH\_22 psi}$ (psig)	$p_{WH\_Auger\_22psi}$ (psig)	p_{WH_15psi} (psig)	$p_{WH\_Auger\_15 psi}$ (psig)
11322.24	5.5	4	4.6	2.4	1.3	2.88
42835.8	11.5	5.678	4.8	3	2	2.73
83973.27	13.2	6.45	8.5	3.5	3	2.69
130205.7	15	4.8	10	3	4	2.31
215122.5	15	3.93	10.3	3.7	5.4	2

Table E.6 Air Flow Rate versus Pressure Loss in the Tubing

With and without Auger Tool (air-water)

Q_G scf/day	Pr loss $_{30psi}$ (psi^2)	Pr loss $_{Auger\_30psi}$ (psi^2)	Pr loss $_{22 psi}$ (psi^2)	Pr loss $_{Auger\_22psi}$ (psi^2)	Pr loss $_{15 psi}$ (psi^2)	pr loss $_{Auger\_15 psi}$ (psi^2)
11322.24	0.759878	0.744926	0.752445	0.744926	0.708371	0.716513
42835.8	8.245546	7.667773	8.106595	7.667773	7.181854	6.883678
83973.27	26.06746	21.10436	24.74037	21.10436	22.3932	18.72925
130205.7	59.11421	34.24412	49.69823	34.24412	47.07114	36.63531
215122.5	127.3236	63.92239	106.9118	63.92239	82.96689	51.46297

Table E.7 Pressure Loss through the Tubing

With and without Auger(air-water) and with and without Auger(air-foam)

30 psi

Q_G scf/day	Pr loss $_{30psi}$ psi^2	Pr loss $_{Auger30psi}$ psi^2	Pr loss $_{Auger\_foam\_30 psi}$	pr loss $_{foam\_30 psi}$
11322.24	0.759878	0.744926	0.753592	0.76081
42835.8	8.245546	7.667773	7.826555	8.062692
83973.27	26.06746	21.10436	19.58872	24.0629
130205.7	59.11421	34.24412	26.85282	43.47274
215122.5	127.3236	63.92239		87.18061

Continued

22 psi

Q_G scf/day	Pr loss 22 psi psi^2	Pr loss Auger_22psi psi^2	Pr loss Auger_foam_22 psi	Pr loss_ foam_22 psi
11322.24	0.752445	0.744926	0.742429	0.752025
42835.8	8.106595	7.667773	6.749914	7.816815
83973.27	24.74037	21.10436	12.87944	20.75563
130205.7	49.69823	34.24412		41.60975
215122.5	106.9118	63.92239		82.80922

15 psi

Q_G scf/day	Pr loss 15 psi psi^2	Pr loss Auger_15 psi psi^2	Pr loss Auger_foam_15 psi psi^2	Pr loss foam_15 psi psi^2
11322.24	0.708371	0.716513	0.703157	0.741348
42835.8	7.181854	6.883678	5.993727	7.008949
83973.27	22.3932	18.72925		22.8481
130205.7	47.07114	36.63531		41.79092
215122.5	82.96689	51.46297		96.36103

Table E.8 Liquid Hold Up (Combined)

Q_G	$\lambda_{L\_30\ psi}$	$\lambda_{L\_Auger\_30\ psi}$	$\lambda_{L\_Auger\_foam\_30\ psi}$	$\lambda_{L\_foam\_30\ psi}$
11322.24	0.495862	0.358015	0.346973	0.556442
42835.8	0.188335	0.105447	0.087084	0.12825
83973.27	0.091381	0.035132	0.017139	0.046536
130205.7	0.050707	0.013604	0.002951	0.012662
215122.5	0.021239	0.003595		0.004917

Q_G	$\lambda_{L\_22\ psi}$	$\lambda_{L\_Auger\_22\ psi}$	$\lambda_{L\_Auger\_foam\_22\ psi}$	$\lambda_{L\_foam\_22\ psi}$
11322.24	0.271172	0.191725	0.182929	0.270418
42835.8	0.114088	0.055495	0.024524	0.069671
83973.27	0.045914	0.018141	0.003771	0.01732
130205.7	0.016533	0.004807		0.008918
215122.5	0.009398	0.001945		0.003428

Q_G	$\lambda_{L\_15\ psi}$	$\lambda_{L\_Auger\_15\ psi}$	$\lambda_{L\_Auger\_foam\_15psi}$	$\lambda_{L\_foam\_15\ psi}$
11322.24	0.062345	0.075239	0.059357	0.153484
42835.8	0.027189	0.021836	0.011769	0.025791
83973.27	0.019719	0.009604		0.012067
130205.7	0.010909	0.004959		0.00495
215122.5	0.003562	0.000658		0.003002

Table E.9 Temperature versus Air Density

	Temperature(^{0}F)	Density of air (g/cc)
1	68	0.00651
2	70	0.00671
3	72	0.00728
4	73	0.00591
5	74	0.0066
7	76	0.017
8	78	0.019
9	78.5	0.01
10	79.2	0.0094

Table E.10 Air Flow Rate versus Efficiency (Auger-foam)

(a) (Auger)

Q_G scf/day	$\eta\_30\ psi$	η_22psi	$\eta\_15\ psi$
11322.24	0.005842	0.009993	0.001
42835.8	0.029572	0.054132	0.041518
83973.27	0.104578	0.146967	0.163619
130205.7	0.230646	0.310959	0.341703
215122.5	0.418888	0.402101	0.479717

(b) (Auger-foam)

Q_G scf/day	$\eta\_Auger\_foam\_30\ psi$	$\eta\_Auger\_foam\_22psi$	$\eta\_Auger\_foam\_15\ psi$
11322.24	0.008272	0.01331	0.007361
42835.8	0.050814	0.167355	0.165434
83973.27	0.248537	0.479416	
130205.7	0.545747		
215122.5			

(c) Foam

QG scf/day	η_foam_30 psi	η_foam_22psi	η_foam_15 psi
11322.24	0.00022	0.000558	0.009914
42835.8	0.022176	0.035746	0.024075
83973.27	0.076899	0.161062	0.002014
130205.7	0.264597	0.162752	0.112175
215122.5	0.315283	0.225443	0.16144

Table E.11 Air Flow Rate versus Wellhead Pressure

Q_G scf/day	$P_{WH\ 30\ psi}$ psig	$P_{WH\_Auger\_30\ psi}$ psig	$P_{WH\_Auger\_foam\_30\ psi}$ psig	$P_{WH\_foam\_30\ psi}$ psig
11322.24	5.5	4	11.068	10
42835.8	11.5	5.678	12.1742	14.84
83973.27	13.2	6.45	16	15.32
130205.7	15	4.8	21	21
215122.5	15	3.93		26

Q_G scf/day	$P_{WH\_22\ psi}$ psig	$P_{WH\_Auger\_22\ psi}$ psig	$P_{WH\_Auger\_foam\_22\ psi}$ psig	$P_{WH\_foam\_22\ psi}$ psig
11322.24	4.6	2.4	7.5128	6
42835.8	4.8	3	7.87	11
83973.27	8.5	3.5	11	13
130205.7	10	3		12
215122.5	10.3	3.7		13
Q_G scf/day	$P_{WH\_15\ psi}$ psig	$P_{WH\_Auger\_15\ psi}$ psig	$P_{WH\_Auger\_foam\_15psi}$ psig	$P_{WH\_foam\_15psi}$ psig
11322.24	1.3	2.88	3.27	6
42835.8	2	2.73	3.48	5
83973.27	3	2.69		7
130205.7	4	2.31		10
215122.5	5.4	2		12

Table E.12 Combined Flow Envelope

Q_G scf/day	$Q_{L\_30\ psi}$ stb/day	$Q_{L\_Auger\_30\ psi}$ stb/day	$Q_{L\_Auger\_foam\_30\ psi}$ stb/day	$Q_{L\_foam\_30\ psi}$ stb/day
11322.23824	920.416	534.17	457.86	1097.69
42835.80134	821.8	427.336	311.11	487.21
83973.26694	698.53	258.867	111.53	316.98
130205.7397	575.26	152.033	29.35	129.14
215122.5265	386.246	65.744		82.18

Q_G scf/day	$Q_{L\_22\ psi}$ stb/day	$Q_{L\_Auger\_22\ psi}$ stb/day	$Q_{L\_Auger\_foam\_22\ psi}$ stb/day	$Q_{L\_foam\_22\ psi}$ stb/day
11322.24	410.9	262.976	234.8	399.16
42835.8	538.279	246.54	99.79	305.24
83973.27	394.464	152.033	29.4674	140.88
130205.7	213.668	61.635		111.53
215122.5	199.2865	41.09		70.44

$Q_{G\_15\ psi}$ scf/day	$Q_{L\_15\ psi}$ stb/day	$Q_{L\_Auger\_15\ psi}$ stb/day	$Q_{L\_Auger\_foam\_15\ psi}$ stb/day	$Q_{L\_foam\_15\ psi}$ stb/day
11322.24	90.398	106.834	82.166	223.022
42835.8	143.815	110.943	58.69	123.249
83973.27	202.9846	94.507		111.511
130205.7	172.578	75.31797		70.428
215122.5	92.4525	16.436		70.428

Table E.13 Liquid Unloading versus Pressure Loss(Combined)

(a) 30 psi

Unloading_ 30 psi	Pr loss__30psi psi^2	Unloading 30 psi_Auger	Pr loss_Auger30psi psi^2	Unloading _30 psi_Auger_foam	Pr loss Auger_foam_30 psi	Unloading 30 psi_foam	pr loss _foam_30 psi
0.08129276	0.759878	0.047179	0.744926	0.040439	0.753592	0.09695	0.76081
0.019184887	8.245546	0.009976	7.667773	0.007263	7.826555	0.011374	8.062692
0.008318481	26.06746	0.003083	21.10436	0.001328	19.58872	0.003775	24.0629
0.004418085	59.11421	0.001168	34.24412	0.000225	26.85282	0.000992	43.47274
0.00179547	127.3236	0.000306	63.92239			0.000382	87.18061

(b) 22 psi

Unloading __22 psi	Pr loss _22 psi psi^2	Unloading 22 psi_Auger	Pr loss _Auger_22psi psi^2	Unloading_ 22 psi_Auger_foam	Pr loss _Auger_foam_22 psi	Unloading foam_22 psi	Pr loss_ foam_22 psi
.036291	0.752445	0.023227	0.744926	0.020738	0.742429	0.035255	0.752025
0.012566	8.106595	0.005755	7.667773	0.00233	6.749914	0.007126	7.816815
0.004697	24.74037	0.00181	21.10436	0.000351	12.87944	0.001678	20.75563
0.001641	49.69823	0.000473	34.24412			0.000857	41.60975
0.000926	106.9118	0.000191	63.92239			0.000327	82.80922

(c) 15 psi

Unloading 15 psi	Pr loss 15 psi psi^2	Unloading 15 psi_Auger	Pr loss Auger_15 psi psi^2	Unloading 15 psi_Auger_foam	Pr loss Auger_foam_15 psi psi^2	Unloading foam_15 psi	Pr loss foam_15 psi psi^2
0.00798411	0.708371	0.009436	0.716513	0.007257	0.703157	0.019698	0.741348
0.003357355	7.181854	0.00259	6.883678	0.00137	5.993727	0.002877	7.008949
0.002417253	22.3932	0.001125	18.72925			0.001328	22.8481
0.001325425	47.07114	0.000578	36.63531			0.000541	41.79092
0.000429767	82.96689	7.64E-05	51.46297			0.000327	96.36103

Table E.14 Efficiency Comparison(Combined)

(a)30 psi

Q_G scf/day	η_Auger_30 psi	η_Auger_foam_30 psi	η_foam_30 psi
11322.24	0.005842	0.008272	0.00022
42835.8	0.029572	0.050814	0.022176
83973.27	0.104578	0.248537	0.076899
130205.7	0.230646	0.545747	0.264597
215122.5	0.418888		0.315283

(b)22 psi

Q_G scf/day	$\eta_{\_Auger\_22psi}$	$\eta_{\_\_Auger\_foam\_22psi}$	$\eta_{\_\_foam\_22psi}$
11322.24	0.009993	0.01331	0.000558
42835.8	0.054132	0.167355	0.035746
83973.27	0.146967	0.479416	0.161062
130205.7	0.310959		0.162752
215122.5	0.402101		0.225443

(c)15 psi

Q_G scf/day	$\eta_{\_Auger\_\_15\ psi}$	$\eta_{\_\_Auger\_foam\_15\ psi}$	$\eta_{\_\_foam\_15\ psi}$
11322.24	0.001	0.007361	0.009914
42835.8	0.041518	0.165434	0.024075
83973.27	0.163619		0.002014
130205.7	0.341703		0.112175
215122.5	0.479717		0.16144

APPENDIX F

DEVELOPMENT OF TERMINAL VELOCITY EQUATIONS

This chapter summarizes the development of the Turner1 equations to calculate the

minimum natural gas velocity to remove liquid droplets from a vertical wellbore.

F.1 Physical Model

Consider natural gas flowing in a vertical wellbore and a liquid droplet transported at a

uniform velocity in the natural gas stream as illustrated in Figure F.1.

The forces acting on the droplet are gravity, pulling the droplet downward, and the

upward drag of the natural gas as it flows around the droplet.

The gravity force is:

$$F_G = \frac{g}{g_c}(\rho_L - \rho_G)X\frac{\pi d^3}{6}$$

and the upward drag force is given by:

$$F_D = \frac{1}{2g_c}\rho_G C_D A_d (V_g - V_d)^2$$

Where g= gravitational constant=32.17 ft/s^2

g_c = 32.17 lbm-ft/lbf-s^2 ,   d= droplet diameter, ρ_L = liquid density
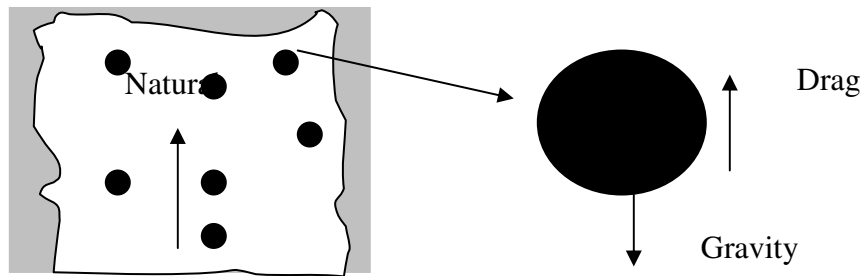
Figure F.1 Liquid droplet transported in a vertical natural gas stream

ρ_G = natural gas density

C_D = drag coefficient

A_d= droplet projected cross sectional area

V_G = natural gas velocity

V_d= droplet velocity

F_G= F_D

Or:

$$\frac{g}{g_c}(\rho_L - \rho_G)\frac{\pi d^3}{6} = \frac{1}{2g_c}\rho_G C_D A_d V_c^2$$

Substituting $A_d = \dfrac{\pi d^2}{4}$ and solving for V_c gives:

$$V_c = \sqrt{\frac{4g(\rho_L - \rho_G)}{3\rho_G C_D}d} \quad\text{...(F.1)}$$

This equation assumes a known droplet diameter. In reality, the droplet diameter is dependent on the natural gas velocity. For liquid droplets entrained in a natural gas stream, Reference[5] shows that this dependence can be expressed in terms of the dimensionless Weber number:

$$N_{WE} = \frac{V_c^2 \rho_G d}{\sigma g_c} = 30$$

Solving for the droplet diameter gives:

$$d = 30 \frac{\sigma g_c}{\rho_G V_c^2}$$

Substituting into Equation F.1 gives:

$$V_c = \sqrt{\frac{4(\rho_L - \rho_G)g\,30\sigma g_c}{3\rho_G C_D \rho_G V_c^2}}$$

or

$$V_c = \left(\frac{40 g g_c}{C_D}\right)^{0.25}\left(\frac{\rho_L - \rho_G}{\rho_G^2}\sigma\right)^{0.25}$$

Turner assumed a drag coefficient of $C_D = .44$ that is valid for fully turbulent conditions. Substituting the turbulent drag coefficient and values for g and gc gives:

$$Vc = 17.514\left(\frac{\rho_L - \rho_G}{\rho_G^2}\sigma\right)^{0.25} \text{ ft/s} \dots\dots(F.2)$$

Where ρ_L = liquid density, lbm/ft^3

ρ_G = natural gas density, lbm/ft^3

σ = surface tension, lbf/ft

Equation A.2 can be written for surface tension in dyne/cm units using the conversion

lbf/ft = .00006852 dyne/cm to give:

$$V_c = 1.593\left(\frac{\rho_L - \rho_G}{\rho_G{}^2}\sigma\right)^{0.25} \text{ ft/s} \dots\dots\dots\dots\dots\dots\dots\dots\dots\dots\dots\dots\dots\dots\dots\dots\dots\dots\dots\dots\dots\dots\text{(F.3)}$$

Where ρ_L = liquid density, lbm/ft^3

ρ_G = natural gas density, lbm/ft^3

ρ = surface tension, dyne/cm

F.2 Equation Simplification

Equation F.3 can be simplified by applying "typical" values for the natural gas and

liquid properties. From the real natural gas law, the natural gas density is given by:

$$\rho_G = 2.715\gamma_G\frac{P}{(460+T)Z} \text{ lbm/ft}^3 \dots\dots\dots\dots\dots\dots\dots\dots\dots\dots\dots\dots\dots\dots\dots\dots\dots\dots\dots\text{(F.4)}$$

Evaluating Equation A-4 for typical values of

Natural gas gravity $\gamma_G = 0.6$

Temperature $T = 120^0\text{F}$

Natural gas deviation factor Z= 0.9

Gives

$$\rho_G = 2.715 X 0.6 \frac{P}{(460+120)X0.9} = 0.0031P \text{ , lbm/ft}^3$$

Typical values for density and surface tension are:

Water density 67 lbm/ft3

Condensate density 45 lbm/ft3

Water surface tension 60 dyne/cm

Condensate surface tension 20 dyne/cm

Foam surface tension 33 dynes/cm

Introducing these typical values and the simplified natural gas density:

$$V_{C,water} = 1.593 \left(\frac{67-0.0031P}{(0.0031P)^2} 60 \right)^{0.25} = 4.434 \left(\frac{67-0.0031P}{(0.0031P)^2} \right)^{0.25} \text{ ft/sec}$$

$$V_{C,condensate} = 1.593 \left(\frac{45-0.0031P}{(0.0031P)^2} 20 \right)^{0.25} = 3.369 \left(\frac{45-0.0031P}{(0.0031P)^2} \right)^{0.25} \text{ ft/sec}$$

F.3 Turner Equations

Turner et al.[2] found that for their field data, where wellhead pressures were typically >
1000 psi, a 20% upward adjustment to the theoretical values was required to match the
field observations. Applying the 20% adjustment then yields:

$$V_{C,water} = 5.321 \left(\frac{67-0.0031P}{(0.0031P)^2} \right)^{0.25} \text{ ft/s}$$

$$V_{C,condensate} = 4.043 \left(\frac{45-0.0031P}{(0.0031P)^2} \right)^{0.25} \text{ ft/s}$$

F.4 Coleman Equation

Coleman et al.[3] found that Equation A.3 was an equation that would fit their data. This was without the 20% adjustment that Turner et al. made to fit their data at higher average wellhead pressures.

$$V_{C,water} = 4.434 \left(\frac{67 - 0.0031P}{(0.0031P)^2} \right)^{0.25} \text{ft/s}$$

$$V_{C,condensate} = 3.369 \left(\frac{45 - 0.0031P}{(0.0031P)^2} \right)^{0.25} \text{ft/s}$$

The multiphase flow in wellbores and pipelines is handled by several multiphase flow equations by Beggs and brills[25].
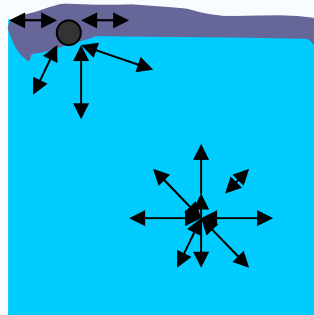
F.4 The Cause Of Surface Tension

Figure F.4.1 Diagram of the forces on a molecule of liquid.

Surface tension is a result of attraction between the molecules of the liquid . Within the bulk of the liquid, each molecule is pulled equally in all directions by the other molecules, causing in a net force of zero. At the surface of the liquid, the molecules are pulled inwards by other molecules to the the liquid more than their attraction to contacting medium. Therefore all of the molecules at the surface are subject to inward of

molecular attraction which can be balanced only by the resistance of the liquid to compression. This causes the liquid squeezes itself together until it has the locally lowest surface area possible.

The boundary molecules have fewer pulling materials than interior molecules and are therefore in a higher state of energy. For the liquid to minimize its energy state, it must minimize its number of boundary molecules and therefore minimize its surface area.

F.5   Weber number

The **Weber number** is a dimensionless number in fluid mechanics. It is used to analyse fluid flows with interfacing between two different fluids, especially for multiphase flows with strongly curved surfaces. It is a measure of the fluid's inertia compared to its surface tension and is useful in analyzing thin film flows and the formation of droplets and bubbles.

It is defined as:

$$Nwe = \rho v^2 l / \sigma$$

Where

ρ is the density of the fluid

v is its velocity

l is its characteristic length

σ is the surface tension.

F.6   Drag coefficient:

The drag coefficient (C_d) is a dimensionless quantity that describes an aerodynamic drag caused by fluid flow, used in the drag equation. Two objects of the same area moving at the same speed through a fluid will experience a drag force proportional to their C_d numbers. Coefficients for rough unstreamlined objects can be 1 or more, for smooth objects much less. For spherical objects it is considered to be 0.44 which is used in Turner equation.

$$F_d = 0.5\ \rho v^2 C_d A$$

Where,

ρ is the density of the fluid

v is its velocity

l is its characteristic length

σ is the surface tension.

A C_d equal to 1 would be obtained in a case where all of the fluid approaching the object is brought to rest, building up stagnation pressure over the whole front surface.

For an object moving through a fluid or natural gas, the drag is the sum of all the aerodynamic or hydrodynamic forces in the direction of the external fluid flow. (Forces perpendicular to this direction are considered lift). It therefore acts to oppose the motion of the object.

In fluid dynamics, drag is the force that resists the movement of a solid object through a fluid (a liquid or natural gas). Drag is made up of friction forces, which act in a direction parallel to the object's surface (primarily along its sides, as friction forces at the front and back cancel themselves out), plus pressure forces, which act in a direction perpendicular to the object's surface.

An object falling through a natural gas or liquid experiences a force in direction opposite to its motion. Terminal velocity is achieved when the drag force is equal to force of gravity pulling it down.

F_d

F_g
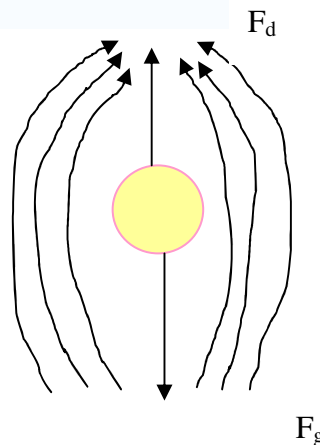
APPENDIX G

FORMULAS USED

The different formulas used to interpret the data are displayed in the appendix. The formulas are grouped in terms of the appendix in which their results are shown.

Conversion of M_L to Q_L

Where,

M_L = Mass Flow Rate of the liquid, lb/min

Q_L = Volumetric Flow Rate of the Liquid, STBD

Here,

Liquid = water

Density of Liquid at standard conditions (1 atm, 32^0 F) 'ρ_L' = 62.415 lb/ft^3

Mass flow at In-situ conditions= Mass Flow Rate at standard conditions

Then,

Q_L STB/day $= M_L / \rho_L$

$= \dfrac{M_L \text{ lb/min X 60X24 min/day}}{62.415 \text{ lb/ft}^3 \text{ X5.615 ft}^3 \text{ /bbl}}$

$= 0.04109\ M_L$ lb/min

Conversion of M_G to Q_G

Here,

M_G = Mass Flow Rate of the Natural gas, kg/min

Q_G = Volumetric Flow Rate of the Natural gas, SCFD

Here,

Natural gas = Air

Density of Natural gas at standard conditions (1 atm, 60^0 F) 'ρ_G' = 0.076313 lb/ft^3

Since ,

Mass flow at In-situ conditions = Mass Flow Rate at standard conditions

Then, Q_G SCF/day = M_G / ρ_G

$$= \frac{M_G \text{ lb/min} \times 60 \times 24 \text{ min/day}}{0.07631 \text{ lb/ft}^3}$$

$$= M_G \text{ lb/min} \times 18870$$

Calculating ΔP

$\Delta P = P_{WF} - P_{WH}$

Where

ΔP = differential pressure, psi

P_{WF} = Bottomhole pressure, psi

P_{WH} = Wellhead Pressure, psig

Natural gas-Liquid Ratio (GLR)

$$\text{GLR SCF/STB} = \frac{Q_G \text{ SCF/day}}{Q_L \text{ STB/day}}$$

Where,

GLR = Natural gas-Liquid Ratio, SCF/STB

Q_G = Volumetric Flow Rate of the Natural gas, SCFD

Q_L = Volumetric Flow Rate of the Liquid, STBD

Conversion of T^0F to T^0R

$T^0R = T^0F + 460$

Conversion of Q_L to q_L

q_L ft^3/day = Q_L STB/day X 5.615 SCF/STB X B_L ft^3/SCF

Where,

q_L = Volumetric Flow Rate of the Liquid, ft^3/day

Q_L = Volumetric Flow Rate of the Natural gas, STBD

B_L = Formation Volume Factor for the Liquid, ft^3/SCF

For water,

$B_L = C_1 + C_2 P_{AVG} + C3 P^2_{AVG}$

$C_1 = 0.9911 + 6.35 \times 10^{-5} T + 8.5 \times 10^{-7} T^2$

$C_2 = 1.093 \times 10^{-6} - 3.497 \times 10^{-9} T + 4.57 \times 10^{-12} T^2$

$C_3 = -5 \times 10^{-11} + 6.429 \times 10^{-13} T - 1.43 \times 10^{-15} T^2$

And

T = Temperature, ^0F

P_{AVG} = average Pressure of the System, psia.

$P_{AVG} = (P_{WF} + P_{WH})/2$

Conversion of Q_G to q_G

q_G ft^3/day = Q_G SCF/day X B_G ft^3/SCF

where,

q_G = Volumetric Flow Rate of the Natural gas, ft^3/day

Q_G= Volumetric Flow Rate of the Natural gas, SCFD

B_G = Formation Volume Factor for the Natural gas, ft^3/SCF

For any Natural gas,

B_G = P_{SC} Z T_{AVG}/ T_{SC} P_{AVG}

$\quad$ = 0.0283 Z T_{AVG}/ P_{AVG}

Where,

$\qquad$ P_{SC} = standard conditions for Pressure, 14.696 psia.

$\qquad$ T_{SC} = standard conditions for Temperature, 520^0 R

$\qquad$ T_{AVG} = average Temperature of the system, ^{0}R

$\qquad$ P_{AVG} = average pressure of the system, psia.

$\qquad$ Z = compressibility Factor at T_{AVG} and P_{AVG}

Z= A+ (1-A) e^{-B} +C P$^D_{PR}$

Here,

A = 1.39(T_{PR} – 0.92)$^{0.5}$ – 0.36 T_{PR} – 0.101

B = P_{PR}(0.62-0.23 T_{PR}) + P_{PR}^{2}[$\underline{0.066}$ - 0.037] + $\underline{0.32\ P_{PR}}$^{6}

$\qquad\qquad\qquad\qquad\qquad$ T_{PR} -0.86 $\qquad\qquad\qquad$ e$^{[20.723(TPR\ -1)]}$

C = 0.132- 0.32 log T_{PR}

$D = e \, (0.715 - 1.128 \, T_{PR} + 0.42 \, T_{PR}{}^2)$

P_{PR} = Pseudoreduced Pressure

T_{PR} = Pseudoreduced Temperature

$$P_{PR} = \frac{P_{AVG}}{P_{PC}}$$

$$T_{PR} = \frac{T_{AVG}}{T_{PC}}$$

P_{PC} = Pseudocritical Pressure, psia

T_{PC} = Pseudocritical Temperature, ^0R

Calculating crossectional area

$A \, ft^2 \; = (\Pi \, (D1 \text{ in inch}^2)*0.45 \, {}^+ \Pi \, (D2 \text{ in inch}^2)*0.55)/ \, 4X144$

$\qquad = 0.021817 \, ft^2$

Conversion of q_L to v_{sL}

$$v_{sL} = \frac{q_L \qquad ft^3/day}{A \, ft^2 \, X \, 86400 \text{ sec}}$$

Where ,

v_{sL} = superficial Liquid Velocity , ft/sec

q_L = Volumetric Flow Rate of the Liquid, ft^3/day

A = cross sectional area of the Pipe, ft^2

Conversion of q_G to vs_G

$$v_{sG} \text{ ft/sec} = \frac{q_G \quad \text{ft}^3/\text{day}}{A \text{ ft}^2 \text{ X } 86400 \text{ sec/day}}$$

Where,

v_{sG} = superficial Natural gas Velocity, ft/sec

q_G = In-situ Volumetric Flow Rate of the Natural gas, ft^3/day

a= cross sectional area of the pipe, ft^2

Calculating the no slip Liquid hold Up

$$\lambda_L = \frac{q_L \quad \text{ft}^3/\text{day}}{q_L \text{ ft}^3/\text{day} + q_G \text{ ft}^3/\text{day}}$$

where,

λ_L = No-slip Liquid hold Up

q_L = In-situ Volumetric Flow Rate of the Liquid, ft^3/day

q_G = In-situ Volumetric Flow Rate of Natural gas, ft^3/day

Calculating the no-slip Natural gas Hold up

$\lambda_G = 1 - \lambda_L$

Back Pressure Equation

The tubing pressure loss in a flowing natural gas well can be determined from

$$p^2_{WF} = p^2_{WH} e^S + C_1 \gamma_g q^2_{SC} T_{AVG} Z_{AVG} f(MD)(e^S - 1)/SD^5$$

Where ,

$S = C_2\,\gamma_g\,q^2_{SC}\,(TVD)/\underline{T}_{AVG}\,Z_{AVG}$

C_1 and C_2 are constants depending on units

p_{WF}, P_{WH} are pressures , psia.

q_{SC} = Flow Rate, MMscfd

TVD= Total Vertical Depth, ft

MD = Measured Depth, ft

D= Inside Pipe Diameter, in

$C_1 = 25$

$C_2 = 0.0375$

T and Z are the average temperature and Z factor existing in the well.

The equation although used for dry natural gas has been modified to be used for the continuously unloaded wells by adjusting the natural gas gravity and replacing that with the mixture gravity.

$\gamma_m = \dfrac{\gamma_g + 4591\,\gamma_L/R}{1 + 1123/R}$

Where γ_g = Natural gas Gravity, (air=1)

γ_L = Liquid Gravity, (water=1)

R= Producing natural gas/liquid Ratio, scf/stb

Efficiency

$$\eta = (p^2_{WF} - p^2_{WH} e^S)_{Auger} - (p^2_{WF} - p^2_{WH} e^S)_{tubing} / (p^2_{WF} - p^2_{WH} e^S)_{tubing}$$

η = Efficiency

$(p^2_{WF} - p^2_{WH} e^S)_{Auger}$ = Pressure Loss with Auger, $psia^2$

$(p^2_{WF} - p^2_{WH} e^S)_{tubing}$ = Pressure Loss without Auger, $psia^2$

APPENDIX H

NATURAL GAS FUNDAMENTALS

H.l Introduction

This Appendix catalogs some commonly used natural gas fundamental expressions that are useful when operating natural gas wells.

H.2 Natural Gas Apparent Molecular Weight and Specific Gravity

Molecular weight is defined for a specific molecule but not for a mixture of different molecular species. For natural gas mixtures, the apparent natural gas molecular weight *M* is defined to represent the average molecular weight of all the molecules in the natural gas. Thus, *M* can be calculated from the mole fraction of each molecular species in the natural gas as:

$$M = \sum_{allspeciesj} y_j M_j$$

Where y_j = mole fraction of molecule j

M_j = molecular weight of molecule j

$$M_{air} = \sum_{allspeciesi} y_i M_i = 0.78 \times 28.01 + 0.21 \times 32 + 0.01 \times 39.94 = 28.97$$

The specific gravity of a natural gas is the ratio of the natural gas apparent molecular weight to the apparent molecular weight of air.

$$\gamma_G = \frac{M_G}{M_{air}} = \frac{M_G}{28.97}$$

Standing and Katz[26] provided correlation for density and compressibility.

H.3 Pressure Increase in Static Column of Natural Gas

$$P_{bot} = P_{top} X \exp\left(\frac{0.01875\gamma_g \frac{g}{g_c} H}{(T+460)Z} \right)$$

The above equation for P_{bot} can be used to calculate the pressure increase down an annulus of a natural gas-lifted or flowing multiphase flow well or to the fluid level in the annulus for a pumping well. It is more accurate if the calculations are broken up into increments and the temperature and Z factor are the averages for each segment of calculation.

H.4 Calculate Pressure Drop in Flowing Dry Natural Gas Well: Cullender And Smith Method[27]

Total drop in tubing= Pressure drop due potential energy change+ Frictional pressure drop+ Pressure drop due to Kinetic energy change

$$\frac{dp}{dl} = \left(\frac{\partial p}{dl} \right)_{el} + \left(\frac{\partial p}{dl} \right)_{f} + \left(\frac{\partial p}{dl} \right)_{acc}$$

Or: $\left(\dfrac{dp}{dl} \right) = \dfrac{g}{g_c} \rho \cos(\theta) + \dfrac{fv^2 \rho}{2 g_c d} + \dfrac{\rho vdv}{g_c dl}$

Where θ is the angle from vertical

Upper half of well:

$$18.75\lambda_g(MD) = (p_{wf} - p_{if})(K_{mf} + K_{if})$$

Lower half of well:

$$18.75\lambda_g(MD) = (p_w - p_{mf})(K_{wf} + K_{mf})$$

Where p_{wf} =flowing bhp to be solved

p_{if} = flowing tubing pressure, input

p_{mf} = flowing pressure midway in well

$$K = \cfrac{\dfrac{p}{Tz}}{\dfrac{0.001(TVD)}{MD}\left(\dfrac{p}{Tz}\right)^2 + F^2}$$

The solution can proceed by first calculating N_{Re}, a friction factor and p_{mf} by assuming

P_{mf} and solving for p_{mf} using the following equation:

$$18.75\gamma_g(MD) = (p_{mf} - p_{if})(K_{mf} + K_{if})$$

Since K_{mf} is a function of P_{mf}, the solution is iterative. Once the intermediate pressure is

solved for, then P_{WF} can be solved for in the two-segment example. In a real case for

accuracy, the solution would be broken into several increments.

H.5 Pressure Drop in A Natural Gas Well Producing Liquids

One of many correlations for natural gas wells producing some liquids is the Gray[28]

correlation. It is a vertical flow correlation for natural gas wells to determine pressure

changes with depth and the bottomhole pressure. The method developed by Gray

accounts for entrained fluids, temperature gradient, fluid acceleration, and

nonhydrocarbon natural gas components. Well test data are required to make the necessary calculations. As per Gray, for two-phase pressure drop can be defined from the following equation.

$$dp = \frac{g}{g_c}\left[\xi\rho_g + (1-\xi)\rho_l\right]dh + \frac{f_t G^2}{2 g_c D \rho_{mf}}dh - \frac{G^2}{g_c}d\left(\frac{1}{\rho_{mi}}\right)$$

Where

ξ = the insitu natural gas volume fraction

D = Conduit traverse dimension

G = mass velocity

ρ = density

h = depth

p = pressure

g_c = dimensionless constant

f_t = irreversible energy loss

Further, as given in API14BM, ξ can be defined as:

$$\xi = \frac{1 - \exp\left[-2.314\left[N_V\left(1+\frac{205.0}{N_D}\right)\right]^B\right]}{R+1}$$

$$B = 0.814\left[1 - 0.0554 Ln\left(1+\frac{730R}{R+1}\right)\right]$$

$$N_V = \frac{\rho_m^2 V_{sm}^4}{g\tau(\rho_l - \rho_g)}$$

where Nv, N_D, and R are velocity, diameter and superficial liquid to natural gas ratio parameters, which mainly influence the hold-up for condensate wells. In Gray's method, superficial liquid and natural gas densities are used and a superficial mixture velocity (V_{sm}) is calculated.

The values of the superficial velocities are determined from:

$$V_S = Q/A$$

The Q values for oil and water are from input of bbls/MMscf for the water and the condensate (oil). The conventional liquid holdup H_L is found as:

$$H_l = 1 - \xi$$

H.6 Natural Gas Well Deliverability Expressions

H.6.1 Backpressure Equation

Perhaps the most widely used inflow expression for natural gas wells is the natural gas backpressure equation[29] :

$$q_G = C_1\left(\overline{P_r}^2 - P_{wf}^2\right)^n$$

Where q_G = natural gas rate, units consistent with C_1

C_1=inflow coefficient

N=inflow exponent

P_r=average reservoir pressure, psia.

P_{wf}= flowing bottomhole pressure, psia.

Once values for *C* and *n* are determined using test data, the backpressure equation can generate a predicted flow rate for any flowing wellbore pressure, P_{wf}. Because there are two constants, C and *n,* a minimum of two pairs of pseudo-stabilized data *(q_g, P_{wf})* are needed but usually at least four data pairs (a "four point" test) are used to determine C and *n* to account for possible errors in the data collection.

The equation can be written as:

$$\log\left(\overline{P}_r^{\,2} - P_{wf}^{\,2}\right) = \log \Delta P^2 = \frac{1}{n}\log(q_g) - \frac{1}{n}\log C$$

A plot of ΔP^2 versus q_g on log-log paper will result in a straight line having a slope of 1/n and an intercept of q_g=C at ΔP^2 =1. The value of C can also be calculated using any point from the best line through the data since $C_1 = \dfrac{q_G}{\left(\overline{P}_r^{\,2} - P_{wf}^{\,2}\right)^n}$

For high permeability wells where the flow rates and pressures attain steady state for each test within a reasonable time (conventional flow-after- flow test), the log-log plot is easily used to generate the needed data.

For tighter permeability wells, isochronal[30] or modified isochronal tests and plots can be used where the slope is generated from shorter flow tests, and a parallel line is drawn though an extended pressure-rate point for final results.

Neely[31] and Fetcovitch[32] wrote the above single-phase flow equation for natural gas

wells as:

$$q_G = C\left(\frac{\overline{P_r}^2 - P_{wf}^2}{\overline{\mu}\,\overline{z}}\right)$$

Where $\overline{\mu}$ = average viscocity that is a function of pressure

$\overline{z}$ = average natural gas deviation factor that is a function of pressure

C= a constant (not the C in back pressure equation) and can be determined from a single

well test if the shut in average pressure is known.

The P_{wf} should be determined from a downhole pressure gauge. The viscosity and Z

factor should be determined at the bottomhole temperature and average bottomhole

pressure. Then C will not change as rates are varied from the well unless damage sets in,

such as scale buildup.

Using this equation can result in a more accurate inflow expression showing a correction

to a higher AOF compared to the old log-log backpressure equation.[32,33]

APPENDIX I

CODE FOR SOLVING THE MINIMUM FLOW EQUATION

I.1   Final 4 Phase Model

```vba
Sub RunSolver(wksht As String, nFrom As Variant, nTo As Variant)

   With ThisWorkbook.Worksheets(wksht)
     For i = nFrom To nTo
        ' Initialize Solver
        Application.ScreenUpdating = False
        Application.Run "Solver.xla!Auto_Open"
        SolverReset
        Application.Run "Solver.xla!Auto_Open"
        SolverOptions MaxTime:=120, Precision:=0.1, Convergence:=0.1,
AssumeNonNeg:=True
        Application.Run "Solver.xla!Auto_Open"
        '.Cells(i, 15) = 100
        changeparm = "$O$" & CStr(i)    ' Decision Variable (Qgm)

        objfn = "$BA$" & CStr(i)        ' Objective Function
        SolverOK SetCell:=Range(objfn), MaxMinVal:=2,
ByChange:=Range(changeparm)
        SolverAdd CellRef:=Range(changeparm), Relation:=3, FormulaText:=0.1
        SolverAdd CellRef:=Range(changeparm), Relation:=1, FormulaText:=10000

        ' Run Solver
        Application.Run "Solver.xla!Auto_Open"
        SolverSolve UserFinish:=True
        Application.Run "Solver.xla!Auto_Open"
        SolverFinish KeepFinal:=1
        Application.ScreenUpdating = True

        ' Change color for 53 columns
        Qg = .Cells(i, 12)
        For j = 1 To 53
          If Qg > .Cells(i, 15).Value() * 1000 Then
             .Cells(i, j).Interior.Color = RGB(255, 255, 200)
          Else
             .Cells(i, j).Interior.Color = RGB(200, 100, 150)
          End If
        Next j
     Next i
```

```
        End With

End Sub

Private Sub UserForm_Initialize()
    'Add list entries to combo box. The value of each
    'entry matches the corresponding ListIndex value
    'in the combo box.

    Call Get_FieldNames

    ' Set focus on first entry in combobox
    FieldName_CB.SetFocus
    If (FieldName_CB.LineCount > 0) Then
       'Combo box values are ListIndex values
       FieldName_CB.BoundColumn = 0
       'Set combo box to first entry
       FieldName_CB.ListIndex = 0
    Else
         ' Deactivate the fieldname combobox
    End If

    End Sub

Private Sub Get_FieldNames()

    FieldName_CB.Clear
    ' Should be picked up from database LATER
    FieldName_CB.AddItem "Field1"
    FieldName_CB.AddItem "Field2"
    ' upscaling provision
    ' FieldName_CB.AddItem "Field3"
    ' FieldName_CB.AddItem "Field4"
    ' Should be picked up from database LATER

End Sub

Private Sub Get_WellNames(fieldname As String)

    WellName_CB.Clear
    ' Should be picked up from database LATER (using fieldname)
    WellName_CB.AddItem "Well1"
    WellName_CB.AddItem "Well2"
  ' upscaling provision ///////////////////////
```

```
        WellName_CB.AddItem "well3"
        WellName_CB.AddItem "well4"
        WellName_CB.AddItem "well5"
        WellName_CB.AddItem "well6"
        WellName_CB.AddItem "well7"
        WellName_CB.AddItem "well8"
        WellName_CB.AddItem "well9"
        WellName_CB.AddItem "well10"
        WellName_CB.AddItem "well11"
        WellName_CB.AddItem "well12"
        WellName_CB.AddItem "well13"
        WellName_CB.AddItem "well14"
        WellName_CB.AddItem "well15"
        WellName_CB.AddItem "well15"
        WellName_CB.AddItem "well16"
        WellName_CB.AddItem "well17"
        WellName_CB.AddItem "well18"
        WellName_CB.AddItem "well19"
        WellName_CB.AddItem "well20"
    '   WellName_CB.AddItem "well21"
    '   WellName_CB.AddItem "well21"
    '   WellName_CB.AddItem "well22"
    '   WellName_CB.AddItem "well23"
    '   WellName_CB.AddItem "well24"
    '   WellName_CB.AddItem "well25"
    '   WellName_CB.AddItem "well26"
    '   WellName_CB.AddItem "well27"
    '   WellName_CB.AddItem "well28"



        ' Should be picked up from database LATER

End Sub

Private Sub Get_From_and_To_Rows(fieldname As Variant, wellname As Variant)

    wksht = fieldname & "_" & wellname
    Worksheets(wksht).Activate
    ' MsgBox wksht
    nRows = Worksheets(wksht).Cells(1, 1)
    If (nRows > 0) Then
        RowRange_From_CB.Clear
        RowRange_To_CB.Clear
```

```
      For i = 1 To nRows
         RowRange_From_CB.AddItem CStr(1 + i)
         RowRange_To_CB.AddItem CStr(1 + i)
      Next i
      RowRange_From_CB.ListIndex = 0
      RowRange_To_CB.ListIndex = 0
   Else
      ' Deactivate From and To combo boxes
   End If

End Sub

Private Sub FieldName_CB_Click()

   Call Get_WellNames(FieldName_CB.Text)
   WellName_CB.SetFocus
   If (WellName_CB.LineCount > 0) Then
      WellName_CB.ListIndex = 0
   Else
      ' Deactivate the wellname combobox
   End If

End Sub

Private Sub WellName_CB_Click()

   WellName_CB.SetFocus
   wellname = WellName_CB.Text
   FieldName_CB.SetFocus
   fieldname = FieldName_CB.Text
   Call Get_From_and_To_Rows(fieldname, wellname)

End Sub

Private Sub RunBatch_BTN_Click()

   ' Run only selected well and date range
   Dim wksht As String

   wksht = FieldName_CB.Text & "_" & WellName_CB.Text
   Call DynSolve(wksht)

End Sub
```

```vb
Private Sub RunAllFields_BTN_Click()

    ' Run all wells in all fields for all date ranges
    Dim nFields, nWells As Integer
    Dim wksht As String

    nFields = FieldName_CB.ListCount
    nWells = FieldName_CB.ListCount

    For i = 1 To nFields
        FieldName_CB.ListIndex = i - 1
        For j = 1 To nWells
            WellName_CB.ListIndex = j - 1
            Call Get_From_and_To_Rows(FieldName_CB.Text, WellName_CB.Text)
            wksht = FieldName_CB.Text & "_" & WellName_CB.Text
            RowRange_To_CB.ListIndex = RowRange_To_CB.ListCount - 1
            Call DynSolve(wksht)
        Next j
    Next i

End Sub

Private Sub DynSolve(wksht As String)

    nFrom = CInt(RowRange_From_CB.Value)
    nTo = CInt(RowRange_To_CB.Value)
    If (nFrom > nTo) Then
        MsgBox "Check if ...From Row < End Row"
    Else
        Call RunSolver(wksht, nFrom, nTo)
    End If

End Sub
```

APPENDIX J

PROCESS DOCUMENTATION LIQUID LOADING PROJECT

J.1   Platform:

Dynamic Surveillance Tool (**DSS**) :

Important elements of handling a Liquid Loading Project by

1. To assign DSS project name

2. Table with field production and well completion data exported to DSS

3. Map name

4. Workbook name (Private and Public)

5. Table adjusted to meet the requirement of DSS (i.e identifying each well by PID etc.)

Microsoft Office Visio: Used for creation of workflow

System Requirement : Operating System NT 4.0 or above , Microsoft Access or Microsoft SQL Server database,6 MB free space harddrive,512 MB RAM,SCADA monitoring preferable for on line data acquisition, Microsoft Excel with Visual Basic add-ons

Process of analysis in DSS

Create a table in DSS with desired name.then choose a primary indexing key combining at least PID; PType which is an entity type and date.

J.2 Liquid loading prediction
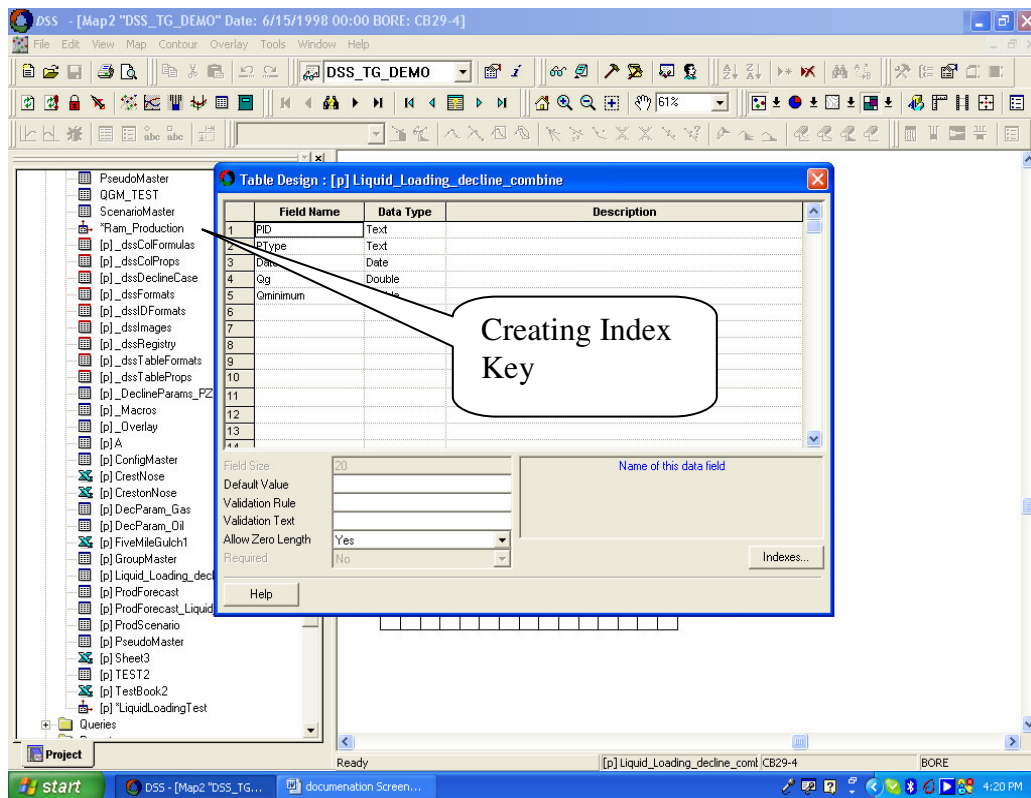
Figure J.2.1 Creating the primary id (pidex_new) involves combining the PID; ptype

and date in a composite primary key and PID should be indexed primary key

Key selection is one of the main criteria concerning the well identification. Once PID

and ptype and date is selected , the formulas and criteria are tabulated to identify the

liquid loaded and liquid unloaded wells based on the criteria 1or 2 depending on whether

the gas production figure is more or less than the calculated minimum flow. If criteria 1

is met, the liquid unloading column puts in the gas figure and liquid loading column gets

blank. If the criteria is 2, the liquid unloading column gets blank and the liquid loading

column gets the gas values. This tabulated column then is mapped to bubble map.
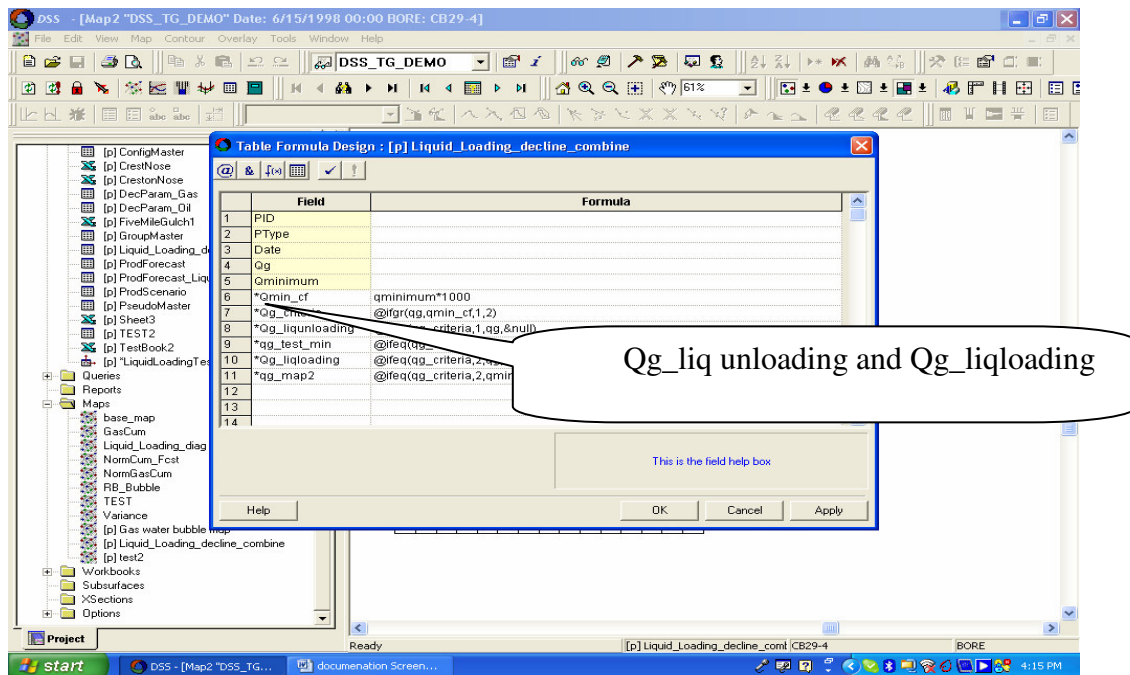
Figure J.2.2 Criteria and formula for table to generate the columns
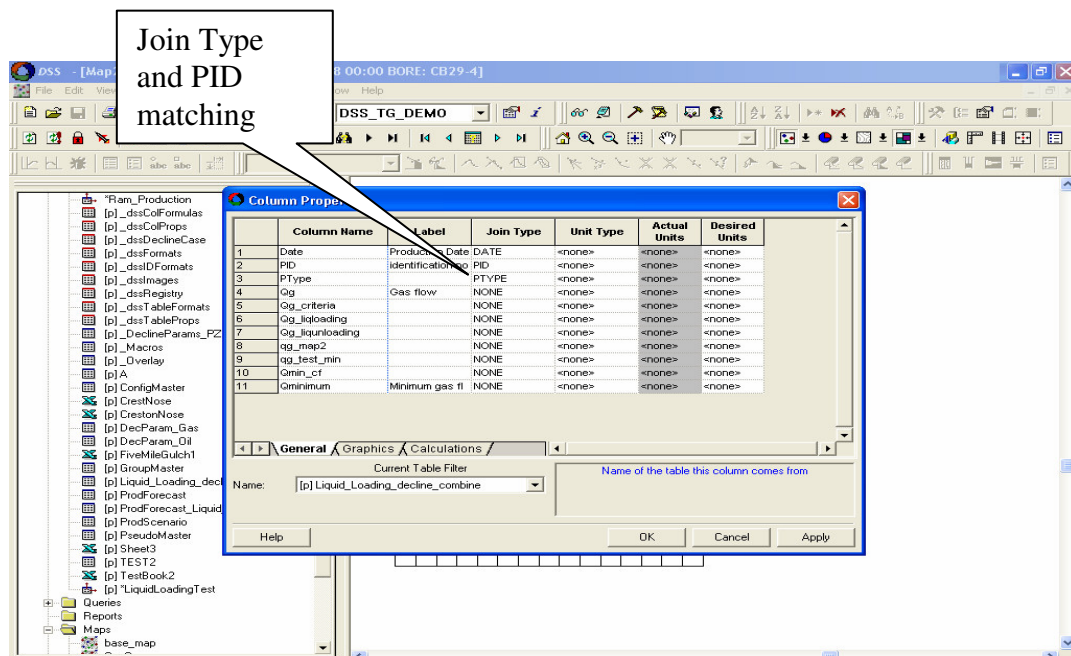
Figure J.2.3 Select the proper join type and match PID with corresponding PID; ptype and date

Choosing the graphics tab and choose the different colors for the columns Qg_liqloading (red) and Qg_liqunloading in green which is used in bubble map.the columns were created by criteria set in the formula section of the table .If the value of the criteria is 1 it will write Qg value in the be liq_unloading column and leave the corresponding Qg_liqunloading cells blank. In case 2 is the value of the Qg_criteria it fills the Qg_loading column with Qg value and leave the Qg_loading cell blank.

The calculations tab. one can average; interpolate; set null as 0.
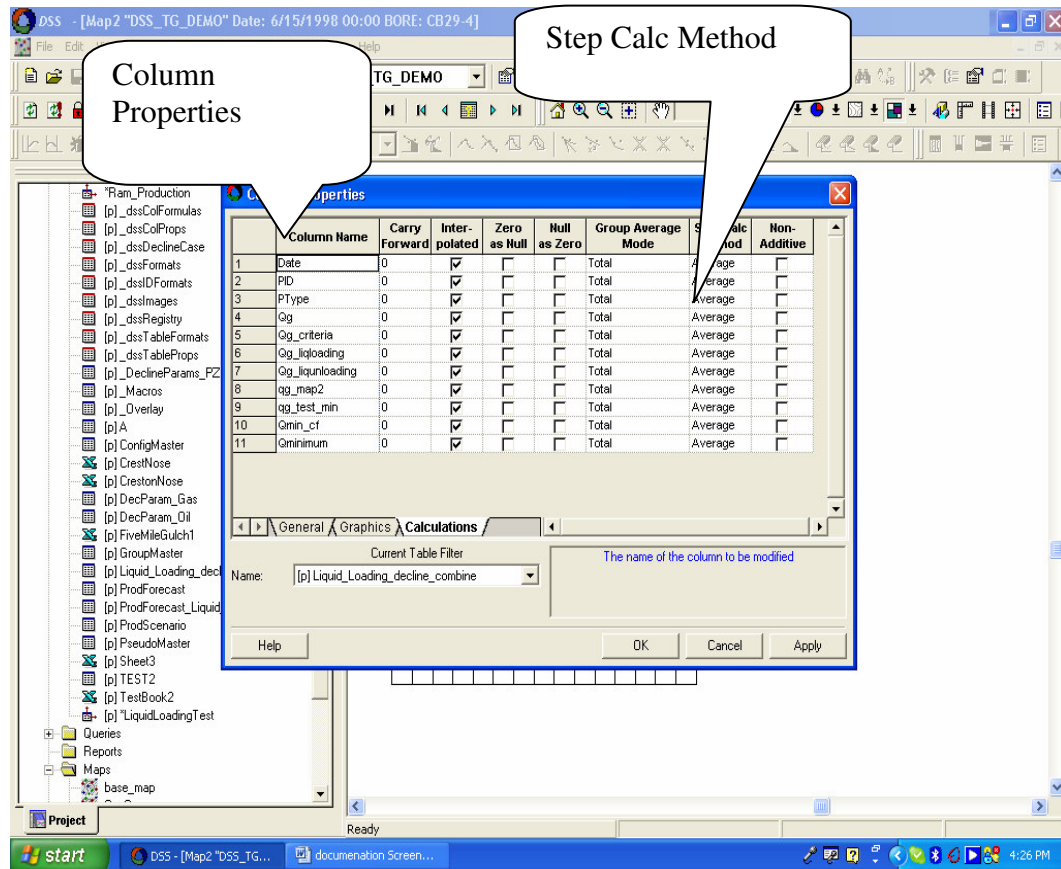
Figure J.2.4 Column properties calculation tab
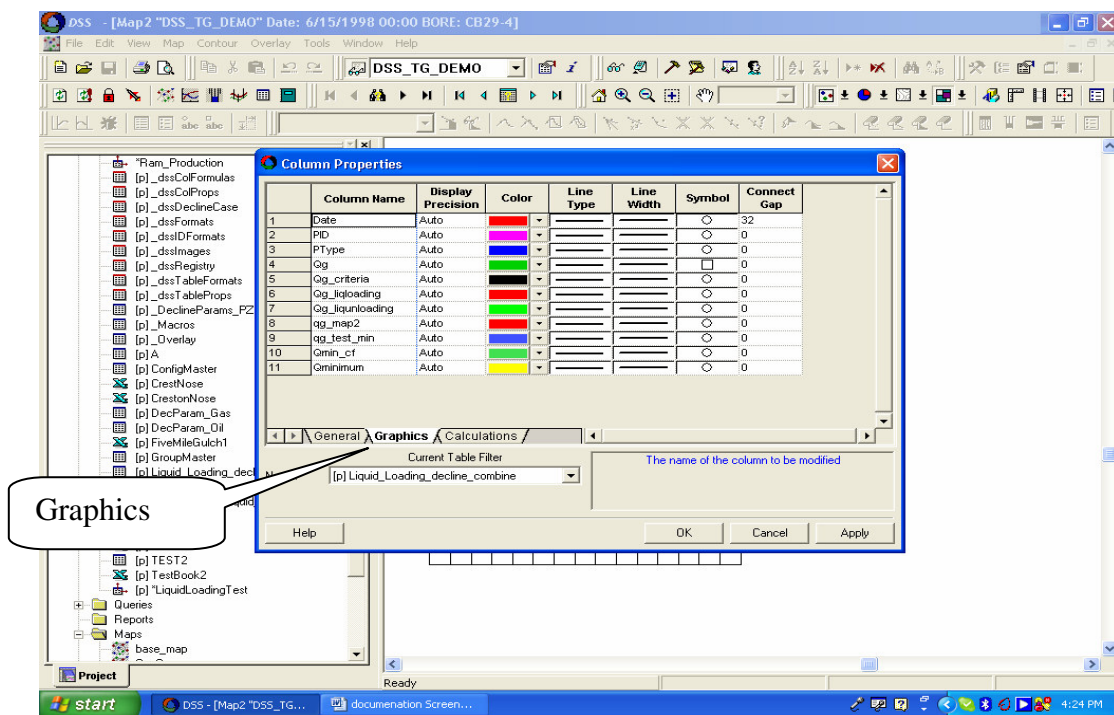
Figure J.2.5 Column properties graphics tab

Figure J.2.6 Screenshot of the bubble map table created with the criteria

Display with the red indicating liquid loaded and the green ones liquid unloaded wells

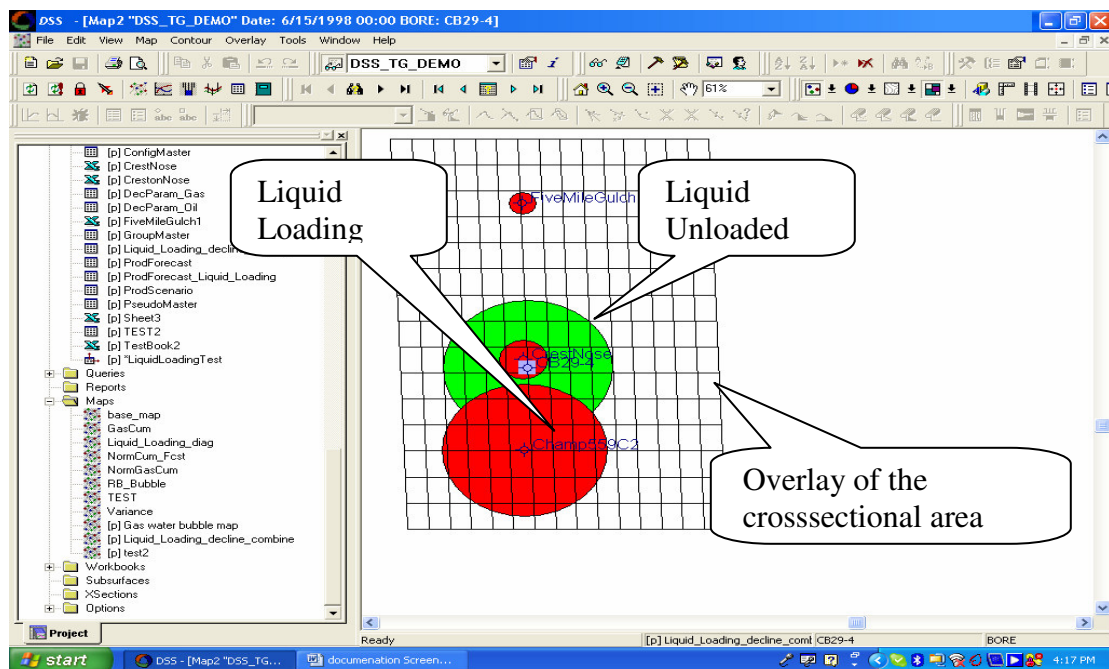on a particular day and time in a bubble map.

Figure J.2.7 Screenshot of the bubble map
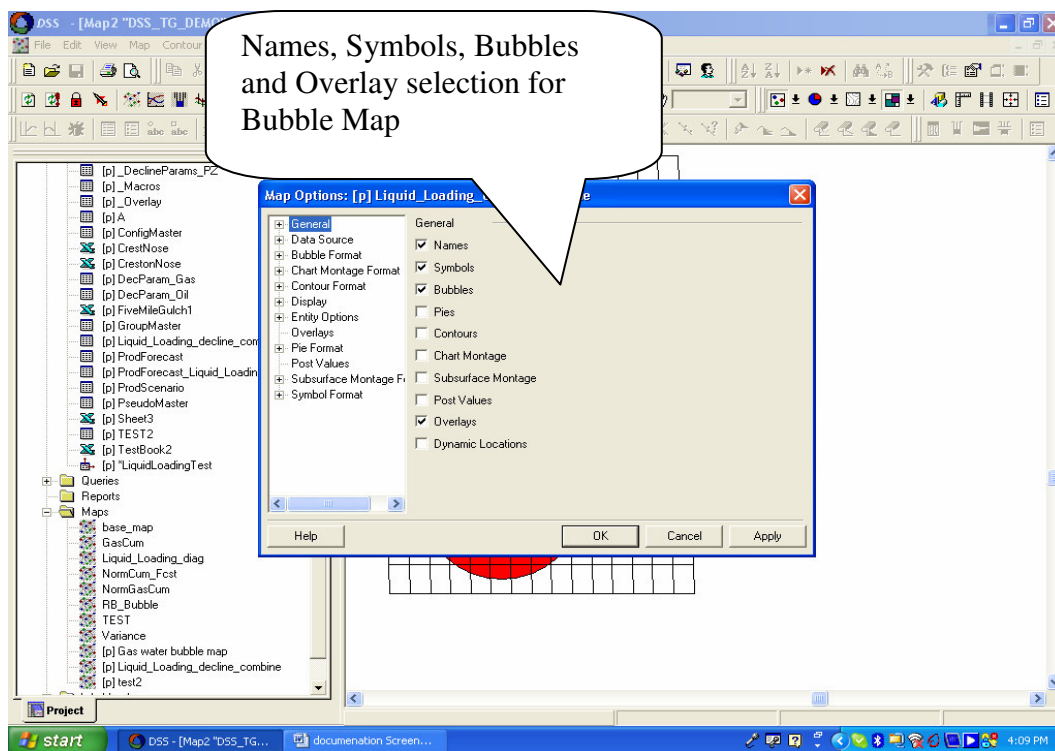
Figure J.2.8 Properties of bubble map
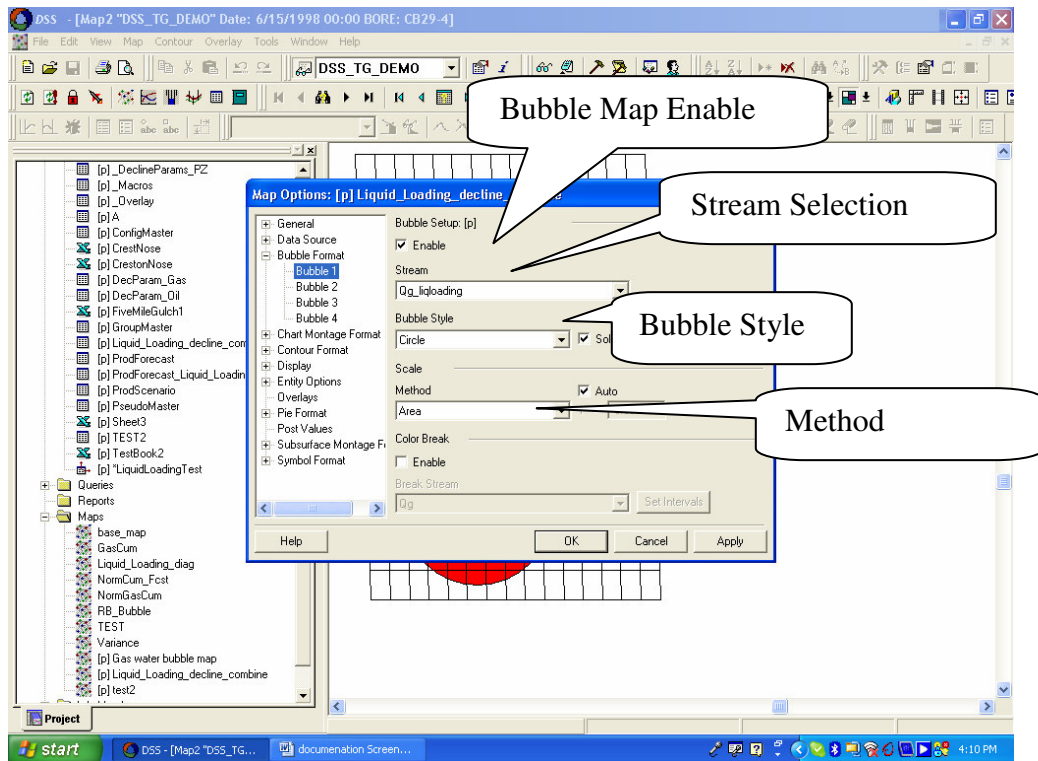
Figure J.2.9 Set up of bubble map style, scale and method
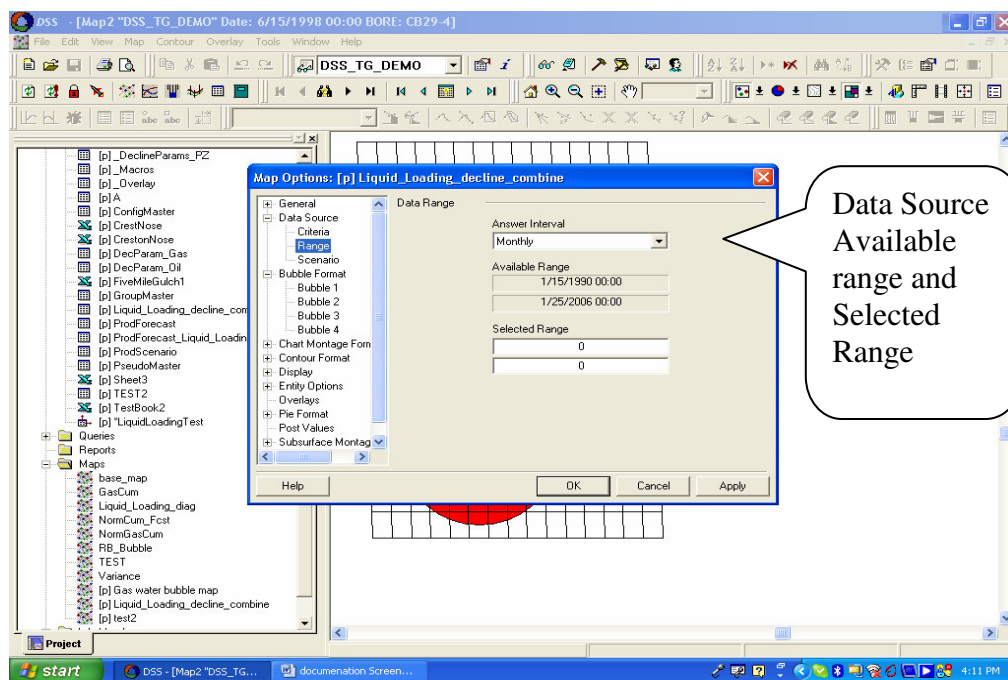
Figure J.2.10 Choosing a data source
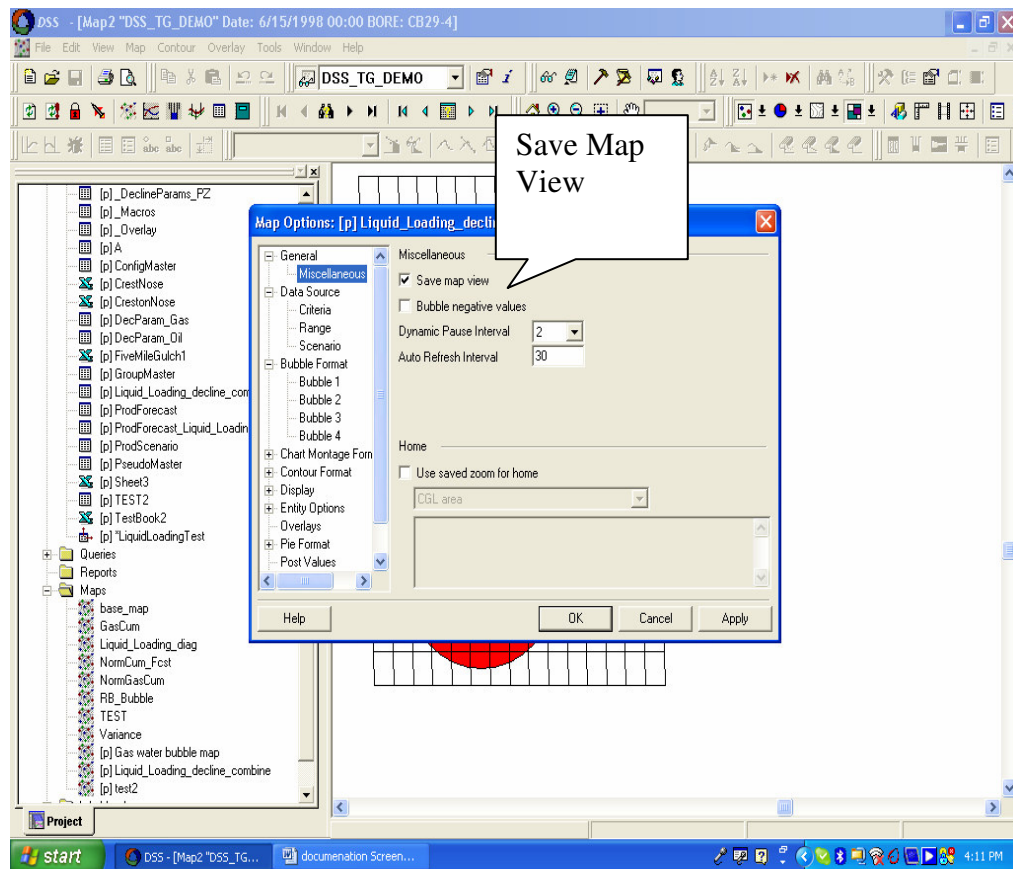
Figure J.2.11 Map view
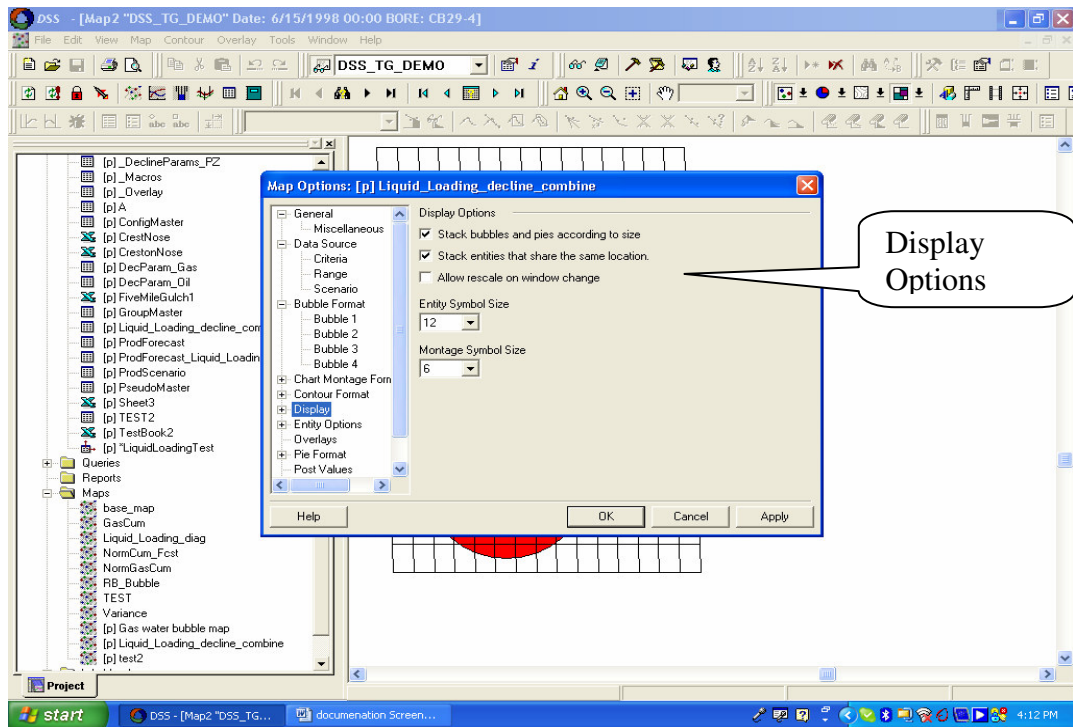
Figure J.2.12 Display options
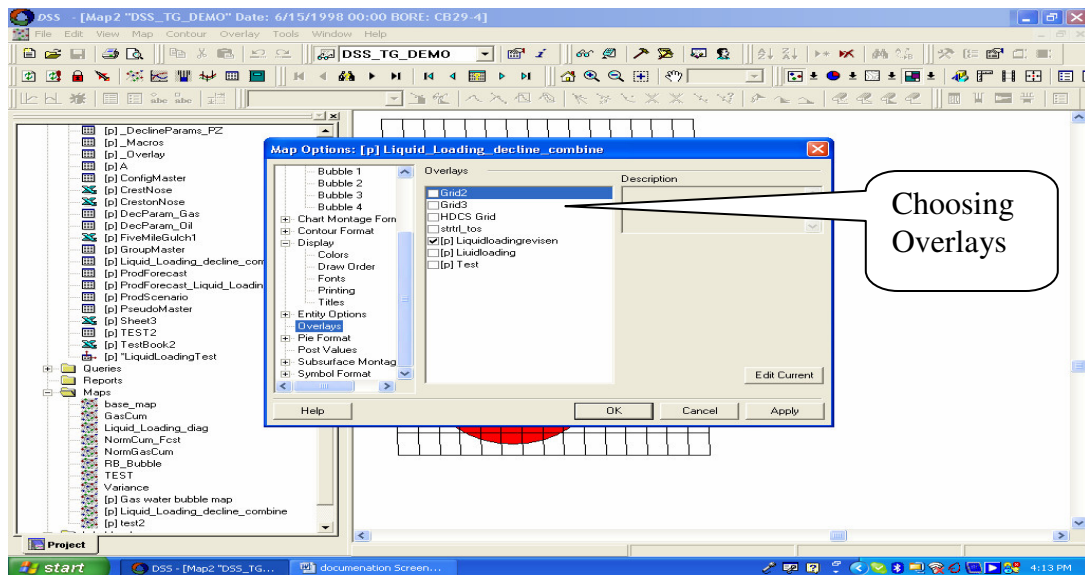
Figure J.2.13 Overlays

J.3 Liquid loading prediction through forecasting by DSS
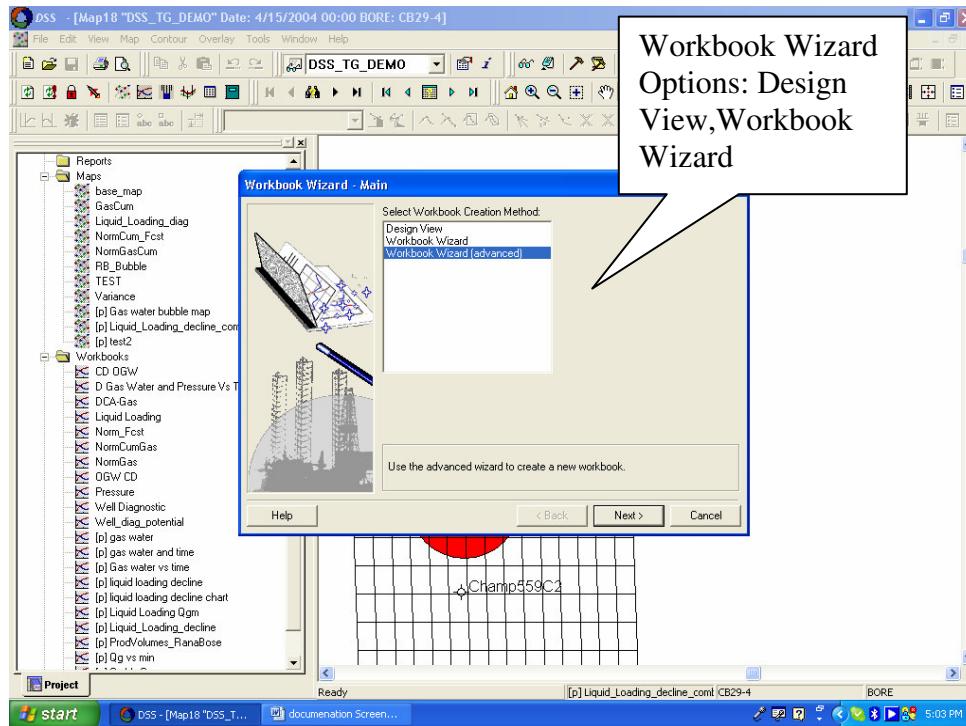
Figure J.3.1 Creation of workbook
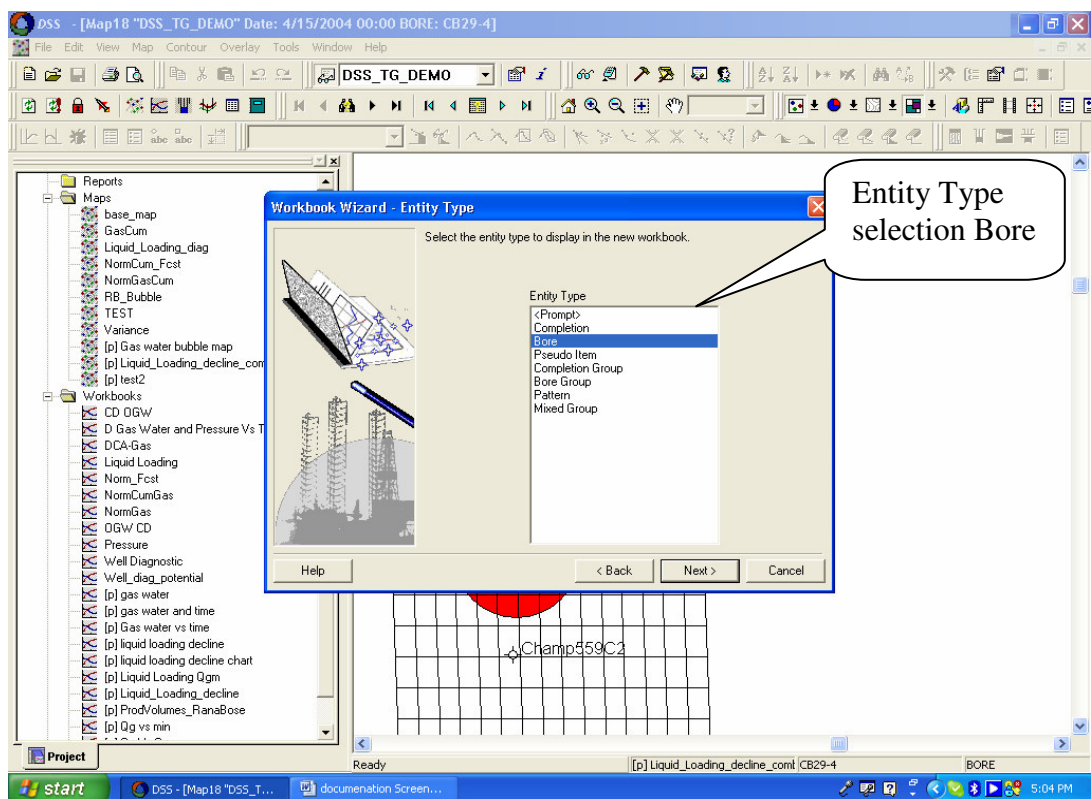
Figure J.3.2 Entity type selection
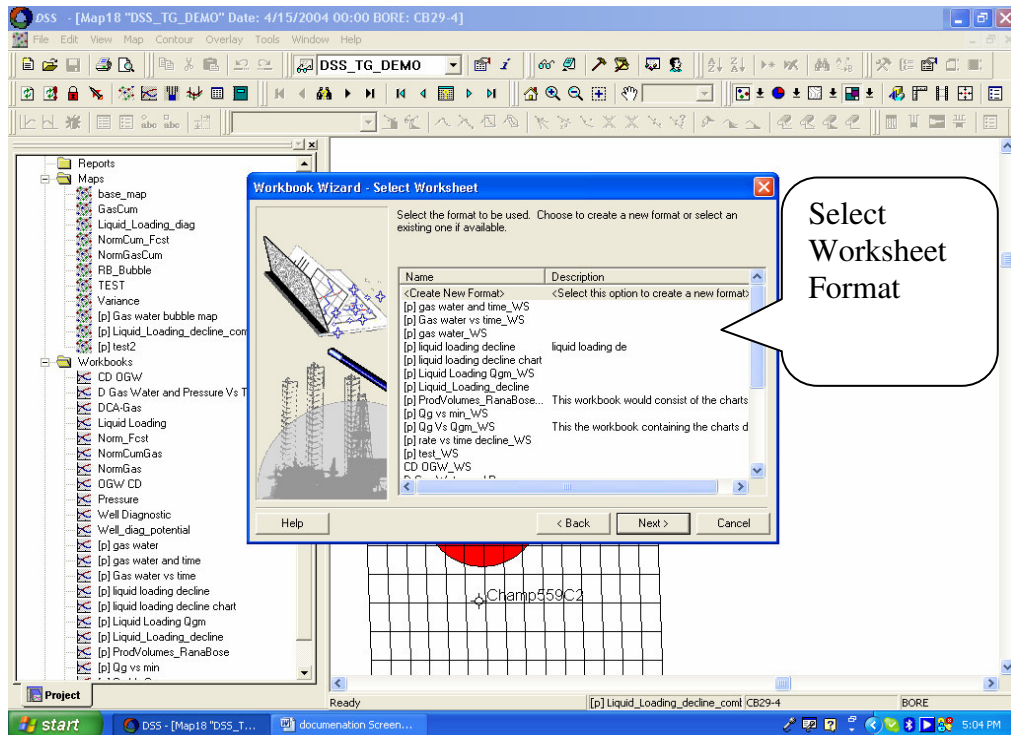
J.3.3 Format selection
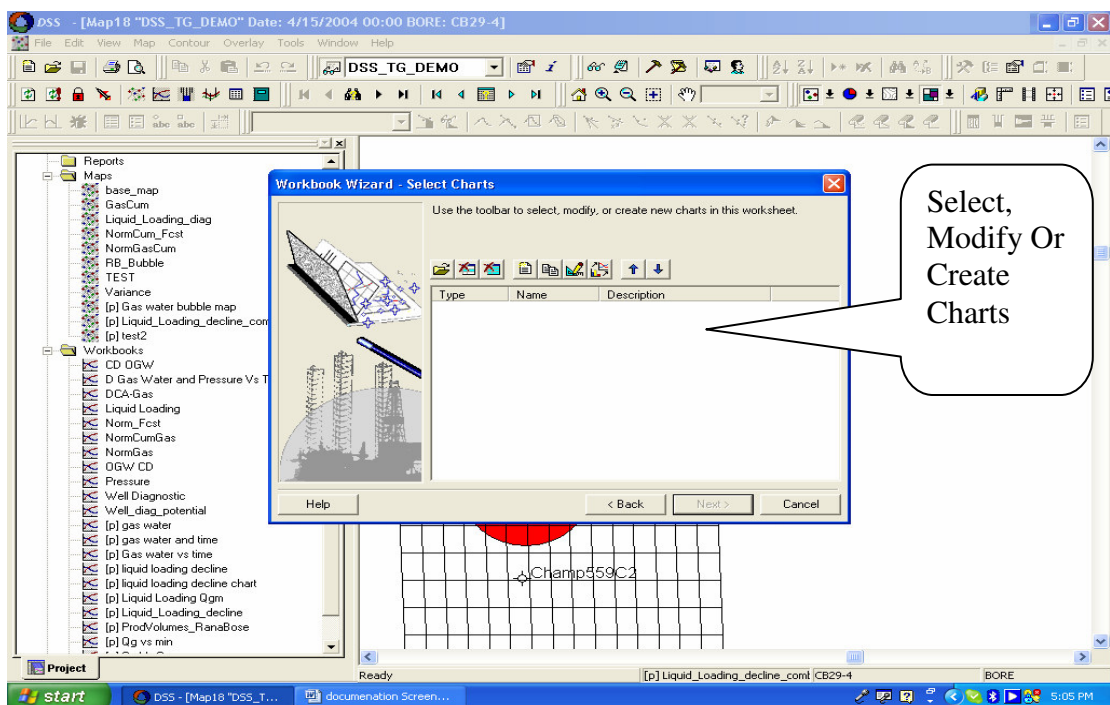
Figure J.3.4 Chart selection
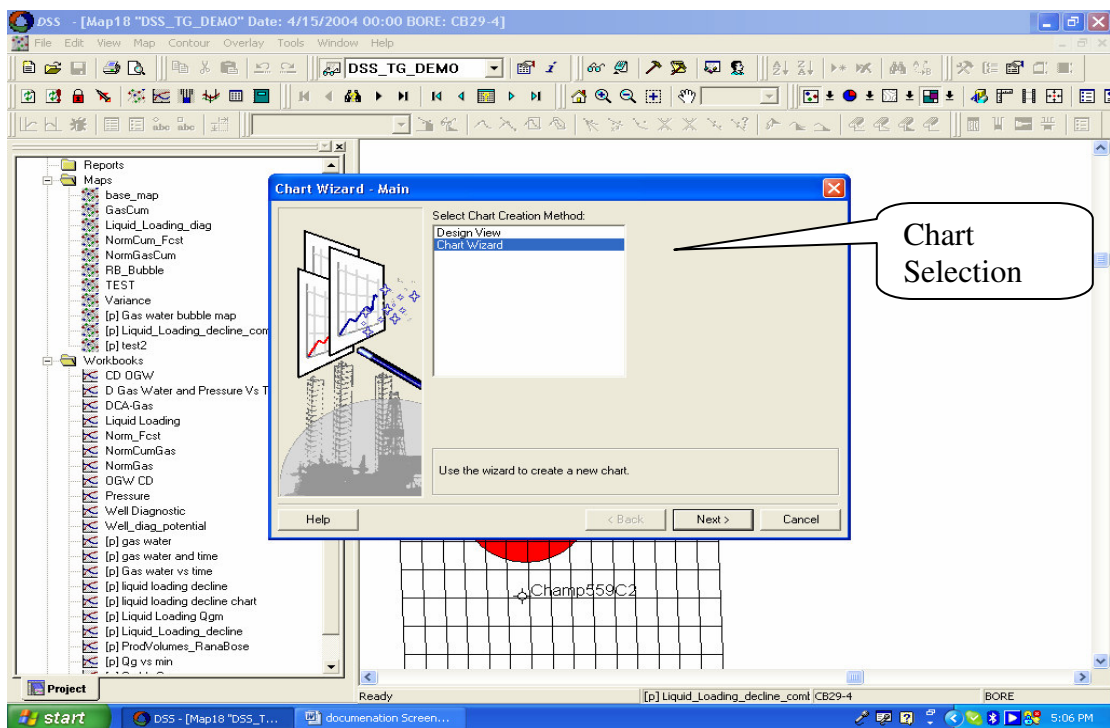
Figure J.3.5 Chart criterion selection
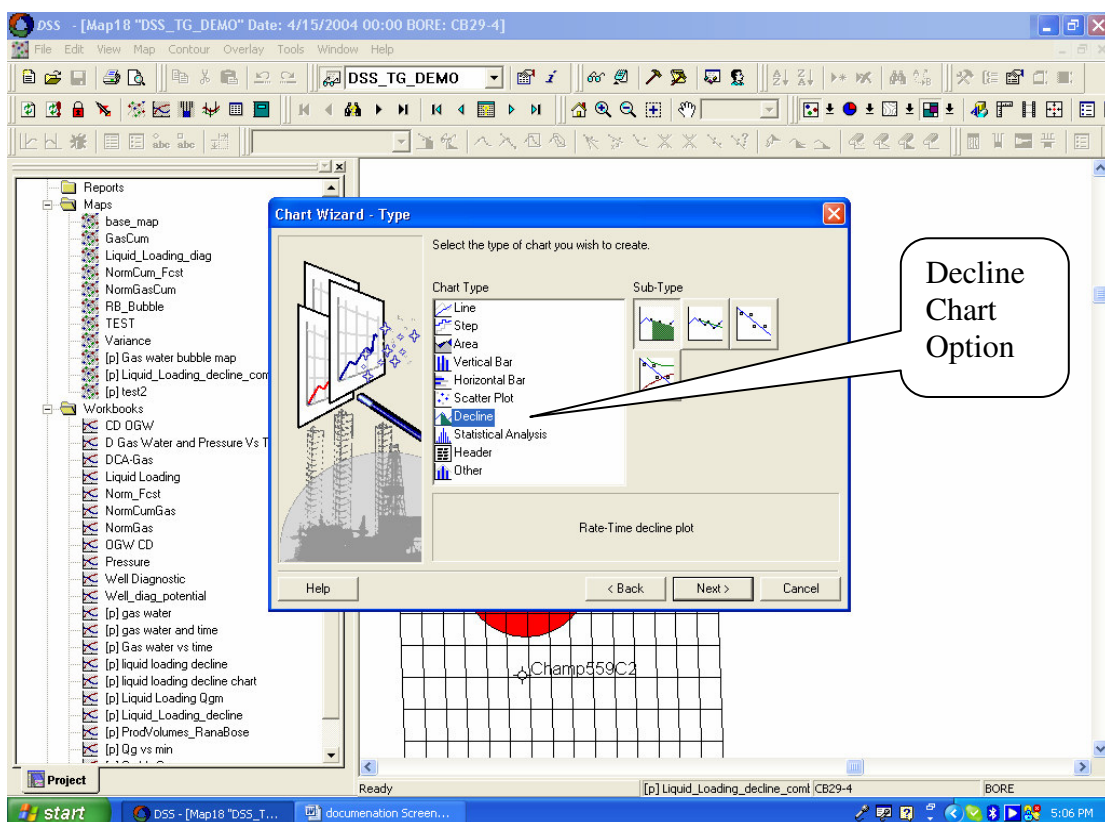
Figure J.3.6 Creation of type of chart
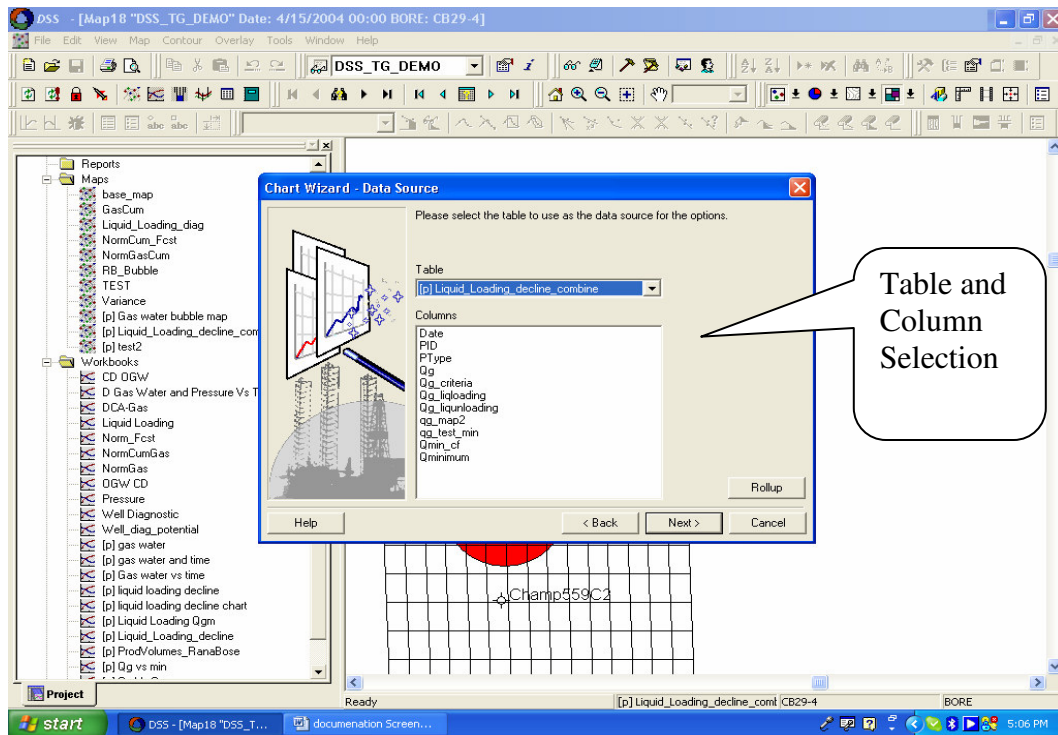
Figure J.3.7 Data table selection
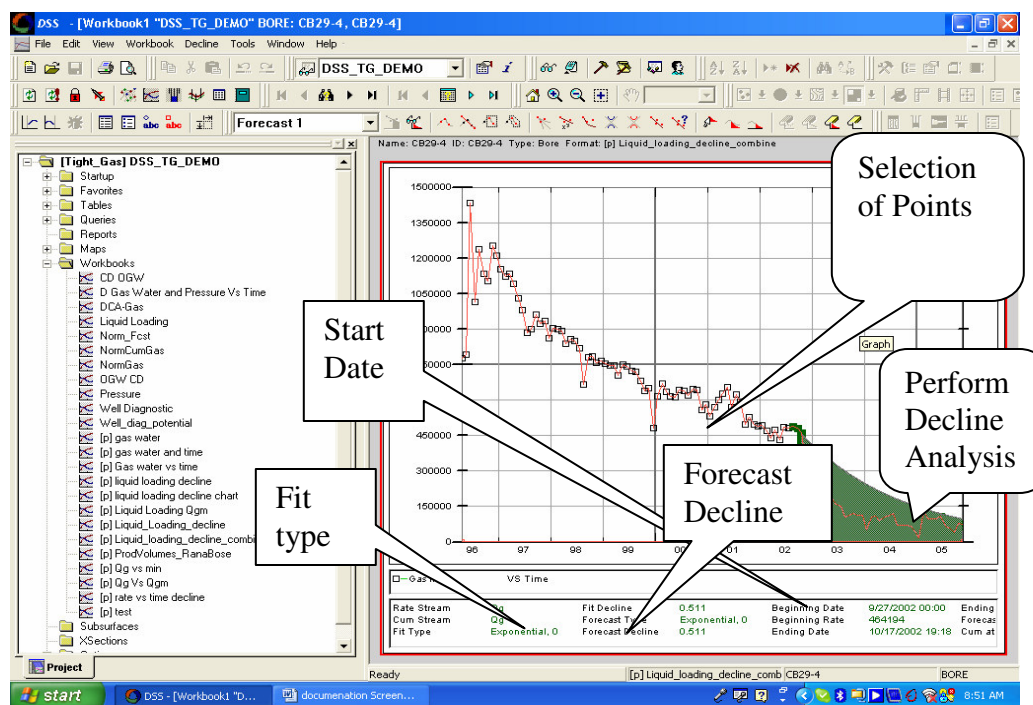
Figure J.3.8 Creation of chart in workbook
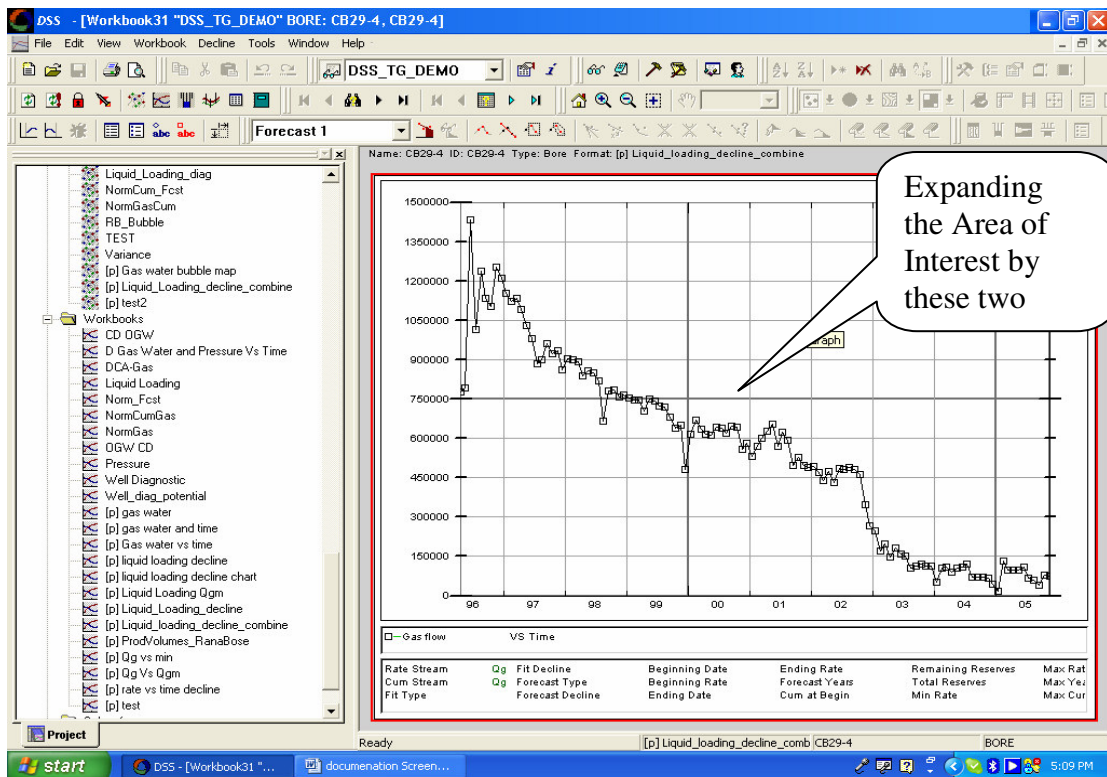
Figure J.3.9 Expanding the area of interest
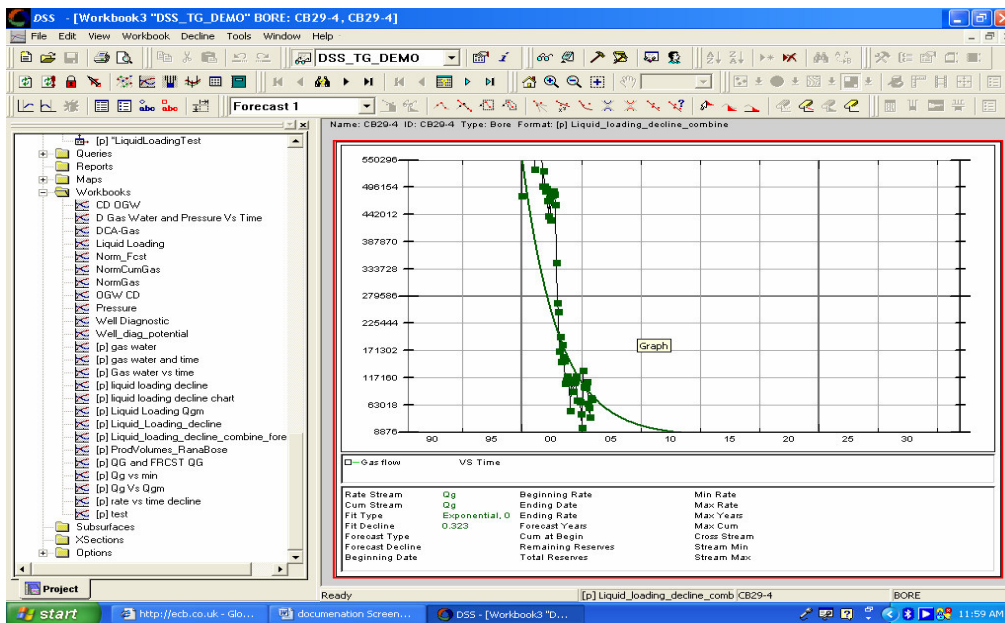
Figure J.3.10 Expand right and left accordingly
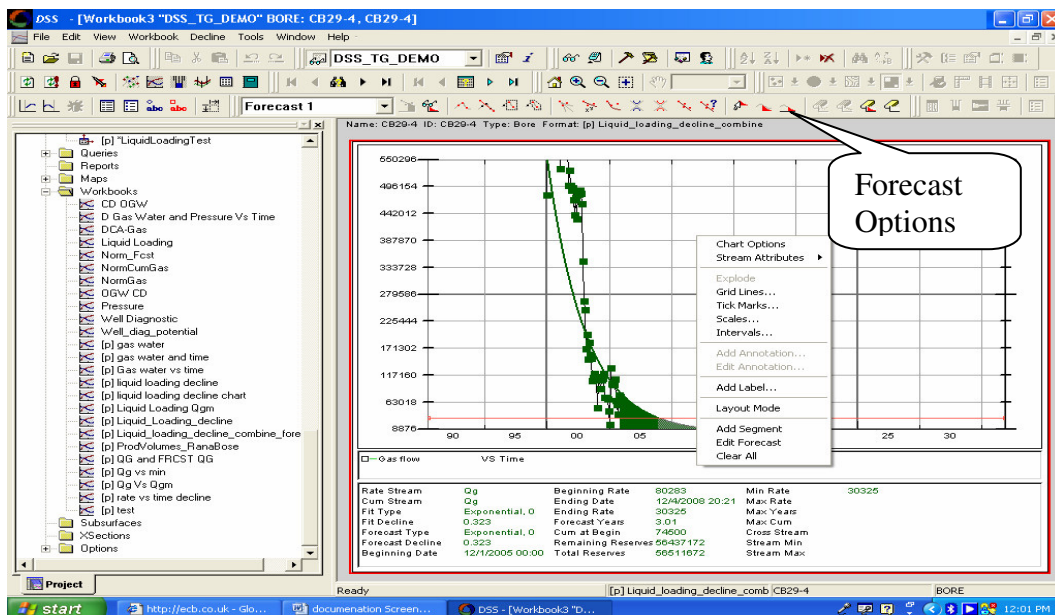
Figure J.3.11 Options available **a)** forecast at **b)** forecast current **c)** forecast last
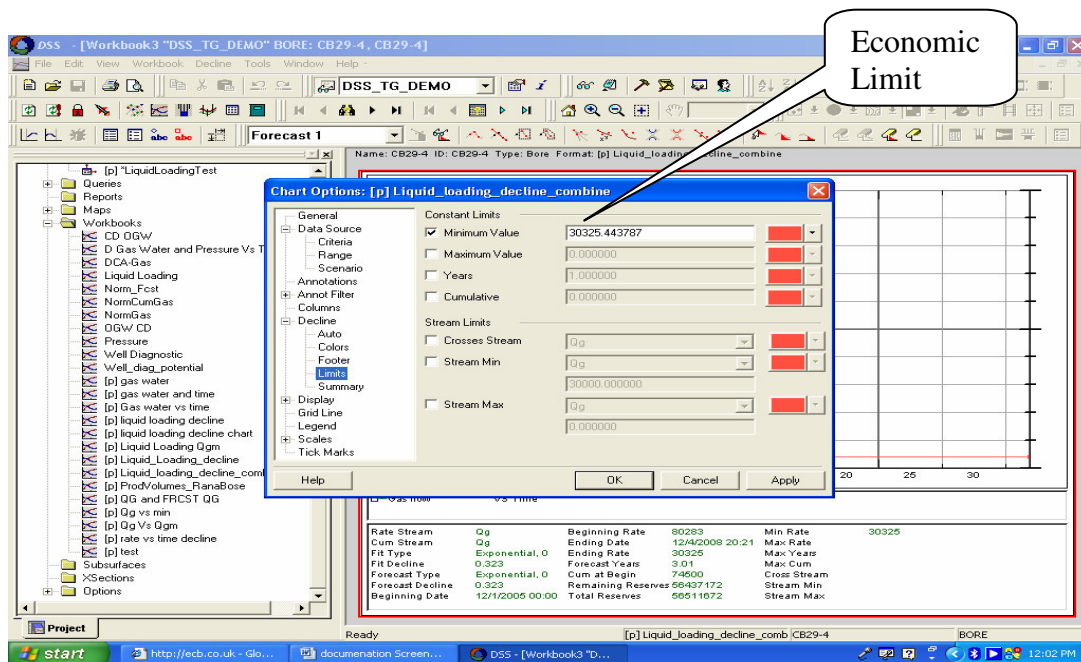
Figure J.3.12 Economic limit selection

The set limit can be adjusted by dragging and placing the decline line.

The layout can be adjusted to display all the decline component; remaining reserves; total reserves; forecast years.

The data hence obtained to predict liquid loading based on Qgm in VBA Excel program can be tabulated in RB_Qg_Prodorecast table

Figure J.3.13 Liquid loading prediction table
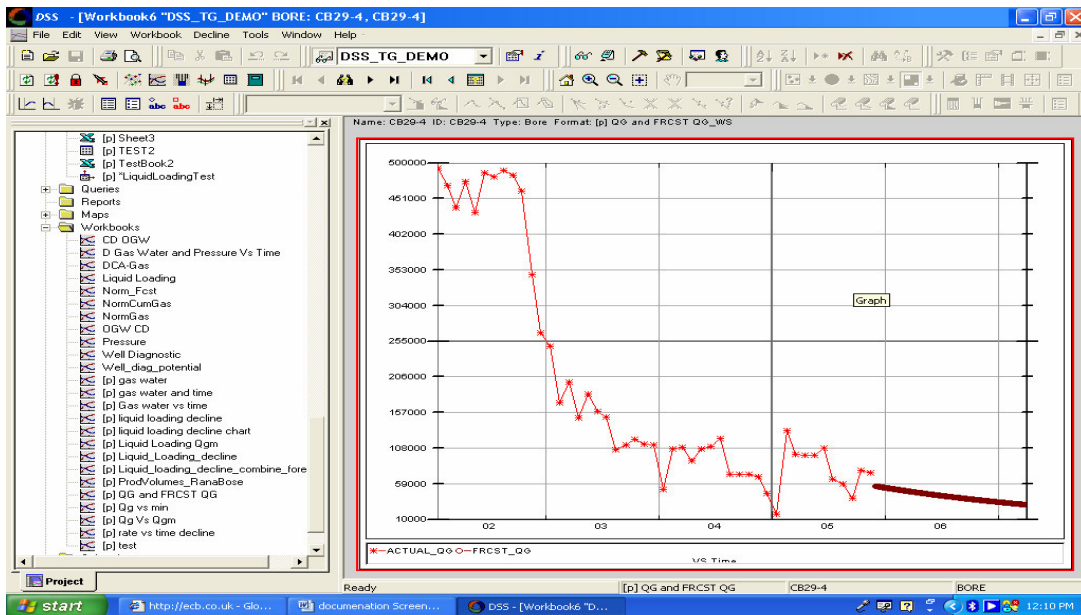
Figure J.3.14 The Q_g and FRCST Q_g workbook provides the production and forecasted production in the same workbook
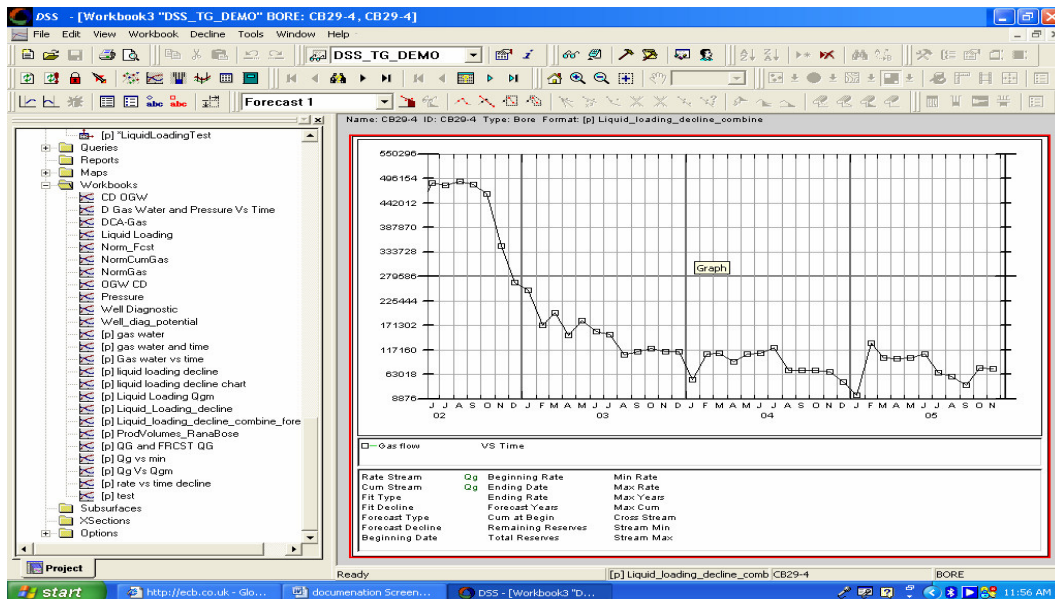
Figure J.3.15 Production history
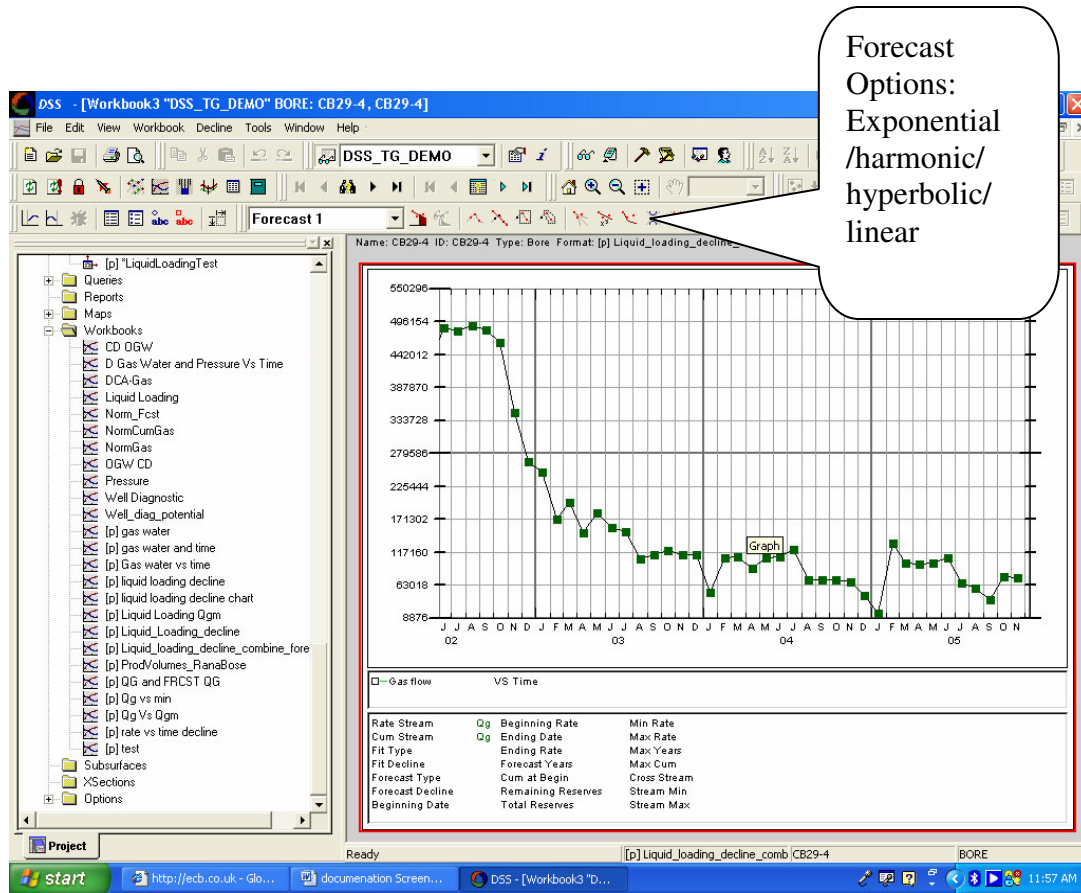
Figure J.3.16 Points selection

J.4 Field Engineer Interface
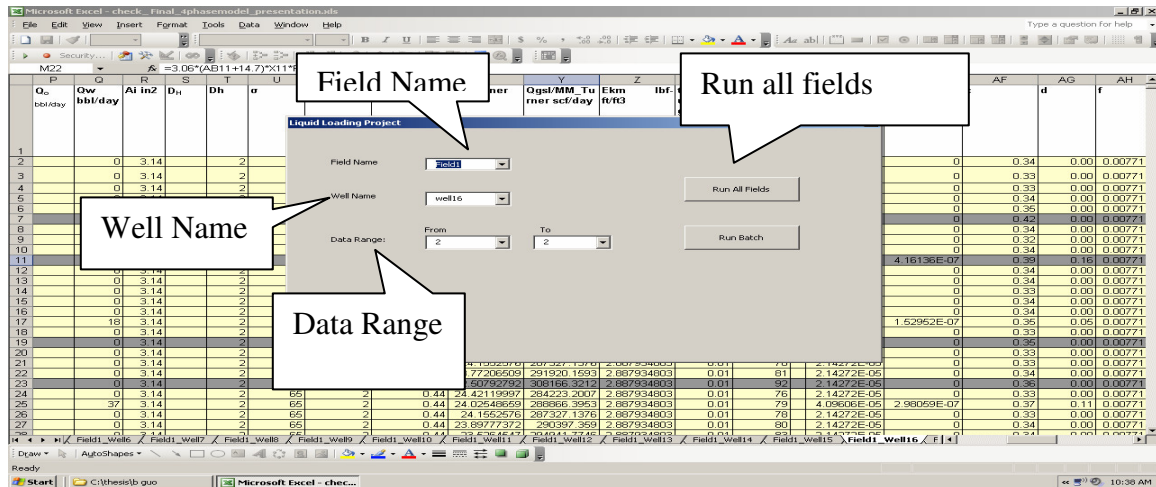
Figure J.4.1 Showing the option of choosing the Field and the well batchwise in "Run Batch" option or can choose all wells for analysis by selecting to "Run All Fields" button

Figure J.4.2 Wells loaded and unloaded colored differently with yellow ones being the liquid unloaded and the grey ones being liquid loaded wells

**Table J.4.1   Comparison between Turner Model and B.Guo's Model
with Field Data**

Field1_well1			Field1_well2		
$Q_{gm\ calculated}$(Mscf/day)	Qgsl/MM_Turner scf/day	Difference%	$Q_{gm\ calculated}$(Mscf/day)	Qgsl/MM_Turner scf/day	Difference%
1012.64	946679.5798	6.96796136	328.9101	339625.3123	-3.155003429
406.09	430888.0558	-5.7561797	327.4770	338320.9715	-3.205243716
477.02	494757.6704	-3.5847552	344.2814	353648.3543	-2.648671854
395.67	421627.6537	-6.1562537	265.6189	282689.0264	-6.038468592
387.68	414544.4074	-6.4811881	258.4387	276338.4594	-6.477480548
477.02	494757.6704	-3.5847552	252.9197	271476.5438	-6.835506018
408.65	433171.7205	-5.6615601	292.5830	306759.0031	-4.621212629
406.09	430888.0558	-5.7561797	260.2523	277939.9167	-6.363818
382.25	409753.1584	-6.710986	344.2814	353648.3543	-2.648671854
395.67	421627.6537	-6.1562537	258.4387	276338.4594	-6.477480548
534.77	547560.294	-2.3365352	276.0393	291951.9522	-5.450430755
393.94	414544.4074	-4.9701973	304.6953	276338.4594	10.26163626
481.38	498719.2897	-3.4766681	318.7427	330384.3052	-3.523658775
390.36	416919.0704	-6.3703366	323.5019	329042.4976	-1.683861872
400.91	426283.4114	-5.9517492	318.7427	330384.3052	-3.523658775
456.89	476513.8927	-4.1175375	267.3839	284254.1552	-5.93492933
376.75	404904.356	-6.9522662	315.7776	327695.0757	-3.636762631
408.65	433171.7205	-5.6615601	267.3839	284254.1552	-5.93492933
461.44	480629.1893	-3.9920597	260.2523	277939.9167	-6.363818
341.90	374475.8954	-8.6993358	245.3682	264853.1191	-7.356875697
435.84	457527.7659	-4.7407777	318.7427	330384.3052	-3.523658775
461.44	480629.1893	-3.9920597	340.1581	349880.9826	-2.778909511
356.84	387448.8899	-7.9011329	245.3682	264853.1191	-7.356875697
353.90	384889.7271	-8.0518286	276.0393	291951.9522	-5.450430755
447.67	468172.5486	-4.3800029	247.2777	266524.6277	-7.221441629
380.24	402457.7232	-5.5211297	298.6247	276338.4594	8.064836154
411.19	435443.2082	-5.5689582	333.1726	343507.9319	-3.008754758
445.33	466063.4176	-4.4483695	262.0534	279532.0589	-6.252824452
387.68	414544.4074	-6.4811881	262.0534	279532.0589	-6.252824452
403.51	428592.0194	-5.8528855	328.9101	339625.3123	-3.155003429

Continued

Field1_well3			Field1_well4		
$Q_{gm\ calculated}$(Mscf/day)	Qgsl/MM_Turner scf/day	Difference	$Q_{gm\ calculated}$(Mscf/day)	Qgsl/MM_Turner scf/day	Difference%
263.84	281115.0442	-6.144404843	353.72	303850.0582	16.41119548
276.04	291951.9522	-5.450430755	353.72	303850.0582	16.41119548
269.14	285810.576	-5.833704663	353.72	303850.0582	16.41119548
267.38	284254.1552	-5.93492933	353.72	303850.0582	16.41119548
237.58	258057.3197	-7.936444951	353.72	303850.0582	16.41119548
196.39	222927.9566	-11.90410592	353.72	303850.0582	16.41119548
196.39	222927.9566	-11.90410592	353.72	303850.0582	16.41119548
256.61	274727.5242	-6.593911915	353.72	303850.0582	16.41119548
252.92	271476.5438	-6.835506018	353.72	303850.0582	16.41119548
251.05	269836.148	-6.96089308	353.72	303850.0582	16.41119548
281.10	296473.1192	-5.183800356	353.72	303850.0582	16.41119548
265.62	282689.0264	-6.038468592	353.72	303850.0582	16.41119548
262.05	279532.0589	-6.252824452	353.72	303850.0582	16.41119548
229.52	251075.1498	-8.584772456	353.72	303850.0582	16.41119548
270.88	287358.4302	-5.734715938	353.72	303850.0582	16.41119548
269.14	285810.576	-5.833704663	353.72	303850.0582	16.41119548
256.61	274727.5242	-6.593911915	353.72	303850.0582	16.41119548
272.61	288897.8555	-5.637888039	353.72	303850.0582	16.41119548
256.61	274727.5242	-6.593911915	353.72	303850.0582	16.41119548
252.92	271476.5438	-6.835506018	353.72	303850.0582	16.41119548
254.77	273106.9432	-6.713216982	353.72	303850.0582	16.41119548
263.84	281115.0442	-6.144404843	353.72	303850.0582	16.41119548
263.84	281115.0442	-6.144404843	353.72	303850.0582	16.41119548
245.37	264853.1191	-7.356875697	353.72	303850.0582	16.41119548
214.70	238358.3972	-9.926726331	353.72	303850.0582	16.41119548
245.37	264853.1191	-7.356875697	353.72	303850.0582	16.41119548
272.61	288897.8555	-5.637888039	353.72	303850.0582	16.41119548
265.62	282689.0264	-6.038468592	353.72	303850.0582	16.41119548
254.77	273106.9432	-6.713216982	353.72	303850.0582	16.41119064
254.77	273106.9432	-6.713216982	353.72	303850.0582	16.41119548

Continued

Field1_well5			Field1_well6		
$Q_{gm\ calculated}$(Mscf/day)	Qgsl/MM_Turner scf/day	Difference%	$Q_{gm\ calculated}$(Mscf/day)	Qgsl/MM_Turner scf/day	Difference%
349.70	300768.3507	16.27003117	338.77	348615.919	-2.823561735
337.38	291322.5645	15.81020854	371.87	378946.5573	-1.868381949
341.54	294505.6706	15.96994321	370.60	377781.3416	-1.901089893
347.00	298695.7519	16.17272625	281.10	296473.1192	-5.183800356
351.05	301799.1748	16.31771147	295.78	309633.9318	-4.474055672
359.00	307909.7667	16.59101324	370.60	377781.3416	-1.901089893
355.04	304870.1899	16.45702516	302.07	315303.6628	-4.195644935
345.64	297653.901	16.12307419	359.00	367123.1834	-2.213988894
347.00	298695.7519	16.17272625	287.72	302394.3914	-4.85279639
258.44	231767.7402	11.50761935	373.13	380108.0973	-1.836057164
269.14	239712.096	12.27519829	297.37	311061.2426	-4.402522193
378.63	315868.478	19.8706254	370.91	369518.9778	0.377101084
270.88	241010.2963	12.39322331	282.77	297964.6668	-5.098525474
262.05	234446.2429	11.77547854	281.10	296473.1192	-5.183800356
265.62	237094.0222	12.03105668	375.64	382420.284	-1.772528436
274.33	243585.6012	12.62162982	294.19	308199.8834	-4.546939174
256.61	230416.6332	11.36879733	297.37	311061.2426	-4.402522193
302.07	264448.2333	14.2282695	375.64	382420.284	-1.772528436
265.62	237094.0222	12.03105668	357.68	365919.2424	-2.250968568
362.90	310918.8272	16.71999404	270.88	287358.4302	-5.734715938
348.36	299733.889	16.2217074	279.43	294973.8965	-5.270836478
359.00	307909.7667	16.59101324	373.13	380108.0973	-1.836057164
356.37	305886.8288	16.50226332	359.00	367123.1834	-2.213988894
366.77	313898.2487	16.84432616	279.43	294973.8965	-5.270836478
352.38	302826.3985	16.36476185	370.60	377781.3416	-1.901089893
365.11	304870.1899	19.76023825	369.27	365919.2424	0.916930127
349.70	300768.3507	16.27003117	282.77	297964.6668	-5.098525474
344.28	296608.2972	16.0727374	366.77	374263.2965	-2.001587538
331.76	287022.1647	15.58615112	270.88	287358.4302	-5.734715938
335.98	290253.581	15.75541747	272.61	288897.8555	-5.637888039

Continued

Field1_well7			Field1_well8		
Q$_{gm\ calculated}$(Mscf/day)	Qgsl/MM_Turner scf/day	Difference%	Q$_{gm\ calculated}$(Mscf/day)	Qgsl/MM_Turner scf/day	Difference%
328.91	284847.0361	15.46901102	308.24	320871.2667	-3.936535782
327.48	283753.0729	15.40919881	270.88	287358.4302	-5.734758785
344.29	296608.2972	16.07600948	262.05	279532.0589	-6.252859208
265.62	237094.0222	12.03101012	265.62	282689.0264	-6.038507637
258.44	231767.7402	11.50789651	280.94	282689.0264	-0.618813426
252.92	227690.0045	11.08072751	231.56	252839.0018	-8.414716921
292.59	257281.7445	13.72271714	258.44	276338.4594	-6.477256102
260.25	233110.8979	11.64341623	272.61	288897.8555	-5.637931648
344.29	296608.2972	16.07597061	302.08	315303.6628	-4.19378613
258.44	231767.7402	11.50763068	258.44	276338.4594	-6.477471042
276.04	244862.9276	12.73212556	311.28	323618.4218	-3.813250216
258.44	231767.7402	11.50780857	326.04	337011.4658	-3.256178755
318.74	277096.514	15.02967541	314.28	326341.97	-3.694691204
317.26	275971.127	14.96274709	274.33	290428.986	-5.543193368
318.74	277096.514	15.02967541	258.44	276338.4594	-6.477321845
267.38	238406.7108	12.15445891	265.62	282689.0264	-6.038507639
315.78	274841.0312	14.89471689	265.62	282689.0264	-6.038507639
267.38	238406.7108	12.15445891	290.98	305311.1941	-4.694172806
260.25	233110.8979	11.64348924	334.03	323618.4218	3.217179479
245.37	264853.1191	-7.354589273	231.56	252839.0018	-8.414717982
318.74	330384.3052	-3.523498046	231.56	252839.0018	-8.414717982
340.16	349880.9826	-2.77696869	227.46	249298.6611	-8.758059484
245.37	264853.1191	-7.354589273	228.75	245706.6755	-6.899360079
276.04	291951.9522	-5.450475348	281.11	296473.1192	-5.181460763
247.28	266524.6277	-7.221455236	0.10	0.1	2.27318E-11
258.44	276338.4594	-6.477321845	0.10	0.1	2.27318E-11
333.18	343507.9319	-3.008054258	0.10	0.1	2.27318E-11
262.05	279532.0589	-6.252859211	0.10	0.1	2.27318E-11
262.05	279532.0589	-6.252859211	0.10	0.1	2.27318E-11
328.91	339625.3123	-3.154847527	1.44	0.1	1440396.107

Continued

Field1_well9			Field1_well10		
$Q_{gm\ calculated}$(Mscf/day)	Qgsl/MM_Turner scf/day	Difference%	$Q_{gm\ calculated}$(Mscf/day)	Qgsl/MM_Turner scf/day	Difference%
432.67	435135.2919	-0.566976353	604.15	594802.1594	1.571426212
334.58	344792.1944	-2.960901401	599.46	590434.5012	1.5285943
267.38	284254.1552	-5.934970132	605.70	596250.3978	1.585572171
334.58	344792.1944	-2.960901401	391.58	397111.7982	-1.392516961
277.74	293466.8811	-5.358317517	289.17	287358.4302	0.629497982
245.37	264853.1191	-7.354598369	237.58	258057.3197	-7.936104281
249.17	268185.5723	-7.08950336	274.33	290428.986	-5.543193365
340.16	349880.9826	-2.776994918	577.89	570335.0076	1.324036573
381.85	388138.7157	-1.619754376	256.62	274727.5242	-6.591847801
241.51	261477.5983	-7.638183353	277.74	293466.8811	-5.359711979
546.08	540691.3975	0.996983025	667.76	653965.828	2.10860485
519.60	516008.3274	0.696083175	237.58	258057.3197	-7.936105719
256.62	274727.5242	-6.591831048	666.35	652656.0251	2.097445147
281.11	296473.1192	-5.181460763	272.61	288897.8555	-5.637931649
263.84	281115.0442	-6.144441959	267.38	284254.1552	-5.934969942
269.14	285810.576	-5.833746527	270.88	287358.4302	-5.734758787
284.44	299448.6539	-5.012211553	265.62	282689.0264	-6.038507639
524.11	520208.2987	0.749418806	272.61	288897.8555	-5.637931649
480.08	479195.7703	0.184214105	278.85	279532.0589	-0.242544862
323.14	334376.7166	-3.360537905	225.39	247509.2637	-8.93773233
227.46	249298.6611	-8.758059484	591.56	583076.874	1.455134864
212.50	236485.2391	-10.14444891	229.52	251075.1498	-8.583804792
225.39	247509.2637	-8.93773233	593.94	585294.5926	1.477443937
229.52	251075.1498	-8.583804792	241.51	261477.5983	-7.638234407
210.27	234596.9581	-10.36964852	594.73	586031.8304	1.484827861
219.04	242060.7459	-9.511878688	229.52	251075.1498	-8.583804792
267.38	284254.1552	-5.934969942	505.84	503186.2589	0.52737129
551.25	545486.1065	1.055889028	597.89	588970.8732	1.514106662
419.42	422854.3435	-0.811981427	254.77	273106.9432	-6.7132359
251.05	269836.148	-6.960900706	595.52	586768.0736	1.492185899

Continued

Field1_well11			Field1_well12		
$Q_{gm\ calculated}$(Mscf/day)	Qgsl/MM_Turner scf/day	Difference%	$Q_{gm\ calculated}$(Mscf/day)	Qgsl/MM_Turner scf/day	Difference%
303.63	316704.9261	-4.129141493	267.52	279532.0589	-4.29716796
282.78	297964.6668	-5.096028859	274.33	290428.986	-5.543193361
265.62	282689.0264	-6.038507638	267.38	284254.1552	-5.934969942
323.14	334376.7166	-3.360545636	265.62	282689.0264	-6.038507637
313.11	306759.0031	2.068892759	265.62	282689.0264	-6.03850764
239.55	259773.1637	-7.785335979	254.77	273106.9432	-6.713235898
279.44	294973.8965	-5.267729877	274.33	290428.986	-5.543193365
323.14	334376.7166	-3.360534496	249.17	268185.5723	-7.089503359
284.44	299448.6539	-5.012210304	256.62	274727.5242	-6.591847801
314.28	326341.97	-3.694685917	256.62	274727.5242	-6.592099042
287.73	302394.3914	-4.849803743	330.34	340924.5474	-3.105248214
316.02	320871.2667	-1.512685944	274.88	274727.5242	0.055460462
263.84	281115.0442	-6.144441959	269.14	285810.576	-5.833746527
309.76	322247.8327	-3.874028924	284.44	299448.6539	-5.012211553
265.62	282689.0264	-6.038507639	320.22	331720.5666	-3.468268358
258.44	276338.4594	-6.477321845	269.14	285810.576	-5.833746527
321.68	333051.3486	-3.413963181	260.25	277939.9167	-6.363525155
300.52	313896.0189	-4.261225437	274.33	290428.986	-5.543193368
268.50	276338.4594	-2.837607326	262.05	279532.0589	-6.252859211
249.17	268185.5723	-7.089503352	256.62	274727.5242	-6.591831048
323.14	334376.7166	-3.360537905	251.05	269836.148	-6.960900706
326.04	337011.4658	-3.256178755	331.76	342218.7349	-3.056285063
317.26	329042.4976	-3.579631477	262.05	279532.0589	-6.252859211
281.11	296473.1192	-5.181460763	249.17	268185.5723	-7.089503352
237.58	258057.3197	-7.936105719	231.56	252839.0018	-8.414717982
239.55	259773.1637	-7.785337843	259.45	258057.3197	0.537874333
323.14	334376.7166	-3.360537905	272.61	288897.8555	-5.637931649
258.44	276338.4594	-6.477321845	260.25	277939.9167	-6.363525155
256.62	274727.5242	-6.591831048	254.77	273106.9432	-6.7132359
323.14	334376.7166	-3.360537905	252.92	271476.5438	-6.835518862

Continued

Field1_well13			Field1_well14		
$Q_{gm \text{ calculated}}$(Mscf/day)	Qgsl/MM_Turner scf/day	Difference%	$Q_{gm \text{ calculated}}$(Mscf/day)	Qgsl/MM_Turner scf/day	Difference%
454.93	369155.8938	23.23467336	258.44	276338.4594	-6.476659843
276.04	244862.9276	12.73212556	277.74	293466.8811	-5.359711957
270.88	241010.2963	12.39317221	272.61	288897.8555	-5.637931651
269.14	239712.096	12.27514837	326.04	337011.4658	-3.256186755
322.08	254847.2674	26.38327339	295.78	309633.9318	-4.474082564
265.62	237094.0222	12.03101012	252.92	271476.5438	-6.835518863
299.93	252388.871	18.83623918	349.72	358608.4181	-2.479595474
449.73	378233.1653	18.90398093	302.08	315303.6628	-4.193761907
296.61	249905.8496	18.6897847	239.55	259773.1637	-7.785338908
260.25	233110.8979	11.64361629	274.33	290428.986	-5.543193372
299.60	249905.8496	19.88560861	340.16	349880.9826	-2.777027857
263.84	235773.908	11.90470382	283.63	290428.986	-2.340023092
421.15	345825.4597	21.78201019	318.74	330384.3052	-3.523498046
281.11	248654.8742	13.05287371	294.19	308199.8834	-4.54652635
279.45	237094.0222	17.86354205	270.88	287358.4302	-5.734758787
272.61	242301.4272	12.50861996	276.04	291951.9522	-5.450475348
427.96	347609.3444	23.11591378	260.25	277939.9167	-6.363525155
272.61	242301.4272	12.50861996	272.61	288897.8555	-5.637931649
273.33	233110.8979	17.25233494	326.04	337011.4658	-3.256178755
247.28	266524.6277	-7.221455236	231.56	252839.0018	-8.414717982
277.19	282689.0264	-1.944105449	300.52	313896.0189	-4.261225437
256.62	274727.5242	-6.591831048	249.17	268185.5723	-7.089503352
274.08	277939.9167	-1.389938057	331.76	342218.7349	-3.056285063
398.72	403706.6406	-1.234354829	298.95	312481.9082	-4.330469636
262.58	266524.6277	-1.480355428	249.17	268185.5723	-7.089503352
260.25	277939.9167	-6.363525155	267.74	276338.4594	-3.112469334
275.88	279532.0589	-1.306773153	258.44	276338.4594	-6.477321845
284.44	299448.6539	-5.012211553	342.92	352397.1506	-2.68902089
277.37	279532.0589	-0.773181628	352.40	361062.2443	-2.399722701
269.14	285810.576	-5.833746527	311.28	323618.4218	-3.813287757

Continued

Field1_well15			Field1_well16		
$Q_{gm \ calculated}$(Mscf/day)	Qgsl/MM_Turner scf/day	Difference%	$Q_{gm \ calculated}$(Mscf/day)	Qgsl/MM_Turner scf/day	Difference%
368.05	375439.7461	-1.967685009	279.43	294973.8965	-5.270833299
288.74	294973.8965	-2.11438156	270.88	287358.4302	-5.734754317
276.04	291951.9522	-5.450475353	267.38	284254.1552	-5.934969017
314.36	313896.0189	0.148480056	272.61	288897.8555	-5.637918305
402.25	406962.6774	-1.15879658	286.08	300925.1924	-4.933087386
296.01	299448.6539	-1.147202371	341.54	351141.3765	-2.734779922
289.36	303856.3573	-4.771036823	274.33	290428.986	-5.543175121
368.31	367123.1834	0.32192382	263.84	281115.0442	-6.14444208
260.25	277939.9167	-6.363519124	276.04	291951.9522	-5.450458789
351.88	348615.919	0.935843294	313.94	290428.986	8.095601113
321.68	333051.3486	-3.413956808	274.33	290428.986	-5.543175121
293.74	299448.6539	-1.90686902	276.04	291951.9522	-5.450458789
347.01	356137.2427	-2.561620177	270.88	287358.4302	-5.734754317
275.68	282689.0264	-2.479500126	274.33	290428.986	-5.543175121
286.09	300925.1924	-4.930166122	277.74	293466.8811	-5.359702128
279.44	294973.8965	-5.267785877	284.71	287358.4302	-0.920697062
347.01	356137.2427	-2.561620177	270.88	287358.4302	-5.734754317
297.37	311061.2426	-4.402161014	281.10	296473.1192	-5.183753065
269.14	285810.576	-5.833746527	270.88	287358.4302	-5.734754317
331.76	342218.7349	-3.056285063	270.88	287358.4302	-5.734754317
269.14	285810.576	-5.833746527	276.04	291951.9522	-5.450458789
260.25	277939.9167	-6.363525155	294.19	308199.8834	-4.546962137
272.61	288897.8555	-5.637931649	267.38	284254.1552	-5.934969017
287.73	302394.3914	-4.849789816	300.32	288897.8555	3.954972287
254.77	273106.9432	-6.7132359	270.88	287358.4302	-5.734754317
371.21	319488.6465	16.19019727	274.33	290428.986	-5.543175121
276.04	291951.9522	-5.450475348	279.43	294973.8965	-5.270833299
268.50	276338.4594	-2.837607326	276.04	291951.9522	-5.450458789
279.44	294973.8965	-5.267785877	276.04	291951.9522	-5.450458789
364.20	371898.9147	-2.070423203	281.10	296473.1192	-5.183753065

Continued

Field1_well17			Field1_well18		
$Q_{gm\ calculated}$(Mscf/day)	Qgsl/MM_Turner scf/day	Difference%	$Q_{gm\ calculated}$(Mscf/day)	Qgsl/MM_Turner scf/day	Difference%
258.44	276338.4594	-6.476659843	399.90	404794.9939	-1.208961405
277.74	293466.8811	-5.359711957	358.77	346071.5773	3.667862102
272.61	288897.8555	-5.637931651	390.38	396001.6312	-1.419850324
326.04	337011.4658	-3.256186755	413.22	401520.7888	2.914873869
269.14	285810.576	-5.833746526	311.28	323618.4218	-3.813260726
265.62	282689.0264	-6.038507639	414.27	400423.2403	3.459206125
384.31	390401.9284	-1.561052693	404.58	409118.4896	-1.109667868
258.44	276338.4594	-6.477261424	272.61	288897.8555	-5.637931648
315.78	327695.0757	-3.636688711	318.00	312481.9082	1.76675451
326.04	337011.4658	-3.256184301	419.01	404794.9939	3.510842437
324.59	335696.7347	-3.307942687	355.05	363499.0726	-2.323702306
282.11	290428.986	-2.866033171	442.97	429040.4217	3.245658576
586.77	578614.0687	1.409792731	433.77	436142.5053	-0.545070665
492.65	490900.4892	0.35658595	429.40	432099.0153	-0.624462936
305.18	318099.8932	-4.062513829	429.40	432099.0153	-0.624462936
270.88	287358.4302	-5.734758787	358.28	352397.1506	1.668651789
260.25	277939.9167	-6.363525155	356.37	364711.219	-2.286488394
282.78	297964.6668	-5.095975061	308.24	320871.2667	-3.935787716
305.18	318099.8932	-4.062513829	305.63	287358.4302	6.359950418
274.33	290428.986	-5.543193368	368.93	357375.0215	3.232905167
247.28	266524.6277	-7.221455236	416.04	419725.844	-0.877609165
318.74	330384.3052	-3.523498046	444.07	430062.4619	3.256987916
312.78	324983.1096	-3.75352617	423.88	426988.7243	-0.727002251
267.38	284254.1552	-5.934969942	445.96	426988.7243	4.442821614
376.89	383570.9964	-1.74121906	411.49	415516.5395	-0.967855859
291.18	296473.1192	-1.786569107	423.76	411262.6169	3.03928994
321.68	333051.3486	-3.413963181	401.08	405880.3314	-1.183730853
311.28	323618.4218	-3.813287757	337.05	333051.3486	1.199852528
256.62	274727.5242	-6.591831048	251.05	269836.148	-6.960900706
252.92	271476.5438	-6.835518862	277.44	276338.4594	0.399809461

Continued

Field1_well19			Field1_well20		
$Q_{gm\ calculated}$(Mscf/day)	Qgsl/MM_Turner scf/day	Difference%	$Q_{gm\ calculated}$(Mscf/day)	Qgsl/MM_Turner scf/day	Difference%
265.62	282689.0264	-6.038468598	492.65	490900.4892	0.35629501
276.04	291951.9522	-5.450430762	400.42	374263.2965	6.987672015
269.14	285810.576	-5.8337464	487.85	486433.6393	0.291980717
274.33	290428.986	-5.543193373	363.90	340924.5474	6.740394612
291.64	288897.8555	0.949911005	495.51	493560.2289	0.394399412
371.87	378946.5573	-1.868382272	378.48	340924.5474	11.01521752
295.78	309633.9318	-4.47408612	480.08	479195.7703	0.184210338
258.44	276338.4594	-6.477261424	516.66	479195.7703	7.817410506
277.74	293466.8811	-5.359711972	386.75	392651.6943	-1.503641947
283.99	293466.8811	-3.23073902	424.49	393771.6068	7.800128243
277.74	293466.8811	-5.359711961	544.36	539083.0924	0.978238661
274.33	290428.986	-5.543193368	496.27	466246.11	6.439515545
410.35	414457.2952	-0.99093427	474.16	473691.2776	0.099591071
274.33	290428.986	-5.543193368	484.00	454839.4538	6.411634293
287.73	302394.3914	-4.849789816	269.14	285810.576	-5.833746527
270.88	287358.4302	-5.734758787	326.70	285810.576	14.30802694
270.88	287358.4302	-5.734758787	393.98	399322.5764	-1.338699816
371.87	378946.5573	-1.868382469	485.93	481015.9432	1.020955813
273.90	281115.0442	-2.565714678	492.65	490900.4892	0.35658595
252.92	271476.5438	-6.835518862	449.73	450970.3125	-0.274086397
272.61	288897.8555	-5.637931649	363.89	339625.3123	7.143885768
263.84	281115.0442	-6.144441959	312.60	302394.3914	3.375516347
274.33	290428.986	-5.543193368	338.78	348615.919	-2.821881032
263.84	281115.0442	-6.144441959	368.60	335696.7347	9.802291019
254.77	273106.9432	-6.7132359	411.49	415516.5395	-0.967855859
380.62	387001.9931	-1.64960481	289.38	281115.0442	2.941228674
265.62	282689.0264	-6.038507639	300.52	313896.0189	-4.261225437
270.88	287358.4302	-5.734758787	344.08	323618.4218	6.324007655
256.62	274727.5242	-6.591831048	435.93	438149.7152	-0.507369701
258.44	276338.4594	-6.477321845	480.67	447066.2689	7.516611566

Continued

Field2_well1			Field2_well2		
$Q_{gm\ calculated}$(Mscf/day)	Qgsl/MM_Turner scf/day	Difference%	$Q_{gm\ calculated}$(Mscf/day)	Qgsl/MM_Turner scf/day	Difference%
1015.30	825754.046	22.95434305	642.31	541378.2598	18.64385388
947.13	773375.7321	22.46736505	594.48	487872.827	21.85241594
925.14	773375.7321	19.6233697	593.23	487872.827	21.59501723
924.81	773375.7321	19.58068676	589.18	487872.827	20.76442025
926.29	773375.7321	19.77180019	580.91	487872.827	19.07098148
925.72	773375.7321	19.69913273	580.91	487872.827	19.07098148
926.11	773375.7321	19.74855992	592.14	487872.827	21.37145145
946.98	773375.7321	22.44703902	592.80	487872.827	21.50610376
925.63	773375.7321	19.68633715	601.45	487872.827	23.28029677
925.63	773375.7321	19.68633715	601.45	487872.827	23.28029677
925.63	773375.7321	19.68633715	601.45	487872.827	23.28029677
925.63	773375.7321	19.68633715	601.45	487872.827	23.28029677
925.63	773375.7321	19.68633715	601.45	487872.827	23.28029677
925.63	773375.7321	19.68633715	601.45	487872.827	23.28029677
925.63	773375.7321	19.68633715	601.45	487872.827	23.28029677
925.63	773375.7321	19.68633715	601.45	487872.827	23.28029677
925.63	773375.7321	19.68633715	601.45	487872.827	23.28029677
925.63	773375.7321	19.68633715	601.45	487872.827	23.28029677
925.63	773375.7321	19.68633715	601.45	487872.827	23.28029677
925.63	773375.7321	19.68633715	601.45	487872.827	23.28029677
925.63	773375.7321	19.68633715	601.45	487872.827	23.28029677
925.63	773375.7321	19.68633715	601.45	487872.827	23.28029677
925.63	773375.7321	19.68633715	601.45	487872.827	23.28029677
925.63	773375.7321	19.68633715	601.45	487872.827	23.28029677
925.63	773375.7321	19.68633715	601.45	487872.827	23.28029677
925.63	773375.7321	19.68633715	601.45	487872.827	23.28029677
925.63	773375.7321	19.68633715	601.45	487872.827	23.28029677
925.63	773375.7321	19.68633715	601.45	487872.827	23.28029677
925.63	773375.7321	19.68633715	601.45	487872.827	23.28029677

The prediction of liquid loading by Turner flow rate corresponding to terminal velocity was found wanting in most real BP well scenario. The actual well names which can be referred to master table, are not disclosed due to technical reasons. The wells tended to show signs of liquid loading even if the predicted Turner flowrate was not suggesting that. This had necessitated to consider B.Guo's model as an alternative model of predicting flowrate.If found successful, it was to be considered for inclusion in DSS upcoming releases and also include it in the engineering workflows.

In field1, well4,5,7,13,20 and Field2 well1,2 justified claim of B.Guo.Most of the wells deviated by 5-6% which proves that the arbitrary 20% adjustment is close enough. But the four phase model has got more scientific explanation.

The claim of B.Guo[1] of Turner flow rate underprediction was found true around 40% wells and 20% more wells was very close by 5-6%. Needs more data to conclude on the applicability range of the model.

VITA

Name:	Rana Bose
Permanent Address:	Flat 8/12, 36 C Ballygunge Circular Road Kolkata-700019 West Bengal, India
Education:	Harold Vance Department of Petroleum Engineering, Texas A&M University M.S in Petroleum Engineering January 2005-May 2007
	Chemical Engineering Department Jadavpur University, Kolkata, India Bachelor in Chemical Engineering May 1986-June 1990
Experience:	October 2005-December 2006 Research Assistant Texas A&M University
	September 1991-December 2004 Deputy Superintendent Engineer (Production), Oil and Natural Gas Corporation Ltd., India